Methodology and quantification of N_2O emissions from grain sorghum production in humid and semi-arid environments using an automated trace gas analyzer system

by

Ashley Elizabeth Trout

B.S., Kansas State University, 2024

A THESIS

submitted in partial fulfillment of the requirements for the degree

MASTER OF SCIENCE

Department of Agronomy
College of Agriculture

KANSAS STATE UNIVERSITY
Manhattan, Kansas

2026

Approved by:

Major Professor
Peter J. Tomlinson, PhD

Copyright

Abstract

The Intergovernmental Panel on Climate Change (IPCC) approximates the global warming potential of N_2O at 300 times that of carbon dioxide. More than one third of all N_2O emissions are anthropogenic and are primarily due to agriculture. This study aims to compare N_2O emissions from sorghum fields under varying precipitation regimes and fertilizer management, to assess whether the IPCC default emissions factor of 1% overestimates these emissions and to evaluate how disaggregating this factor based on environmental and management factors could improve its accuracy. Field trials were conducted over six site years with a range of annual precipitation (350 mm -700 mm). All analyses evaluated six nitrogen application rates of streamed UAN (including a no nitrogen control), along with three additional product & placement combinations, evaluated both at planting and one month prior to planting. N_2O fluxes were measured using an N_2O / H_2O trace gas flux analyzer (Model 7820, LI-COR) and a portable automated chamber system (Model 8200-01, LI-COR). Data collected from chambers were processed using Soil Flux Pro software (Version 5.3.1, LI-COR). Nitrous oxide (N_2O) emissions have high spatial and temporal variability across the landscape, and agricultural management can introduce additional spatial variability, making quantification even more difficult. In addition to the main analysis of N_2O emissions, this study also focused on the methods used to collect N_2O flux estimates by evaluating sampling time and chamber placement.

A study was conducted to identify the optimum sampling duration for different time intervals: 180 seconds, 120 seconds (recommended by the manufacturer), and 90 seconds, to identify an optimum sampling time and minimize time spent obtaining N_2O measurements while maintaining data quality. Chamber fluxes were analyzed using SAS Version 9.4 using PROC REG procedure. Regression analysis with all sites combined resulted in high r^2 ($r^2 > 0.97$) in each

comparison group. However, with all sites combined, all slope values were different from one ($p < 0.0019$). Under the assumption that the longer duration is most reliable, the low RMSE values indicated that samples can be collected at the shorter sampling duration of 120-seconds without compromising data quality. The manufacturer's recommended sampling duration of 120-seconds is likely a reliable balance between data quality and labor required for measurements.

The analysis of chamber placement's impact N_2O flux in banded (38 cm centers) and non-banded nitrogen fertilizer treatments was conducted by collecting N_2O flux from two chambers in each plot, one adjacent to the row and over the fertilizer band (on-band), and one centered in the inter-row area between the fertilizer bands (inter-row). In non-banded treatments, two chambers were placed in the same positions. Data were evaluated in two subsets, rate treatments and placement treatments. Statistical analysis was conducted using SAS Version 9.4. PROC MIXED procedures. When evaluating rate treatments, there was an interaction between chamber position and nitrogen fertilizer rate ($p = 0.0043$). At high rates (>100.8 kg ha^{-1}), the on-band chambers had higher flux values than the inter-row treatments ($p < 0.05$). On sampling days with high N_2O flux levels, differences between the two chamber placements were the largest. Since these two chamber placements had significant differences from one another, plots missing on-band chambers should be omitted from daily flux calculations to avoid underestimating or overestimating flux. Across all fertilizer placement treatments (broadcast urea with urease inhibitor – NBPT (N-(n-butyl) thiophosphoric triamide), streamed UAN, coultered UAN, and no nitrogen control) and at all sites, the interaction between fertilizer placement and chamber position was not significant at $\alpha = 0.05$ but was significant at $\alpha = 0.1$. Streamed UAN placements applied in a band at both application timings did show differences between flux values in the inter-row and on-band chambers ($p = 0.0768$). There was no statistical difference between the on-band and inter-row chambers in the broadcast urea with urease inhibitor - NBPT and no nitrogen control treatments. However, the mean flux for the on-band chamber overall was 0.45 nmol N_2O m^{-2} s^{-1} and the mean flux for the inter-row chamber overall was 0.29 nmol N_2O m^{-2} s^{-1} indicating a strong overriding influence of chamber position ($p = 0.0001$). Given the variability of collected results, plots with banded fertilizer application where either the on-band or inter-row chamber had missing data, should be omitted from analysis because of the potential of influence from the high concentration of fertilizer in one area. Chamber position as a main effect was highly significant when all sites were evaluated, meaning that regardless of fertilizer rate or placement relative to the chamber, there is enough inherent spatial variability that plots missing one of the two chambers should be omitted from the dataset.

Analysis of cumulative N_2O emissions data show an influence of nitrogen application rate on cumulative N_2O flux at all evaluated site years ($p < 0.0001$). Increasing nitrogen fertilizer application rates resulted in higher cumulative N_2O emissions ($p < 0.05$). Overall, nitrogen fertilizer applied one month prior to planting did not show any differences between nitrogen fertilizer application methods. Sorghum grown in dryer environments generally did result in lower cumulative N_2O emissions compared to sorghum grown in wetter environments with similar nitrogen treatments. N_2O emissions from grain sorghum did not always peak within the first two weeks following nitrogen application, but a peak was observed within the first month following nitrogen application, typically following a rainfall event. Overall, increasing nitrogen rate did not result in increased N_2O emission factors and subsurface placement with a coulter or addition of a urease inhibitor did not clearly reflect a reduction in emissions factors in evaluated environments. The EF values calculated, specifically those from the more characteristic rainfall year, 2025, are largely in-line with IPCC’s disaggregated EF value for arid and semiarid environments of 0.5 percent (IPCC, 2019).

Table of Contents

List of Equations

List of Figures

List of Tables

Acknowledgements

I would like to thank my advisor, Dr. Peter Tomlinson, for his mentorship, guidance, and encouragement. My sincere appreciation goes out to my committee members, Drs. Lucas Haag, Eduardo Santos, and Dorivar Ruiz Diaz, for their commitment to this project and my development through the program. I am also appreciative of the funding sources that made this research possible, including United States Sorghum Checkoff Program, FFAR AgMission Initiative, and the Kansas Fertilizer Fund.

To my best friend and fellow graduate student, Molly Kane, thank you for making every day feel like a new adventure. I am forever grateful to have shared this part of my life with you, thank you for being yourself and bringing the happiest energy to my world each day.

As a part of the Environmental Quality Lab, it has been a privilege to learn from those who came before and mentor those who have come after me. Kathy, Oscar, Taylor, Heston, Grace, Sydney, Bethany, Quinten, and Nathan, thank you for being a part of this project and making my time here wonderful.

As always, I am blessed to be surrounded by the most supportive and loving family including my husband, Landon Trout, my parents, Eric and Jackie Chandler, and my sisters, Maggie and Jerica. Thank you for seeing me through this degree and for supporting me every single day.

Dedication

This thesis is dedicated to my most supportive, kind, and genuine friends who have loved me through this phase of life.

Chapter 1 - Literature Review

Grain Sorghum Production

Grain sorghum is native to Northeastern Africa and is estimated to have been domesticated between 3000 B.C. and 4000 B.C. (Winchell et al., 2017; Venkateswaran et al., 2019). Since this domestication, grain sorghum has been an important crop across cultures in semiarid regions around the world (Rooney, 2016). It is believed sorghum spread to India from Northeastern Africa around 1700 B.C. and from there spread across the Asian continent (Venkateswaran et al., 2019). In 1757 A.D., Benjamin Franklin documented sorghum growing in the United States (Venkateswaran et al., 2019). Following this introduction, sorghum was brought to Central and South America in the 1800s (Venkateswaran et al., 2019). Modern hybrid grain sorghum was developed in 1956 and was widely adopted in the first five years of availability to the market (Rooney, 2016). Since its introduction, sorghum has become an important crop around the world.

Sorghum is well known for heat and drought tolerance and is therefore grown in semiarid, subtropical, and tropical climates around the globe (Rooney, 2016). It is the world's fifth most prevalent cereal grain after wheat, corn, rice, and barley (Taylor, 2003). A significant portion of global grain sorghum production occurs in the United States, Nigeria, Brazil, Sudan, Mexico, India, Ethiopia, Argentina, China, and Australia (United States Department of Agriculture, 2024). In 2024, the United States represented 15% of global grain sorghum production, with 55% of that production being in Kansas (United States Department of Agriculture, 2024).

Grain sorghum has various uses which are largely dependent on the production regions. In the United States and Australia, sorghum grain is primarily used in animal feed (Rooney, 2016). Sorghum can contribute to animal feed rations for poultry, beef, dairy, swine, and pets (Sorghum Checkoff; Zhao and Dahlberg, 2019). In Africa, Asia, and Central America, sorghum grain is prevalent as a food crop for human consumption (Hadebe et al., 2016; Taylor, 2003; Venkateswaran et al., 2019). In addition, sorghum is gluten free and non-GMO, which is filling a niche in food markets in the United States and around the globe (Sorghum Checkoff). Aside from its use in food, sorghum is becoming an important crop for fuel production. In the United States, sorghum is used as a starch source for ethanol production (Rooney, 2016; Rooney et al., 2007). In fact, one third of sorghum in the United States is used for renewable fuel production (Sorghum Checkoff). Ethanol made from grain sorghum qualifies as a renewable fuel under the Renewable Fuel Standard Program because it achieves at least a 20% reduction in emissions compared to the baseline petroleum fuel it would replace (US Environmental Protection Agency, 2012). An average gallon of grain sorghum ethanol reduces greenhouse gas emissions by 32% compared to the petroleum fuel baseline (US Environmental Protection Agency, 2012). While corn is the most prevalent feedstock for ethanol production (US Department of Energy), sorghum produces the same amount of ethanol per bushel but uses one third less water (Sorghum Checkoff). This variety of uses makes sorghum an important crop in many different industries around the world.

Grain Sorghum is a warm season crop and requires temperatures of at least 15°C to initiate germination (Rooney, 2016). To accomplish this, grain sorghum crops in the United

States are typically planted in May or June and are harvested in September and October (Hawkins et al.). Final stands of 49,000 – 74,000 plants ha^{-1} typically result in yields of 3766 – 5021 kg ha^{-1} (Ciampitti and Carcedo, 2022). To achieve these yields, nutrient demands of the crop must be met. Nitrogen, phosphorus, and potassium are the main nutrients required for sorghum growth (Rooney, 2016). Of all required nutrients for grain sorghum growth, nitrogen is often the most limiting (Ciampitti et al., 2022).

In addition to nutrient challenges, drought and heat are significant stresses that can result in yield reduction in sorghum crops (Rooney, 2016). Grain sorghum requires 46-66 centimeters of water to produce a normal yield in areas of lower humidity (Ciampitti et al., 2022). Of this requirement, 15 centimeters of water are required to initiate the reproductive growth stages and grain yield, with yields increasing at 100 kg cm^{-1} of water use (Ciampitti et al., 2022). In general, sorghum is regarded as water efficient with a high water use efficiency compared to corn, miscanthus, and switchgrass, all common biofuel feedstocks in the United States (Oikawa et al., 2014). Compared with corn, grain sorghum uses 40-77 cm of water per season, while corn requires 50-80 cm of water per season (Ciampitti et al., 2023). Higher water use efficiency in grain sorghum (Ciampitti et al., 2022) is complemented by the drought tolerant traits of the crop.

Drought tolerance allows plants to maintain critical cellular and metabolic functions including osmotic adjustment, antioxidant capacity, and cell membrane stability while under a water deficit (Ciampitti and Prasad, 2020, pp. 241–273; Wagaw, 2019). Sorghum plants use a variety of traits to overcome drought (Ciampitti and Prasad, 2020, pp. 241–273). Stay green is a trait that allows sorghum plants to maintain higher levels of chlorophyll in their leaves during terminal drought stress conditions (Ciampitti and Prasad, 2020, pp. 241–273). Sorghum reduces transpiration through leaf rolling and stomatal closure (Wagaw, 2019) and lowers canopy temperatures to allow the plants to transpire less (Ciampitti and Prasad, 2020, pp. 241–273). Under extreme drought, sorghum plants can reduce metabolic processes to near dormancy (Wagaw, 2019). In addition to these traits, sorghum crops can also compensate for differences in stand by developing more heads per plant through tiller development (Ciampitti et al., 2022). Finally, sorghum has a sophisticated root structure that allows the crop to scavenge for water and nutrients like nitrogen (Wagaw, 2019; Zhao and Dahlberg, 2019). These traits help sorghum to overcome drought and create yield even when faced with adversity.

Nitrogen fertilizer is a significant input in grain sorghum production. Grain sorghum uses nitrogen for a variety of plant outcomes, many of which can be displayed by increasing nitrogen fertilizer application rates. Increased nitrogen application rates improved grain sorghum yields and plant height (Abunyewa et al., 2017; Vasilyevich Baranovsky et al., 2020). With increased application rates, sorghum plants tend to consume more nitrogen, causing nitrogen uptake and stem and leaf nitrogen concentrations to increase (Abunyewa et al., 2017; Muchow, 1998). Continuous application of nitrogen is necessary as approximately 50% of nitrogen taken up by the plant is removed with the grain (Espinoza and Kelley, n.d.). Nitrogen fertilizer recommendations range based on expected yield, residual nitrogen in the soil, soil organic matter, and grain price relative to the price of nitrogen fertilizer (Wortmann et al., 2013). Typically, grain sorghum removes 15 g of nitrogen per kg of grain (0.85 pounds of nitrogen per bushel) (Ciampitti et al., 2022). Thus, nitrogen application recommendations for producers range from 112-134 kg ha^{-1} (100-120 pounds $acre^{-1}$) (Espinoza and Kelley, n.d.). Nitrogen fertilizer recommendations can change significantly based on the assumed nitrogen use efficiency.

The nitrogen use efficiency of a cropping system is the proportion of all nitrogen inputs that are retained in harvested crop biomass, contained in crop residues, incorporated into the soil organic matter, and remain in inorganic nitrogen pools in the soil (Cassman et al., 2002). Crop, environmental, and management factors affect nitrogen use efficiency (Haroon et al., 2019). Nitrogen use efficiency can be improved by achieving greater uptake efficiency or by reducing the nitrogen lost from the soil (Cassman et al., 2002). Most crops have a nitrogen use efficiency of 30-50% (Haroon et al., 2019). Grain sorghum tends to have higher nitrogen use efficiency due to root scavenging and production systems that allow for greater nitrogen accumulation in the soil (Zhao and Dahlberg, 2019). In sorghum studies, increasing nitrogen application rates decreased nitrogen use efficiency, with efficiencies as high as 50% in low application rates and as low as 5% in high application rates (Abunyewa et al., 2017; Buah et al., 1998; Rowlings et al., 2022). Environmental factors like rainfall can also have a significant impact on nitrogen use efficiency by driving nitrogen losses. In some cases, rainfall can have a larger impact on nitrogen losses than application rates (Rowlings et al., 2022). However, plant growth limited by moisture can cause nitrogen use efficiency to decline due to decreased plant uptake (Muchow, 1998). All these factors contribute to the variability of nitrogen use efficiency in grain sorghum cropping systems.

Nitrous Oxide Emissions and Agricultural Production

Greenhouse gases are gases that can originate from both natural and anthropogenic sources and absorb and emit radiation at specific wavelengths which result in the greenhouse effect (IPCC, 2012). Water vapor (H_2O), carbon dioxide (CO_2), nitrous oxide (N_2O), methane (CH_4), and ozone (O_3) are the primary greenhouse gases in the Earth's atmosphere (IPCC, 2012). As concentrations of greenhouse gases increase from anthropogenic sources, Earth's temperature is increasing above past levels (US Environmental Protection Agency, 2024). Changes in atmospheric concentrations of CO_2, CH_4, N_2O, and halocarbons from 1750-2011 have contributed to warming of the Earth's atmosphere (IPCC, 2021). The Intergovernmental Panel on Climate Change (IPCC) has put forward the recommendation that rapid reductions in anthropogenic greenhouse gas emissions that restrict warming to "well-below" 2°C would greatly reduce the negative impacts on land ecosystems (Arneth et al., 2019).

Greenhouse gases originate from a variety of sources, both natural and anthropogenic. Natural greenhouse effect drivers include natural sources and sinks of water vapor, CO_2, CH_4, and SO_2 (IPCC, 2021). Anthropogenic sources like energy, waste, and agriculture also contribute to greenhouse gas emissions. Fossil fuel combustion is a major emitter of CO_2 (IPCC, 2021). Methane emissions are the result of fossil fuel extraction, natural gas pipeline leaks, agriculture, and landfills (IPCC, 2021). Agriculture contributions include emission of methane, carbon dioxide, and nitrous oxide (Adegbeye et al., 2020; IPCC 2007). However, agriculture has unique opportunities to offset emissions of these greenhouse gases.

The greenhouse gas N_2O contributes to ozone depletion and requires 114 years to decay in the atmosphere, compared to methane's 12 years (IPCC, 2007; Ravishankara et al., 2009).

Over a 100-year timeline, N_2O has a global warming potential that is approximately 300 times that of carbon dioxide (IPCC, 2007; US Environmental Protection Agency, 2024). More than one third of all N_2O emissions are anthropogenic and are primarily due to agriculture (IPCC, 2007). N_2O emissions have increased over time. The global atmospheric N_2O concentration has increased from a pre-industrial level of approximately 270 ppb to 319 ppb in 2005 (IPCC, 2007). In 2019, the concentration of N_2O in the atmosphere reached 332 ppb (IPCC, 2021). This increase in N_2O concentration is largely attributed to the increased use of nitrogen fertilizers and manure in land-based agriculture (IPCC, 2021; Tian et al., 2020). Increased nitrogen fertilizer use accounted for 64% of the agricultural soil N_2O emissions increase since 1900 (Lu et al., 2022). Nitrous oxide is primarily derived from two parts of the global nitrogen cycle, nitrification, and denitrification (Gruber and Galloway, 2008).

First, denitrification is the anaerobic microbial reduction of nitrate (NO_3^-) to nitrite (NO_2^-) and then to gases NO, N_2O, and N_2 (Smith et al., 2000). At high levels of soil moisture, NO_3^- denitrifies all the way to N_2 (Butterbach-Bahl et al., 2013). The incomplete denitrification process results in emission of N_2O (Barton et al., 2007). Denitrification becomes the main pathway of N_2O emission in high moisture conditions (Rudaz et al., 1990; Wang et al., 2023). The potential for denitrification losses of nitrogen as N_2O is high, particularly if high intensity rainfall occurs early in the growing season (Schwenke and Haigh, 2016).

Second, nitrification is the aerobic microbial oxidation of ammonium ions to nitrite via NH_2OH and then to nitrate (Smith et al., 2000). This process is completed in two steps. First, autotrophic nitrifiers use CO_2 as a carbon source and oxidize NH_4^+ for energy, transforming

NH_4^+ to NO_2^- (Granli and Bøckman, 1994). Second, NO_2^- is further oxidized to NO_3^- (Granli and Bøckman, 1994). This process can create N_2O when ammonium oxidizers use NO_2^- as an alternate electron acceptor when oxygen is limiting, thereby creating N_2O and causing natural N_2O emissions (Granli and Bøckman, 1994). Nitrification is the main N_2O producing pathway in low moisture conditions (Wang et al., 2023).

Approximately 20% of the world's human population lives in semiarid and arid regions (Galbally et al., 2008). These drier climates can have different impacts on N_2O emissions than temperate climates. Since grain sorghum is commonly grown in semiarid and arid regions, these impacts on N_2O emissions are relevant to grain sorghum cropping systems. In grain sorghum experiments, dry weather resulted in lower N_2O emissions and fewer detectable fluxes (Barton et al., 2007; Storlien et al., 2013). However, in hot and dry climates, soil moistened through rainfall and irrigation results in more rapid and intense production of N_2O than is observed in a temperate agricultural system (Galbally et al., 2008). Rainfall and irrigation can have a variety of impacts on N_2O emission in agriculture. Daily N_2O emissions are best correlated with precipitation and water filled pore space (Barton et al., 2007; Malhi and Lemke, 2007).

N_2O production in all soils increases with increasing soil moisture, with little N_2O emitted from dry soils (Barton et al., 2007; Pihlatie et al., 2004; Storlien et al., 2014; Storlien et al., 2013). Rainfall or irrigation events can cause small, short-term peaks of N_2O emissions (Barton et al., 2007; Xiao-Tang and Zhang, 2017; Rudaz et al., 1990; Storlien et al., 2014). These peaks, or pulses, after rainfall are common and driven by denitrification (Aguilera et al., 2013). As a result, frequent wetting and drying cycles of the soil can cause increased annual N_2O

emissions (Liu et al., 2018; Storlien et al., 2014). High N_2O emissions were observed in the first wetting event after a drought (Kitzler et al., 2006; Liu et al., 2018). In addition to rainfall, water-filled pore space in the soil can significantly impact N_2O emissions.

Multiple studies report water filled pore space (WFPS) as a strongly connected variable with N_2O fluxes (Corre et al., 1999; Linn and Doran, 1984). Most N_2O emissions occurred when WFPS was high, above 60-70% (Barrat et al., 2020; Xiao-Tang and Zhang, 2017). Denitrification is the main N_2O producing pathway in conditions above 60-70% WFPS (Wang et al., 2023). At low WFPS levels, less than 50%, low N_2O emissions were observed (Xiao-Tang and Zhang, 2017). N_2O emissions observed when WFPS is lower, are hypothesized to be from the nitrification process (Storlien et al., 2013). Beyond moisture impacts, nitrogen fertilizer management can have major impacts on N_2O emissions.

In addition to precipitation and irrigation, fertilization events can result in high fluxes of N_2O (Storlien et al., 2014). Fertilizer timing, placement, rate, and source can all impact N_2O emissions within a cropping system. N_2O emissions can occur at various times during the growing season. Across multiple studies, N_2O emissions peaked within two weeks following fertilization (Barton et al., 2007; Gehl et al., 2020; Storlien et al., 2014). Fertilizer timing during the growing season can impact N_2O emissions from the crop. In two sorghum studies, N_2O flux was lower in plots receiving split application of nitrogen fertilizer than plots receiving all nitrogen fertilizer at planting (Duval et al., 2022; Schwenke and Haigh, 2019). In one of these studies, this split application reduced the proportion of nitrogen emitted as N_2O by 59% while maintaining nitrogen uptake and grain yield (Schwenke and Haigh, 2019). However, in a corn study, higher levels of N_2O emissions were observed from in-season applications of nitrogen fertilizer compared to preplant applications (Ma et al., 2009).

Fertilizer placement and rate can have significant impacts on N_2O emissions. Consistently, deeper placement on nitrogen fertilizer within the soil results in lower N_2O emissions in sorghum systems (Fertitta-Roberts et al., 2017; Van Kessel et al., 2012). Shallow and surface placement result in higher N_2O emissions across multiple studies (Fertitta-Roberts et al., 2017; Halvorson and Del Grosso, 2013; Rychel et al., 2020). Higher rates of nitrogen fertilizer application have increased N_2O emissions across many studies and cropping systems (Malhi and Lemke, 2007; Preza-Fontes et al., 2020; Schwenke and Haigh, 2016). When nitrogen fertilizer is applied in excess of crop requirement, the proportion of nitrogen lost as N_2O emissions increases substantially (Malhi and Lemke, 2007; Preza-Fontes et al., 2020). Conversely, increased fertilizer rates did not increase N_2O emissions according to Barton et al. (2007) and Gehl et al. (2020). In addition to fertilizer rate, soil nitrogen concentration has had differing effects on N_2O emission. In many cases, soil NO_2^- and NO_3^- concentrations were correlated with N_2O emission rates (Butterbach-Bahl et al., 2013; Chantigny et al., 2010; Liu et al., 2018; Zebarth et al., 2008). However, in other systems no relationship was established between N_2O emissions and soil mineral nitrogen concentrations (Corre et al., 1999; Linn and Doran, 1984).

Use of different nitrogen fertilizer products can impact N_2O emissions from the crop. Enhanced efficiency fertilizers with nitrification inhibitors or urease inhibitors can have varying effects on N_2O emissions. Enhanced efficiency fertilizers were found to reduce N_2O emissions under a wide range of conditions (Maaz et al., 2021). When used together in one product, nitrification and urease inhibited urea resulted in significantly lower emissions when compared with traditional urea (Halvorson and Del Grosso, 2013). However, urease inhibitors and slow-release urea have not been shown to reduce N_2O emissions on their own (Wood et al., 2023).

Nitrous Oxide Emission Estimation

There are three well-established methods of estimating soil N_2O flux emissions, which include eddy covariance, static chamber, and automated chamber (Tallec et al., 2019). Automated soil gas flux systems offer a new automated chamber technology that allows users to collect low concentration soil flux data both quickly and accurately. These systems use optical feedback cavity enhanced absorption spectroscopy to collect measurements of soil gas flux, in this case N_2O, at a rate of one sample per second (LICOR Environmental, 2024). The system's settings are customizable, allowing users to configure the system to best suit their specific research needs. Even with the use of this system, customization and appropriate use are necessary to best capture data that is representative of the evaluated system. Manufacturer's literature recommends observation times of 90 to 180 seconds for sampling N_2O fluxes (LICOR Environmental, 2024b). Observation time is important for maintaining consistent environmental conditions and limiting the effect of altered diffusion (LICOR Environmental, 2024b).

Spatial variability, both expected and unexpected, can have an influence on N_2O flux estimation. When this variability is expected, experimental design can be adjusted to best capture representative data. Nitrification and denitrification are processes that are driven by microbial activity and soil properties, which in turn influence N_2O emissions. Landscape position, inorganic nitrogen concentration, and total organic carbon can influence the spatial variability of denitrification across a landscape (Johnson et al., 2022). When large spatial variability is expected to exist, experiment structure, chamber number, and chamber placement may need to be adjusted to reduce variability (Chadwick et al., 2014). In row crop experiments evaluated with static chambers, variability from applied fertilizer between rows is best captured using rectangular chambers that cover the entire row area (Clough et al., 2020). However, with the use of automated chambers, chamber dimensions are limited by the size and shape of available instrumentation, most of which are small, round chambers. Static chamber guidance literature suggests the avoidance of round chambers for N_2O flux estimation in row crop experiments, which creates a conflict for users in this context (Clough et al., 2020). The limitations of such systems make it difficult to adjust chamber size to cover a large, representative row area, since the volume and area are fixed in these systems. Multiple experiments using the static chamber method across environments report significant influence of chamber placement on N_2O emission estimation when using a static chamber method (Cai et al., 2012; Chadwick et al., 2014; Liu et al., 2023). Additionally, fertilizer application method had a significant influence on the impact chamber placement made on N_2O emission estimation using the static chamber method (Liu et al., 2023). Literature does not yet describe the influence of chamber placement on estimation of N_2O emissions when using an automated chamber system.

Carbon Intensity and Grain Sorghum

Biofuels are liquid fuels produced from renewable biological sources (Department of Energy, 2024). Currently available biofuels are made from sugar crops (sugarcane, sugarbeet); starch crops (corn, sorghum, potatoes); oilseed crops (soybean, sunflower, rapeseed); and animal fats (US Environmental Protection Agency, 2021). Ethanol is a renewable fuel that can be made from various plant materials, collectively known as biomass (Office of Energy Efficiency & Renewable Energy, 2024). In the United States, most ethanol is made from plant starches and sugars – particularly corn starch (Wang et al., 2008). Grain sorghum is a viable feedstock for ethanol and has similar ethanol yield compared to ethanol from corn grain (Wang et al., 2008). Sorghum is more tolerant to water stress than corn and is often grown in drier regions, which can reduce the water footprint of the crop, and, in turn, the fuel made from it (Wang et al., 2008).

Biofuel production and consumption in the United States have increased linearly since the early 1980s (U.S. Energy Information Administration, 2022). Replacing fossil fuels with biofuels has the potential to reduce some undesirable environmental impacts of fossil fuel production and use, including conventional and greenhouse gas pollutant emissions, resource depletion, and dependence on unstable foreign suppliers (US Environmental Protection Agency, 2021). Two prominent government programs, the federal Renewable Fuel Standard (RFS) program, and California's Low Carbon Fuel Standard (LCFS), have contributed to increased US biofuel production and consumption over the past 15 years (U.S. Energy Information Administration, 2022). The RFS program under the Clean Air Act was created under the Energy Policy Act of 2005 (US Environmental Protection Agency, 2015). Renewable Fuel Standard is a national policy that requires a certain volume of renewable fuel to be used to replace or reduce the quantity of fossil fuel in transportation fuel, home heating oil, or jet fuel (US Environmental

Protection Agency, 2015). Renewable fuels under the RFS program must have a certain reduction in greenhouse gas emissions as compared to a 2005 petroleum baseline (US Environmental Protection Agency, 2015).

Ethanol is the most widely used biofuel (US Environmental Protection Agency, 2021). A major driver of increased ethanol demand has been the value of ethanol as an oxygenate, replacing methyl tert-butyl ether in gasoline (Wang et al., 2008). While the most common blend of ethanol in gasoline is E10 (10% ethanol by volume), most vehicles built after 2000 can use gasoline ethanol blends containing up to 15% ethanol by volume (Office of Energy Efficiency & Renewable Energy, 2024; US Environmental Protection Agency, 2021). Some vehicles are even designed to run on E85, a gasoline ethanol blend that can range from 51-83% ethanol by volume (Office of Energy Efficiency & Renewable Energy, 2024). These advances in biofuel technology have improved the total greenhouse gas emissions from the transportation sector and will continue to develop over time.

The Low Carbon Fuel Standard was originally adopted in 2009 with the goal of reducing the carbon intensity (CI) of transportation fuel by at least 20% by 2030 and is overseen by the California Air Resources Board (CARB) (California Air Resources Board, 2007). The Low Carbon Fuel Standard requires fuel producers to reduce the carbon intensity of fuels sold in California and encourages the production of renewable alternatives (California Air Resources Board, 2023). The program requires higher carbon fuel producers to buy credits from companies that sell cleaner fuels to meet mandated targets (California Air Resources Board, 2023). Low Carbon Fuel Standard sets annual carbon intensity targets, which reduce over time for gasoline, diesel, and fuels that replace them (California Air Resources Board, 2007). In addition to California, other states have adopted variations of the LCFS program. The Pacific Coast Collaborative is a regional agreement between California, Oregon, Washington, and British Columbia to align policies, reduce greenhouse gases, and promote clean energy (California Air Resources Board). Over time, these LCFS programs will build an integrated West Coast market for low-carbon fuels that will create greater market pull, increased confidence for investors of low-carbon alternative fuels, and improved enforcement programs (California Air Resources Board).

All transportation fuels need a carbon intensity score to participate in LCFS (California Air Resources Board, 2007). A fuel pathway carbon intensity score consists of the sum of the greenhouse gases emitted throughout each stage of a fuel's production and use (California Air Resources Board, 2024). Carbon intensity, sometimes referred to as a carbon intensity score or CI score, is a form of complete life cycle analysis that considers all the steps of production, transportation, and consumption of a fuel (California Air Resources Board, 2007). Carbon intensity is measured in grams of CO_2-e, defined as an amount of greenhouse gas adjusted for its global warming potential, per megajoule of energy (California Air Resources Board, 2007). Carbon intensity scores include the direct effects of producing and using this fuel and indirect effects associated with how it affects other products and markets (California Air Resources Board, 2024).

Carbon intensity for crop-based biofuels is calculated with the California Greenhouse Gases, Regulated Emissions and Energy Use in Transportation (CA-GREET) model (California

Air Resources Board, 2007). The Low Carbon Fuel Standard does allow individual biofuel conversion facilities to submit custom CIs with their own data (Liu et al., 2020b). There are three different ways that carbon intensity can be certified by CARB. First, and most simply, lookup tables have CI scores that are predetermined based on fuel types and industry averages (California Air Resources Board, 2007). Second, tier 1 applications use a simplified CI calculation that determines site-specific fuel production and transportation emissions (California Air Resources Board, 2007). Finally, tier 2 applications are designed for innovative next generation pathways with unique feedstocks or carbon sequestration (California Air Resources Board, 2007). Tier 2 applications involve a fully customizable California GREET model to determine site-specific CI scores (California Air Resources Board, 2007).

With annually declining CI score targets, there is a strong incentive for innovation within the LCFS program. The LCFS structure creates a strong incentive to deploy only the lowest carbon fuels to California and to continually innovate to reduce the carbon intensity of existing fuels (California Air Resources Board, 2023). While the entire fuel supply chain considers items like feedstock conversion, fuel transportation and distribution, and fuel combustion when calculating a life cycle analysis for biofuels, improvements can be made at the farm level to improve the feedstock carbon intensity (Liu et al., 2020b). Key parameters affecting biofuel feedstock CI include yield, fertilizers/chemical application rates, and agronomic practices (Liu, 2021). Adopting conservation tillage, reducing nitrogen fertilizer use, and implementing cover crops can reduce greenhouse gas emissions per unit of corn produced compared to a baseline corn-soybean rotation (Liu et al., 2020a). Nitrogen fertilizer has been shown to have major impacts on greenhouse gas emissions and, in turn, CI scores. Argonne National Laboratory’s

Feedstock Carbon Intensity Calculator is integrated into the GREET model which analyzes improvements made at the farm level and provides farm gate CI estimates, which can be used to assess lifecycle emissions and compare practice change outcomes (Liu et al., 2020b).

Reducing nitrogen fertilizer inputs while maintaining yield is a highly effective way to reduce the cradle to farm gate greenhouse gas emissions (Liu et al., 2020a). Fertilizer application rate, application method, and source all contribute to emission intensities (Fertitta-Roberts et al., 2017). Nitrogen fertilizer type and rate applied were identified as factors contributing most to CI variations at the farm level in corn for ethanol (Liu, 2021). N_2O emissions were by far the largest contributor to overall life cycle greenhouse gas emissions, frequently accounting for more than half of total emissions (Liu et al., 2020a; Storlien et al., 2013). Efficient use of nitrogen is an important pathway for minimizing life cycle emissions on an energy yield basis (Fertitta-Roberts et al., 2017). High rates of nitrogen fertilizer can support low greenhouse gas intensities and pollutant loads from cellulosic fuels on an energy yield basis if there is sufficient yield response (Fertitta-Roberts et al., 2017). Using nitrogen efficiently in the cropping system is an important part of improving the carbon intensity score of a feedstock.

The proportion of nitrogen lost from the system is most important in determining life cycle greenhouse gas emissions. The percentage of added nitrogen fertilizer lost to the atmosphere as N_2O-N is considered a nitrogen emissions factor by the Intergovernmental Panel on Climate Change (IPCC) (Schwenke et al., 2015; Storlien et al., 2013). Emissions factors for N_2O emissions from nitrogen inputs are measured as kg of N_2O-N per kg of nitrogen input (IPCC, 2006). Emission factors have been found to significantly vary due to nitrogen source, nitrogen application rate, type of crop, and climate regime (Storlien et al., 2013). The default IPCC emissions factor for N_2O emissions from managed soils receiving nitrogen addition as mineral fertilizers, organic amendments and crop residues is 1% (IPCC, 2006). This emissions factor (EF) was set at 1.25% in 1999 and was later lowered to 1% in 2006 and remains at 1% following the 2019 revision with exceptions (IPCC, 2019; IPCC, 2006; Smith et al., 2000). One such exception allows for the disaggregation of emission factors by climatic zones (IPCC, 2019). In dry climates, the default EF value has been adjusted to 0.5% for both organic and synthetic nitrogen inputs, as well as crop residues (IPCC, 2019). Dry climates are defined by the IPCC as temperate areas where the ratio of annual precipitation: potential evapotranspiration is less than 1 (IPCC, 2019). Since grain sorghum has strong drought tolerance and is commonly grown in dry climates, its expanded use in biofuels depends on further research in this area (Rooney, 2016).

Research Hypotheses & Objectives

The objectives of this study were (i) determine the optimal observation time for collecting N_2O flux data using a trace gas analyzer system across different environments; (ii) assess how chamber placement relative to grain sorghum crop rows and nitrogen application bands influences cumulative N_2O emission measurements; (iii) quantify N_2O emissions during a grain sorghum growing season across a rainfall gradient under various nitrogen management practices. The hypotheses were: (i) data collected using the 180-second sampling duration would be more stable, while 90 and 120-second sampling duration would underestimate fluxes compared to the longest duration and likely have more variability; (ii) chamber position significantly impacts N_2O emissions in streamed treatments, and influence increases at higher nitrogen application rates; (iii) chamber position does not have a significant impact on non-streamed treatments; (iv) sorghum grown in dryer environments with similar nitrogen treatments will exhibit lower N_2O emissions throughout the growing season compared to sorghum grown in wetter environments; (v) N_2O emissions from sorghum crops will peak in the first two weeks following nitrogen application; (vi) nitrogen management practices involving lower application rates, the use of urease inhibitors, and deeper placement will result in reduced N_2O emissions over the growing season.

References

Abunyewa, A.A., R.B. Ferguson, C.S. Wortmann, and S.C. Mason. 2017. Grain Sorghum Nitrogen Use as Affected by Planting Practice and Nitrogen Rate. Journal of Soil Science and Plant Nutrition 17(1). doi: https://doi.org/10.4067/s0718-95162017005000012.

Adegbeye, M.J., P. Ravi Kanth Reddy, A.I. Obaisi, M.M.M.Y. Elghandour, K.J. Oyebamiji, et al. 2020. Sustainable agriculture options for production, greenhouse gasses and pollution alleviation, and nutrient recycling in emerging and transitional nations - An overview. Journal of Cleaner Production 242: 118319. doi: https://doi.org/10.1016/j.jclepro.2019.118319.

Aguilera, E., L. Lassaletta, A. Sanz-Cobena, J. Garnier, and A. Vallejo. 2013. The Potential of Organic Fertilizers and Water Management to Reduce N_2O Emissions in Mediterranean Climate Cropping systems. A Review. Agriculture, Ecosystems & Environment 164: 32–52. doi: https://doi.org/10.1016/j.agee.2012.09.006.

Barrat, H.A., J. Evans, D.R. Chadwick, I.M. Clark, K. Le Cocq, et al. 2020. The Impact of Drought and Rewetting on N_2O Emissions from Soil in Temperate and Mediterranean Climates. European Journal of Soil Science 72(6): 2504–2516. doi: https://doi.org/10.1111/ejss.13015.

Barton, L., R. Kiese, D. Gatter, K. Butterbach-Bahl, R. Buck, et al. 2007. Nitrous Oxide Emissions from a Cropped Soil in a Semi-arid Climate. Global Change Biology 14(1): 177–192. doi: https://doi.org/10.1111/j.1365-2486.2007.01474.x.

Buah, S.S.J., J.W. Maranville, A. Traore, and P.J. BrameI-Cox. 1998. Response of nitrogen use efficient sorghums to nitrogen fertilizer. Journal of Plant Nutrition 21(11). doi: https://doi.org/10.1080/01904169809365564.

Butterbach-Bahl, K., E.M. Baggs, M. Dannenmann, R. Kiese, and S. Zechmeister-Boltenstern. 2013. Nitrous Oxide Emissions from soils: How Well Do We Understand the Processes and Their controls? Philosophical Transactions of the Royal Society B: Biological Sciences 368(1621): 20130122. doi: https://doi.org/10.1098/rstb.2013.0122.

Cai, Y., W. Ding, and J. Luo. 2012. Spatial variation of nitrous oxide emission between interrow soil and interrow plus row soil in a long-term maize cultivated sandy loam soil. Geoderma 181-182: 2–10. doi: https://doi.org/10.1016/j.geoderma.2012.03.005.

California Air Resources Board. 2007. Low Carbon Fuel Standard Basics. California Air Resources Board. https://ww2.arb.ca.gov/sites/default/files/2020-09/basics-notes.pdf.

California Air Resources Board. 2023. FAQ: The Standardized Regulatory Impact Assessment for the Low Carbon Fuel Standard | California Air Resources Board. ww2.arb.ca.gov. https://ww2.arb.ca.gov/resources/documents/faq-standardized-regulatory-impact-assessment-low-carbon-fuel-standard.

California Air Resources Board. 2024. Apply for an LCFS Fuel Pathway | California Air Resources Board. Ca.gov. https://ww2.arb.ca.gov/resources/documents/apply-lcfs-fuel-pathway (accessed 13 August 2024).

California Air Resources Board. Low Carbon Fuel Standard - About. ww2.arb.ca.gov. https://ww2.arb.ca.gov/our-work/programs/low-carbon-fuel-standard/about.

Cassman, K.G., A. Dobermann, and D.T. Walters. 2002. Agroecosystems, Nitrogen-use Efficiency, and Nitrogen Management. AMBIO: A Journal of the Human Environment 31(2): 132–140. doi: https://doi.org/10.1579/0044-7447-31.2.132.

Chadwick, D.R., L. Cardenas, T.H. Misselbrook, K.A. Smith, R.M. Rees, et al. 2014. Optimizing chamber methods for measuring nitrous oxide emissions from plot-based agricultural experiments. European Journal of Soil Science 65(2): 295–307. doi: https://doi.org/10.1111/ejss.12117.

Chantigny, M.H., P. Rochette, D.A. Angers, S. Bittman, K. Buckley, et al. 2010. Soil Nitrous Oxide Emissions following Band-Incorporation of Fertilizer Nitrogen and Swine Manure. Journal of Environmental Quality 39(5): 1545–1553. doi: https://doi.org/10.2134/jeq2009.0482.

Ciampitti, I., and A. Carcedo. 2022. Agronomy eUpdate May 26th, 2022 : Issue 908. Ksu.edu. https://eupdate.agronomy.ksu.edu/article_new/sorghum-management-considerations-planting-practices-496 (accessed 12 August 2024).

Ciampitti, I., A. Carcedo, V. Gimenez, S. Lancaster, D. Ruiz Diaz, et al. 2023. Kansas Corn Management 2024. Kansas State University. https://bookstore.ksre.k-state.edu/download/kansas-corn-management-2024_MF3208.

Ciampitti, I., A. Carcedo, D. Ruiz Diaz, R. Onofre, S. Lancaster, et al. 2022. Kansas Sorghum Management 2022. Kansas State University Agricultural Experiment Station and Cooperative Extension Service. https://bookstore.ksre.ksu.edu/pubs/kansas-sorghum-management-2022_MF3046.pdf

Ciampitti, I.A., and V. Prasad. 2020. Sorghum. John Wiley & Sons.

Clough, T.J., P. Rochette, S.M. Thomas, M. Pihlatie, J.R. Christiansen, et al. 2020. Global Research Alliance N_2O chamber methodology guidelines: Design considerations. Journal of Environmental Quality 49(5): 1081–1091. doi: https://doi.org/10.1002/jeq2.20117.

Corre, M.D., D.J. Pennock, C. Van Kessel, and D. Kirkelliott. 1999. Estimation of Annual Nitrous Oxide Emissions from a Transitional grassland-forest Region in Saskatchewan, Canada. Biogeochemistry 44(1): 29–49. doi: https://doi.org/10.1007/bf00992997.

Department of Energy. 2024. DOE Explains...Biofuels. Energy.gov. https://www.energy.gov/science/doe-explainsbiofuels.

Duval, B.D., J. Martin, and M.A. Marsalis. 2022. The Effect of Variable Fertilizer and Irrigation Treatments on Greenhouse Gas Fluxes from Aridland Sorghum. Agronomy 12(12): 3109. doi: https://doi.org/10.3390/agronomy12123109.

Espinoza, L., and J. Kelley. Grain Sorghum Production Handbook. https://www.uaex.uada.edu/publications/pdf/mp297/MP297.pdf (Accessed 4/14/2026)

Fertitta-Roberts, C., S. Spatari, D.A. Grantz, and G.D. Jenerette. 2017. Trade-offs across productivity, GHG intensity, and Pollutant Loads from Second-generation Sorghum Bioenergy. GCB Bioenergy: 1764–1779. doi: https://doi.org/10.1111/gcbb.12471.

Galbally, I.E., W.V. Kirstine, C.P. (Mick) Meyer, and Y.P. Wang. 2008. Soil–Atmosphere Trace Gas Exchange in Semiarid and Arid Zones. Journal of Environmental Quality 37(2): 599–607. doi: https://doi.org/10.2134/jeq2006.0445.

Gehl, K.A., L. Haag, J. Warren, S. Sharma, and P.J. Tomlinson. 2020. Dryland Sorghum Nitrogen Management: Implications for Utilization as Ethanol Feedstock. Kansas Agricultural Experiment Station Research Reports 6(5). doi: https://doi.org/10.4148/2378-5977.7926.

Granli, T., and O. Bøckman. 1994. Nitrous Oxide from Agriculture. Norwegian Journal of Agricultural Sciences. https://agris.fao.org/search/en/providers/122535/records/65ddf8500f3e94b9e5c86f8d

Gruber, N., and J.N. Galloway. 2008. An Earth-system perspective of the global nitrogen cycle. Nature 451(7176): 293–296. doi: https://doi.org/10.1038/nature06592.

Hadebe, S.T., A.T. Modi, and T. Mabhaudhi. 2016. Drought Tolerance and Water Use of Cereal Crops: A Focus on Sorghum as a Food Security Crop in Sub-Saharan Africa. Journal of Agronomy and Crop Science 203(3): 177–191. doi: https://doi.org/10.1111/jac.12191.

Halvorson, A.D., and S.J. Del Grosso. 2013. Nitrogen Placement and Source Effects on Nitrous Oxide Emissions and Yields of Irrigated Corn. Journal of Environmental Quality 42(2): 312–322. doi: https://doi.org/10.2134/jeq2012.0315.

Haroon, M., F. Idrees, H.A. Naushahi, R. Afzal, M. Usman, et al. 2019. Nitrogen Use Efficiency: Farming Practices and Sustainability. Journal of Experimental Agriculture International 36(3): 1–11. doi: https://doi.org/10.9734/jeai/2019/v36i330235.

Hawkins, S., B. Massey, E. Williams, and M. Hodges. 2017. Grain Sorghum Production Calendar. Oklahoma Cooperative Extension Service - Oklahoma State University. https://extension.okstate.edu/fact-sheets/grain-sorghum-production-calendar

IPCC, 2006: 2006 IPCC Guidelines for National Greenhouse Gas Inventories, Prepared by the National Greenhouse Gas Inventories Programme [Eggleston H.S., Buendia L., Miwa K., Ngara T. and Tanabe K. (eds)]. IGES, Japan. https://www.ipcc-nggip.iges.or.jp/public/2006gl/

IPCC, 2007: Climate Change 2007: The Physical Science Basis. Contribution of Working Group I to the Fourth Assessment Report of the Intergovernmental Panel on Climate Change [Solomon, S., D. Qin, M. Manning, Z. Chen, M. Marquis, K.B. Averyt, M. Tignor and H.L. Miller (eds.)]. Cambridge University Press, Cambridge, United Kingdom and New York, NY, USA. https://www.ipcc.ch/site/assets/uploads/2020/02/ar4-wg1-sum_vol_en.pdf

IPCC, 2012: Glossary of terms. In: Managing the Risks of Extreme Events and Disasters to Advance Climate Change Adaptation [Field, C.B., V. Barros, T.F. Stocker, D. Qin, D.J. Dokken, K.L. Ebi, M.D. Mastrandrea, K.J. Mach, G.-K. Plattner, S.K. Allen, M. Tignor, and P.M. Midgley (eds.)]. A Special Report of Working Groups I and II of the Intergovernmental Panel on Climate Change (IPCC). Cambridge University Press, Cambridge, UK, and New York, NY, USA, pp. 555-564. https://archive.ipcc.ch/pdf/special-reports/srex/SREX-Annex_Glossary.pdf

IPCC, 2019: 2019 Refinement to the 2006 IPCC Guidelines for National Greenhouse Gas Inventories [Calvo Buendia, E., Tanabe, K., Kranjc, A., Baasansuren, J., Fukuda, M., Ngarize, S., Osako, A., Pyrozhenko, Y., Shermanau, P. and Federici, S. (eds)]. IPCC, Switzerland. https://www.ipcc.ch/report/2019-refinement-to-the-2006-ipcc-guidelines-for-national-greenhouse-gas-inventories/

IPCC, 2021: Climate Change 2021: The Physical Science Basis. Contribution of Working Group I to the Sixth Assessment Report of the Intergovernmental Panel on Climate Change [Masson-Delmotte, V., P. Zhai, A. Pirani, S.L. Connors, C. Péan, S. Berger, N. Caud, Y. Chen, L. Goldfarb, M.I. Gomis, M. Huang, K. Leitzell, E. Lonnoy, J.B.R. Matthews, T.K. Maycock, T. Waterfield, O. Yelekçi, R. Yu, and B. Zhou (eds.)]. Cambridge University Press, Cambridge, United Kingdom and New York, NY, USA, 2391 pp. doi:10.1017/9781009157896. https://www.ipcc.ch/report/ar6/wg1/

Johnson, F.E., R.N. Lerch, P.P. Motavalli, K.S. Veum, and P.C. Scharf. 2022. Spatial variability of denitrification enzyme activity and actual denitrification emissions on Missouri claypan soils. Soil Science Society of America Journal 86(6): 1582–1596. doi: https://doi.org/10.1002/saj2.20457.

Kitzler, B., S. Zechmeister-Boltenstern, C. Holtermann, U. Skiba, and K. Butterbach-Bahl. 2006. Nitrogen Oxides Emission from Two Beech Forests Subjected to Different Nitrogen Loads. Biogeosciences 3(3): 293–310. doi: https://doi.org/10.5194/bg-3-293-2006.

LICOR Environmental. 2024a. LI-7820 N_2O/H_2O Trace Gas Analyzer. Licor.com/env. https://www.licor.com/env/products/trace-gas/LI-7820.

LICOR Environmental. 2024b. Smart Chamber Initial setup. Licor.com. https://www.licor.com/env/support/Smart-Chamber/topics/intial-setup.html#Installingsoilcollars.

Linn, D.M., and J.W. Doran. 1984. Effect of Water Filled Pore Space on Carbon Dioxide and Nitrous Oxide Production in Tilled and Nontilled Soils. Soil Science Society of America. Doi: https://doi.org/10.2136/sssaj1984.03615995004800060013x

Liu, X. 2021. Varied Farm-Level Carbon Intensities of Corn Feedstock Help Reduce Corn Ethanol Greenhouse Gas Emissions. Environmental Research. doi: https://doi.org/10.1088/1748-9326/ac018f.

Liu, X., H. Kwon, D. Northrup, and M. Wang. 2020a. Shifting Agricultural Practices to Produce Sustainable, Low Carbon Intensity Feedstocks for Biofuel Production. Environmental Research. doi: https://doi.org/10.1088/1748-9326/ab794e.

Liu, X., H. Kwon, M. Wang, and Argonne National Laboratory. 2020b. Feedstock Carbon Intensity Calculator (FD-CIC) Users' Manual and Technical Documentation. https://greet.anl.gov/files/fd-cic-tool-2020-user-guide

Liu, C., Y. Liu, W. Gao, K. Gao, J. Li, et al. 2023. The effect of chamber placement site on N_2O emission under different fertilizer regimes from maize field. Agriculture, Ecosystems & Environment 341: 108210. doi: https://doi.org/10.1016/j.agee.2022.108210.

Liu, S., M. Schloter, and N. Brüggemann. 2018. Accumulation of NO_2^- during Periods of Drying Stimulates Soil N_2O Emissions during Subsequent Rewetting. European Journal of Soil Science 69(5): 936–946. doi: https://doi.org/10.1111/ejss.12683.

Lu, C., Z. Yu, J. Zhang, P. Cao, H. Tian, et al. 2022. Century-long Changes and Drivers of Soil Nitrous Oxide (N_2O) Emissions across the Contiguous United States. Global Change Biology 28(7): 2505–2524. doi: https://doi.org/10.1111/gcb.16061.

Ma, B.L., T.Y. Wu, N. Tremblay, W. Deen, M.J. Morrison, et al. 2009. Nitrous Oxide Fluxes from Corn fields: On-farm Assessment of the Amount and Timing of Nitrogen Fertilizer. Global Change Biology 16(1): 156–170. doi: https://doi.org/10.1111/j.1365-2486.2009.01932.x.

Maaz, T.M., T.B. Sapkota, A.J. Eagle, M.B. Kantar, T.W. Bruulsema, et al. 2021. Meta-Analysis of Yield and Nitrous Oxide Outcomes for Nitrogen Management in Agriculture. Global Change Biology 27(11): 2343–2360. doi: https://doi.org/10.1111/gcb.15588.

Malhi, S.S., and R. Lemke. 2007. Tillage, Crop Residue and N Fertilizer Effects on Crop yield, Nutrient uptake, Soil Quality and Nitrous Oxide Gas Emissions in a Second 4-yr Rotation Cycle. Soil and Tillage Research 96(1-2): 269–283. doi: https://doi.org/10.1016/j.still.2007.06.011.

Muchow, R.C. 1998. Nitrogen Utilization Efficiency in Maize and Grain Sorghum. Field Crops Research 56: 209–216. doi: https://doi.org/10.1016/S0378-4290(97)00132-9

Office of Energy Efficiency & Renewable Energy. 2024. Biofuel Basics. Energy.gov. https://www.energy.gov/eere/bioenergy/biofuel-basics.

Oikawa, P.Y., G.D. Jenerette, and D.A. Grantz. 2014. Offsetting high water demands with high productivity: Sorghum as a biofuel crop in a high irradiance arid ecosystem. GCB Bioenergy 7(5): 974–983. doi: https://doi.org/10.1111/gcbb.12190.

Pihlatie, M., E. Syväsalo, A. Simojoki, M. Esala, and K. Regina. 2004. Contribution of Nitrification and Denitrification to N_2O Production in peat, Clay and Loamy Sand Soils under Different Soil Moisture Conditions. Nutrient Cycling in Agroecosystems 70(2): 135–141. doi: https://doi.org/10.1023/b:fres.0000048475.81211.3c.

Preza-Fontes, G., P.J. Tomlinson, K.L. Roozeboom, J. Warren, and D.A. Ruiz Diaz. 2020. Nitrogen Fertilization Offsets the N2O Mitigating Effects of Cover-Crops and Double-Crop Soybean in a Wheat–Sorghum System. Agronomy Journal 112(2): 772–785. doi: https://doi.org/10.1002/agj2.20095.

Ravishankara, A.R., J.S. Daniel, and R.W. Portmann. 2009. Nitrous Oxide (N_2O): the Dominant Ozone-Depleting Substance Emitted in the 21st Century. Science 326(5949): 123–125. doi: https://doi.org/10.1126/science.1176985.

Rooney, W.L. 2016. Sorghum Production and Improvement Practices. Reference Module in Food Science. doi: https://doi.org/10.1016/b978-0-08-100596-5.00198-0.

Rooney, W.L., J. Blumenthal, B. Bean, and J.E. Mullet. 2007. Designing sorghum as a dedicated bioenergy feedstock. Biofuels, Bioproducts and Biorefining 1(2): 147–157. doi: https://doi.org/10.1002/bbb.15.

Rowlings, D.W., D.W. Lester, P.R. Grace, C. Scheer, Daniele De Rosa, et al. 2022. Seasonal Rainfall Distribution Drives Nitrogen Use Efficiency and Losses in Dryland Summer Sorghum. Field Crops Research 283. doi: https://doi.org/10.1016/j.fcr.2022.108527.

Rudaz, A., E. Davidson, and M. Firestone. 1990. Source of Nitrous Oxide Production following Wetting of Dry Soil. https://www.sciencedirect.com/science/article/abs/pii/0378109791905077

Rychel, K., K. Meurer, G. Börjesson, M. Strömgren, G. Tarekegn Getahun, et al. 2020. Deep N Fertilizer Placement Mitigated N_2O Emissions in a Swedish Field Trial with Cereals. Nutrient Cycling in Agroecosystems 118. doi: https://doi.org/10.1007/s10705-020-10089-3.

Schwenke, G.D., and B.M. Haigh. 2016. The Interaction of Seasonal Rainfall and Nitrogen Fertiliser Rate on Soil N_2O Emission, Total N Loss and Crop Yield of Dryland Sorghum and Sunflower Grown on sub-tropical Vertosols. Soil Research 54(5): 604. doi: https://doi.org/10.1071/sr15286.

Schwenke, G.D., and B.M. Haigh. 2019. Can Split or Delayed Application of N Fertiliser to Grain Sorghum Reduce Soil N_2O Emissions from sub-tropical Vertosols and Maintain Grain Yields? Soil Research 57(8): 859. doi: https://doi.org/10.1071/sr19080.

Schwenke, G.D., D.F. Herridge, C. Scheer, D.W. Rowlings, B.M. Haigh, et al. 2015. Soil N_2O Emissions under N_2-fixing Legumes and N-fertilised canola: a Reappraisal of Emissions Factor Calculations. Agriculture, Ecosystems & Environment 202: 232–242. doi: https://doi.org/10.1016/j.agee.2015.01.017.

Smith, K., L. Bouwman, and B. Braatz. 2000. N_2O: Direct Emissions from Agricultural Soils. IPCC. https://www.ipcc-nggip.iges.or.jp/public/gp/bgp/4_5_N2O_Agricultural_Soils.pdf

Sorghum Checkoff. Sorghum 101. Sorghum Checkoff. https://www.sorghumcheckoff.com/sorghum-101/#:~:text=In%20the%20United%20States%20and.

Storlien, J., J. Heilman, T. Boutton, and D. Baltensperger. 2013. The Carbon Footprint of Bioenergy Sorghum Production in Central Texas: Production Implications on Greenhouse Gas Emissions, Carbon cycling, and Life Cycle Analysis. https://www.proquest.com/docview/1497271563?parentSessionId=9iUFOycEih3pXBoHrhTAWzEwGQ%2F4bOm%2FwAiX8IKZ6mU%3D&pq-origsite=primo&accountid=11789&sourcetype=Dissertations%20&%20Theses

Storlien, J., F.M. Hons, J.P. Wight, and J.L. Heilman. 2014. Carbon Dioxide and Nitrous Oxide Emissions Impacted by Bioenergy Sorghum Management. Soil Science Society of America Journal 78(5): 1694–1706. doi: https://doi.org/10.2136/sssaj2014.04.0176.

Tallec, T., A. Brut, L. Joly, N. Dumelié, D. Serça, et al. 2019. N_2O flux measurements over an irrigated maize crop: A comparison of three methods. Agricultural and Forest Meteorology 264: 56–72. doi: https://doi.org/10.1016/j.agrformet.2018.09.017.

Taylor, J. 2003. Overview: Importance of sorghum in Africa. Afripro, Pretoria, South Africa.

Tian, H., R. Xu, J.G. Canadell, R.L. Thompson, W. Winiwarter, et al. 2020. A Comprehensive Quantification of Global Nitrous Oxide Sources and Sinks. Nature 586(7828): 248–256. doi: https://doi.org/10.1038/s41586-020-2780-0.

U.S. Energy Information Administration. 2022. Biofuels Explained - U.S. Energy Information Administration (EIA). Eia.gov. https://www.eia.gov/energyexplained/biofuels/.

United States Department of Agriculture. 2024. Sorghum Explorer. ipad.fas.usda.gov. https://ipad.fas.usda.gov/cropexplorer/cropview/commodityView.aspx?cropid=0459200.

US Department of Energy. Alternative Fuels Data Center: Ethanol Production. afdc.energy.gov. https://afdc.energy.gov/fuels/ethanol-production#:~:text=Ethanol%20is%20a%20domestically%20produced.

US Environmental Protection Agency. 2012. Supplemental Determination for Renewable Fuels Produced Under the Final FRS2 Program From Grain Sorghum. https://www.epa.gov/renewable-fuel-standard/supplemental-determination-renewable-fuels-produced-under-renewable-fuel

US Environmental Protection Agency. 2015. Overview of the Renewable Fuel Standard Program. www.epa.gov. https://www.epa.gov/renewable-fuel-standard-program/overview-renewable-fuel-standard-program.

US Environmental Protection Agency. 2021. Biofuels and the Environment. www.epa.gov. https://www.epa.gov/risk/biofuels-and-environment.

US Environmental Protection Agency. 2024. Inventory of U.S. Greenhouse Gas Emissions and Sinks: 1990-2022. www.epa.gov. https://www.epa.gov/ghgemissions/inventory-us-greenhouse-gas-emissions-and-sinks-1990-2022.

Van Kessel, C., R. Venterea, J. Six, M.A. Adviento-Borbe, B. Linquist, et al. 2012. Climate, Duration, and N Placement Determine N_2O Emissions in Reduced Tillage systems: A Meta-Analysis. Global Change Biology 19(1): 33–44. doi: https://doi.org/10.1111/j.1365-2486.2012.02779.x.

Vasilyevich Baranovsky, A., T. Mikhailovna Kosogova, S. Ivanovich Kapustin, and A. Sergeevich Kapustin. 2020. The Effect of Nitrogen Fertilizers on the Productivity of Grain Sorghum. Bioscience Research 17(1). https://elibrary.ru/item.asp?id=44149968

Venkateswaran, K., M. Elangovan, and N. Sivaraj. 2019. Origin, Domestication and Diffusion of Sorghum bicolor. Breeding Sorghum for Diverse End Uses: 15–31. doi: https://doi.org/10.1016/b978-0-08-101879-8.00002-4.

Wagaw, K. 2019. Review on Mechanisms of Drought Tolerance in Sorghum (Sorghum bicolor (L.) Moench) Basis and Breeding Methods. Academic Research Journal of Agricultural Science and Research 7(2). doi: https://doi.org/10.14662/ARJASR2019.007.

Wang, D., S. Bean, J. McLaren, P. Seib, R. Madl, et al. 2008. Grain Sorghum Is a Viable Feedstock for Ethanol Production. Journal of Industrial Microbiology & Biotechnology 35(5): 313–320. doi: https://doi.org/10.1007/s10295-008-0313-1.

Wang, H., Z. Yan, X. Ju, X. Song, J. Zhang, et al. 2023. Quantifying Nitrous Oxide Production Rates from Nitrification and Denitrification under Various Moisture Conditions in Agricultural Soils: Laboratory Study and Literature Synthesis. Frontiers in Microbiology 13. doi: https://doi.org/10.3389/fmicb.2022.1110151.

Winchell, F., C.J. Stevens, C. Murphy, L. Champion, and D.Q. Fuller. 2017. Evidence for Sorghum Domestication in Fourth Millennium BC Eastern Sudan: Spikelet Morphology from Ceramic Impressions of the Butana Group. Current Anthropology 58(5): 673–683. doi: https://doi.org/10.1086/693898.

Wood, M.D., X. Gao, K.H.D. Tiessen, M. Tenuta, and D.N. Flaten. 2023. Enhanced Efficiency Urea Fertilizers and Timing Effects on N_2O Emissions from Spring Wheat Production in Manitoba. Agronomy Journal 116(1): 51–72. doi: https://doi.org/10.1002/agj2.21448.

Wortmann, C., R. Ferguson, G. Hergert, C. Shapiro, and T. Shaver. 2013. Nutrient Management Suggestions for Grain Sorghum. University of Nebraska - Lincoln. https://extensionpubs.unl.edu/publication/g1669/2013/pdf/view/g1669-2013.pdf

Xiao-Tang, J., and C. Zhang. 2017. Nitrogen Cycling and Environmental Impacts in Upland Agricultural Soils in North China: A Review. Journal of Integrative Agriculture 2017(12): 2848–2862. doi: https://doi.org/10.1016/S2095-3119(17)61743-X.

Zebarth, B.J., P. Rochette, D.L. Burton, and M. Price. 2008. Effect of Fertilizer Nitrogen Management on N_2O Emissions in Commercial Corn Fields. Canadian Journal of Soil Science 88(2): 189–195. doi: https://doi.org/10.4141/cjss06010.

Zhao, Z.-Y., and J. Dahlberg. 2019. Sorghum. Springer Science + Business Media. https://link.springer.com/content/pdf/10.1007/978-1-4939-9039-9.pdf

Chapter 2 - Comparison of Sampling Duration Using LICOR's 7820 Trace Gas Analyzer

Abstract

Automated Soil Gas Flux Systems offer a new, efficient method of collecting soil gas flux data. However, limited external literature provides guidance on using the system's settings to minimize time spent obtaining measurements while maintaining data quality. This study compares three sampling durations – 180 seconds, 120 seconds (LICOR recommendation), and 90 seconds; using N_2O flux data collected with a N_2O/H_2O trace gas flux analyzer (Model 7820, LI-COR) and 8200 portable Smart Chamber system (Model 8200-01, LI-COR). All data were processed using Soil Flux Pro software (Version 5.3.1, LI-COR) and analyzed using SAS Version 9.4 using PROC REG procedure. Regression analysis with all sites combined resulted in high r^2 values ($r^2 > 0.97$) in each comparison group. However, with all sites combined, all slope values were different from one ($p < 0.0019$). Under the assumption that the longer duration is most reliable, the low RMSE values indicated that samples can be collected at the shorter sampling duration without compromising data quality. Given these results, the manufacturer's recommended sampling duration of 120-seconds is likely a reliable balance between data quality and the labor required for measurements.

Key Findings

- The 120-second and 180-second comparison at the easternmost site had the highest agreement between the two sampling durations, with the slope having no difference from 1.

- Sites with lower average daily N_2O flux values represented lower RMSE values between all comparisons, indicating that sites with higher expected daily flux values should use a longer sampling duration to capture additional variability.

- Consistent high r^2 values ($r^2 > 0.97$) and low RMSE values indicate that samples can be collected at a shorter sampling duration (120-seconds) without compromising data quality.

Introduction

Rising labor costs coupled with a consistent demand for high quality data have created a tradeoff in academic field research. Finding efficient methods for collecting data without compromising quality is critical, especially in labor intensive, time-consuming field trials with many treatments.

The static chamber method, as described by the USDA-ARS GRACEnet Project Protocol (Parkin et al., 2010,) has been the previous prevalent method for estimating nitrous oxide (N_2O) flux. N_2O concentrations are measured with the static chamber method by determining the rate of change in gas concentration in a chamber headspace. These chambers are typically closed for a period of 30-60 minutes to collect a sample. Samples are drawn from the closed chamber at time 0, and at least two other evenly spaced time intervals, often 10-20 minutes apart. These concentrations are then analyzed using gas chromatography and then processed using linear or quadratic regression to calculate the slope of concentration versus time, providing a flux measurement.

Automated soil gas flux systems offer a new technology that allows users to collect low concentration soil flux data both quickly and accurately. LICOR's system uses optical feedback cavity-enhanced absorption spectroscopy to measure soil gas flux (in this case, N_2O) at a rate of one sample per second (LICOR Environmental, 2024a). The system's settings are customizable, allowing users to configure the system to best suit their specific research needs. LICOR's literature recommends observation times (sampling durations) of 90 to 180 seconds for sampling N_2O fluxes (LICOR Environmental, 2024b). However, limited external literature provides guidance on how to use the system's settings to balance time efficiency and data quality. Observation time (sampling duration) is important for maintaining consistent environmental conditions including temperature, pressure, and soil moisture, which can all impact N_2O emissions, and limiting the effect of altered diffusion, a disruption of the natural soil-atmosphere gas exchange process (LICOR Environmental, 2024b). There is scarce information on how to modify the system's settings to account for various environmental conditions. In this study, we use N_2O flux data collected with a N_2O/H_2O Trace Gas Flux Analyzer (Model 7820, LI-COR) and Portable Smart Chamber system (Model 8200-01, LI-COR) to compare sampling durations of 90 seconds, 120 seconds, and 180 seconds, across three locations representing an annual precipitation gradient of 400mm while obtaining measurements from plots subjected to a wide range of nitrogen management treatments.

The objective of this analysis was to determine the optimal observation time (sampling duration) for collecting N_2O flux data using LICOR's Trace Gas Analyzer System across different environments, specifically humid and semi-arid environments. The hypothesis was that data collected with a 180-second sampling duration would be more stable, while 90- and 120-second sampling durations would underestimate fluxes relative to the longest duration and likely exhibit greater variability.

Materials and Methods

Site Descriptions

Three site locations in Kansas across a precipitation and climate gradient were used to conduct experiments during 2024 (Figure 2.1). The eastern Kansas location (MRD) was in Morris County (Lat/Long: 38° 47' 35.5914", -96° 48' 53.8554") at an approximate elevation of 416 meters. The soil type is classified as Irwin silty clay loam, with a taxonomic classification of fine, mixed, superactive, mesic Pachic Argiustoll (USDA NRCS, 2019). The region has a humid subtropical climate (Köppen Climate Classification: Cfa), obtained from Climate Change & Infectious Diseases Group and Brugger, (2017) based on the data of Kotteck et al. (2006). The region also has an average annual precipitation of 860 mm and an average annual temperature of 13 °C (30-year average) (Office of the Kansas State Climatologist, 2020).

The southwest Kansas location (GYD) was in Gray County (Lat/Long: 37° 34' 32.412", -100° 24' 32.2554") at an approximate elevation of 851 meters. The soil type is classified as mainly Richfield silt loam, with a taxonomic classification of fine, smectitic, mesic Aridic Argiustoll (USDA NRCS, 2019). The region has a cold semi-arid climate (Köppen Climate Classification: Bsk), obtained from Climate Change & Infectious Diseases Group and Brugger, (2017) based on the data of Kotteck et al. (2006). The area has an average annual precipitation of 550 mm and an average annual temperature of 13 °C (30-year average) (Office of the Kansas State Climatologist, 2020).

The northwest Kansas location (THD) was in Thomas County (Lat/Long: 39° 14' 5.4954", -101° 12' 11.8434"°) at an approximate elevation of 1005 meters. The soil type is classified as mainly Keith silt loam, with a taxonomic classification of fine-silty, mixed, superactive, mesic Aridic Argiustoll (USDA NRCS, 2019). The region has a cold semi-arid climate (Köppen Climate Classification: Bsk), obtained from Climate Change & Infectious Diseases Group and Brugger, (2017) based on the data of Kotteck et al. (2006). The area also has an average annual precipitation of 500 mm and an average annual temperature of 11 °C (30-year average) (Office of the Kansas State Climatologist, 2020).

Experimental Design

The experiment was designed with treatments in a randomized complete block design with four replications at each of three sites. Treatments included both a nitrogen rate ramp with seven nitrogen application rates as well as a nitrogen application method component with three treatments. Nitrogen rate treatments were 0, 33.6, 67.3, 100.8, 134.5, 168.1, and 201.8 kg N ha^{-1}. All rate treatments were applied as streamed UAN immediately prior to planting. Nitrogen placement treatments were applied immediately prior to planting at a rate of 67.3 kg N ha^{-1}. Placement treatments included broadcast urea treated with a urease inhibitor – NBPT (N-(n-butyl) thiophosphoric triamide) (Agrotain, 1.05 L metric ton $urea^{-1}$), streamed UAN, and coultered UAN placed approximately 7.6 cm deep on 38.1 cm spacing, placing the fertilizer band 19.1 cm from both sides of the planted row (Model Generation III Fertilizer Coulter, Yetter Mfg. Co.). One site (MRD) also included placement treatments that were applied one month prior to grain sorghum planting. These treatments also included broadcast urea treated with a urease inhibitor – NBPT (Agrotain, 1.05 L metric ton $urea^{-1}$), streamed UAN, and coultered UAN placed at approximately 7.6 cm deep on 38.1 cm spacing, placing the fertilizer band 19.1 cm from the plant on both sides (Model Generation III Fertilizer Coulter, Yetter Mfg. Co.).

Soil Nitrous Oxide Emission Measurements

Soil nitrous oxide (N_2O) emissions were measured using a LI-COR N_2O/H_2O Trace Gas Analyzer (Model 7820, LI-COR) paired with a LI-COR Portable Smart Chamber (Model 8200-01, LI-COR). Measurements were collected from soil collars constructed from PVC pipe (19.7 cm inner diameter x 11 cm long), inserted approximately 6 cm into the soil, leaving 5 cm of collar extending above the soil surface. Two of these PVC collars were installed in the second row of each plot, to represent 50% of the total row width of 76.2 cm, with placement resulting in less than 2.2% overlap between chambers. The collars were installed after planting/fertilization and remained in place throughout the duration of the growing season.

N_2O flux measurements were collected weekly at all site locations during the growing season. Measurements were generally taken between 6:00 and 14:00 (CST). At each sampling, the portable smart chamber head was placed over the soil collar. N_2O flux measurements were then collected with a 180 second sampling duration, a 25 second deadband, and a 45 second post purge (LI-COR Environmental, 2024c). Realtime data viewing in the field was used to monitor analyzer performance. Data were collected and stored in the Portable Smart Chamber, including N_2O flux, diagnostic code values, total chamber volume, date, and time.

Data were downloaded and initially processed using Soil Flux Pro software (Version 5.3.1, LI-COR). This software was also used to input collar height information to adjust the total volume and evaluate each individual flux measurement to verify proper chamber and analyzer operation, omitting data collected when a diagnostic code was issued from the analyzer. As data were evaluated in Soil Flux Pro, flux measurements that displayed irregular patterns or signs of analyzer malfunction, such as skips where N_2O concentration was not collected, major N_2O concentration jumps, or major N_2O concentration drops, indicating an issue with the chamber seal or analyzer pressure, were reviewed and excluded from the dataset to ensure data quality.

N_2O fluxes were calculated by the LI-COR 8200-01 Portable Smart Chamber (Model 8200-01, LI-COR) using one-second interval N_2O concentration data recorded by the trace gas analyzer (Model 7820, LI-COR) over the 180-second sampling interval. Soil Flux Pro software (Version 5.3.1, LI-COR) was used to calculate simulated 90-second, 120-second, and 180-second readings from the complete 180-second sample by adjusting the stop time value thus truncating data beyond the desired measurement window. All samples utilized a 25-second deadband time. The unit of flux output from the system was nmol N_2O m^{-2} s^{-1}. Appropriate unit conversion and the molar mass of the nitrogen molecule (28.0134 g mol^{-1}) were used to adjust the flux to a nitrogen mass per area-time basis (g N_2O-N ha^{-1} day^{-1}) (Equation 2.1).

$$\text{Daily Flux (g N}_2\text{O-N ha}^{-1}\text{)} = \frac{nmol\ N_2O}{m^2 \cdot s} \cdot \frac{mol\ N_2O}{(1 \cdot 10^9)nmol\ N_2O} \cdot \frac{3600\ s}{h} \cdot \frac{24\ h}{d} \cdot \frac{28.0134\ g\ of\ N}{mol\ N_2O} \cdot \frac{10,000\ m^2}{ha}$$

Equation 2.1 Daily flux calculation where m is meters, s is seconds, h is hours, d is days, g is grams, and ha is hectare.

Statistical Analysis

Data were analyzed in SAS Version 9.4 (SAS Institute Inc.) using the PROC REG procedure to regress the fluxes obtained from the simulated 90-and 120-second sampling duration (treated as independent variables) against the flux value from the 180-second sampling duration (treated as the dependent variables). Additionally, an analysis was conducted regressing the flux from the 90-second sampling duration against the flux value from the 120-second sampling duration (treated as the dependent variable). This created regressions for 90-second versus 180-second, 120-second versus 180-second, and 90-second versus 120-second sampling durations. Regression analysis was run for each location across sampling dates, and across all locations and sampling dates. In addition, for each regression, a t-test was conducted on the regression slope term to test the null hypothesis that the slope was equal to 1 using the TEST procedure in PROC REG. Statistical significance was analyzed at an alpha level of 0.05.

Results

At 90 seconds, THD had a mean daily N_2O flux of 32.80 g of N_2O-N ha^{-1} d^{-1}, compared to 39.20 g of N_2O-N ha^{-1} d^{-1} at MRD and 52.75 g of N_2O-N ha^{-1} d^{-1} at GYD (Table 2.1). When evaluated at the manufacturer's recommended default sampling duration of 120 seconds (LICOR Environmental, 2024c), THD had a mean daily N_2O flux of 17.22 g of N_2O-N ha^{-1} d^{-1}, compared to 39.96 g of N_2O-N ha^{-1} d^{-1} at MRD and 56.97 g of N_2O-N ha^{-1} d^{-1} at GYD (Table 2.1). When evaluated at 180 seconds, the longest sampling duration, THD had a mean daily N_2O flux of 16.22 g of N_2O-N ha^{-1} d^{-1}, compared to 40.68 g of N_2O-N ha^{-1} d^{-1} at MRD and 59.55 g of N_2O-N ha^{-1} d^{-1} at GYD (Table 2.1). Mean flux levels were consistently lowest at THD across all sampling durations, and were consistently highest across all sampling durations at GYD. Median flux values were consistently lower than the mean for all sites and sampling durations, indicating a positively skewed distribution of data.

A comparison between 90-second and 180-second reading resulted in mixed findings. At each site individually, r^2 values were high ($r^2 > 0.97$) (Table 2.2) (Figure 2.2). Slope values at all three sites (MRD: 0.984, GYD: 0.920, THD: 1.042) were different from one ($p \leq 0.0006$). Although these slopes were all different than 1, THD was the only site with an overestimation (slope > 1) while MRD and GYD both display an underestimation (slope < 1). Intercept values at GYD (1.069) and THD (0.022) were not different from zero at each site and ($p > 0.05$). The comparison at MRD was found to have an intercept (-0.815) that was different from zero ($p =$ 0.0006). The regression on the data from THD produced the lowest RMSE (3.40), indicating higher agreement between the two sampling durations at this site. Data from MRD also produced a relatively low RMSE (3.51), which indicates high agreement between the two sampling durations at this site. Data from GYD produced a higher RMSE (29.24), indicating lower agreement between the two sampling durations at this site.

All sites were combined for comparison between the 90-second and 180-second readings (Table 2.3). Across all sites combined, r^2 values remained high ($r^2 = 0.9813$). Overall, the slope value (0.939) was found to be different from one ($p < 0.0001$). When all three sites are combined, the intercept of this comparison (0.960) was not found to be different from zero ($p = 0.0742$). The RMSE value for this comparison was the highest (16.89) among the sampling duration comparisons across sites (Table 2.3). Additionally, at all locations individually and combined, the 90-second sampling duration compared to the 180-second sampling duration had the highest RMSE of all comparisons.

A comparison between 120-second and 180-second readings resulted in mixed results, specifically at the MRD site (Table 2.4) (Figure 2.3). At each site individually, r^2 values were consistently high ($r^2 > 0.99$). Slope values at GYD (0.938) and THD (1.027) were different from one ($p < 0.0001$), while the slope value at MRD (0.998) was not different from one ($p = 0.4678$). THD was the only site with an overestimation (slope > 1) while GYD displayed an underestimation (slope < 1). Intercept values were found not different from zero at GYD (1.250) and THD (0.085) ($p > 0.05$), while the MRD comparison had an intercept value (-0.643) that was different than zero ($p = 0.0002$). The RMSE for MRD (1.94) and THD (2.93) were notably less than GYD (19.92).

Data were analyzed across-sties to compare the 120-second and 180-second readings (Table 2.3). The resulting regression had a high r^2 value ($r^2 = 0.9912$). Overall, the slope value for the 120-second to 180-second comparison (0.952) was found to be different from one ($p < 0.0001$). The intercept of the regression (0.946) was found to be different than zero ($p = 0.0110$). The RMSE value for this comparison was (11.67) (Table 2.3).

A comparison between 90-second and 120-second readings resulted in consistent results at each site (Table 2.5) (Figure 2.4). At each site individually, r^2 values of the linear regressions were high ($r^2 > 0.997$). Slope values at all three sites (MRD: 0.986, GYD 0.985, THD: 1.015) were all different from one ($p \leq 0.0001$). Although these slopes were all different than 1, THD was the only site with an overestimation (slope > 1) while MRD and GYD both display an underestimation (slope < 1). Regression intercept values at all three sites were not different from zero ($p > 0.05$). This comparison at GYD showed a higher root mean squared error (RMSE) (10.75) than MRD (2.69) and THD, which had the lowest RMSE value (0.91), indicating a higher agreement between the two sample durations at THD and MRD compared to GYD.

Data comparing the 90-second and 120-second sampling durations were also evaluated across all sites (Table 2.3). A high r^2 value was observed ($r^2 = 0.9976$). The slope value (0.990) was found to be different from one ($p < 0.0001$). The RMSE value for this comparison was the lowest (6.08) among the sampling duration comparisons across sites (Table 2.3).

Discussion

High r^2 values between sampling durations were observed at MRD when comparing the 120-second and the 180-second data ($r^2 = 0.9986$, Slope: 0.998, $p = 0.468$) (Table 2.5). This was the only slope value evaluated that was not different from 1. Additionally, this comparison had a low RMSE value (RMSE = 1.94) (Table 2.4), indicating high agreement between the two evaluated sampling durations. This suggests that the 120-second duration can be used to collect samples with the assumption that data quality will be statistically similar to the 180-second values. This is supported by work done by Hutchinson & Livingston (1993) with static chambers which suggested that shorter deployment times result in smaller disturbance of the microsite beneath the chamber. The 90-second and 180-second comparison resulted in an intercept that was different from zero, although this is likely not of any practical significance and likely shows a systemic bias in the 90-second sampling duration.

Contrastingly, daily N_2O fluxes at GYD calculated from integrating a 90-second sampling duration were underestimated when compared to flux calculated from 120-second (Slope: 0.985, $p < 0.0001$) and 180-second sampling durations (Slope: 0.920, $p < 0.0001$), with slope being less than 1 in both comparisons. When comparing daily fluxes calculated from integrating 120- and 180-second sampling durations at GYD, the 120-second data resulted in an underestimation compared to the 180-second data (Slope: 0.938, $p < 0.0001$). This underestimation was also observed at MRD when comparing fluxes calculated from the 90-second sampling duration data compared to both the 120-second (Slope: 0.986, $p = 0.0001$) and 180-second data (Slope: 0.984, $p = 0.0006$). This underestimation compared to the longer durations is further supported by De Klien and Harvey (2015) who reported that longer deployment times integrate flux estimates over a longer period, providing a more reliable estimate.

Daily N_2O fluxes, when calculated from a 90-second sampling duration, were consistently overestimated at THD when compared to 120-second (Slope: 1.015, $p < 0.0001$) and 180-second sampling durations (Slope: 1.042, $p < 0.0001$) with slope being greater than 1 in both comparisons. Additionally, at THD, the 120-second integration resulted in an overestimation of daily N_2O fluxes when compared to the 180-second integration (Slope: 1.027 $p < 0.0001$),

The overestimation observed at THD could be the result of the overall lower N_2O flux levels that were observed at THD compared to the other two sites. THD at 120 seconds had an average daily N_2O flux of 17.22 g of N_2O-N ha^{-1} d^{-1}, compared to 39.96 g of N_2O-N ha^{-1} d^{-1} at MRD and 56.97 g of N_2O-N ha^{-1} d^{-1} at GYD. This lower magnitude of fluxes overall at THD likely contributes to the lower RMSE and overall higher agreement between sample duration comparisons at this site. Comparatively, GYD had much higher fluxes throughout the season, which likely increased the influence of sampling duration on the estimated flux values, resulting in higher RMSE values and lower r^2 values by comparison overall. This indicates that higher expected levels of flux might be a justifiable reason to default towards a longer sampling duration, to capture this higher variability. This choice to use longer sampling duration for higher expected flux levels is further supported by De Klien and Harvey (2015) who reported that longer deployment times integrate flux estimates over a longer period, providing a more reliable estimate.

Conclusion

When comparing the 90-, 120- and 180-second sampling durations using the automated trace gas analyzer system, the 120-second and 180-second comparison at MRD had the highest agreement between the two sampling durations, with the slope having no difference from 1. Overall, a high agreement is observed between all the evaluated sampling duration comparisons, especially in lower flux conditions. Agreement between sampling durations was especially high in environments with lower season average flux values, supported by the consistently low RMSE values at THD. Future work should include the investigation of this data by sampling date to determine conditions that result in an underestimation compared to an overestimation. Under the assumption that the longer duration (180-seconds) is most reliable, the consistent low RMSE values across all sites indicate that samples can be collected at the shorter sampling durations, especially in environments with expected low flux values, without compromising data quality. Given these results, the manufacturer's recommended sampling duration of 120-seconds is likely a reliable balance between data quality and labor required for measurements.

References

Climate Change & Infectious Diseases Group, and K. Brugger. 2017. World Maps of Köppen-Geiger Climate Classification. Vu-wien.ac.at. https://koeppen-geiger.vu-wien.ac.at/usa.htm.

De Klien, C., and M. Harvey. 2015. Nitrous Oxide Chamber Methodology Guidelines Version 1.1. https://www.ars.usda.gov/ARSUserFiles/31831/2012%20Chamber_Methodology_Guidelines_Chapter6.pdf

Hutchinson, G.L., and G.P. Livingston. 2015. Use of Chamber Systems to Measure Trace Gas Fluxes. American Society of Agronomy Special Publication: 63–78. doi: https://doi.org/10.2134/asaspecpub55.c4.

LICOR Environmental. 2024a. LI-7820 N_2O/H_2O Trace Gas Analyzer. Licor.com/env. https://www.licor.com/env/products/trace-gas/LI-7820.

LICOR Environmental. 2024b. Soil gas flux measurement theory. Licor.com/env. https://www.licor.com/env/support/LI-8250/topics/theory.html#Measurementtime.

LICOR Environmental. 2024c. Smart Chamber Initial setup. Licor.com. https://www.licor.com/env/support/Smart-Chamber/topics/intial-setup.html#Installingsoilcollars.

Office of the Kansas State Climatologist. 2020. Office of the Kansas State Climatologist. ksu.edu. https://climate.ksu.edu/products/climatology/ (accessed 27 February 2026).

Parkin, T., P. Gov, A. Mosier, J. Smith, R. Venterea, et al. 2010. USDA-ARS GRACEnet Chamber-based Trace Gas Flux Measurement Protocol. https://www.ars.usda.gov/ARSUserFiles/31831/2003GRACEnetTraceGasProtocol.pdf

USDA NRCS. 2019. Web Soil Survey. usda.gov. https://websoilsurvey.nrcs.usda.gov/app/.

Tables

Table 2.1 Flux magnitude estimated using LICOR 7820 N_2O/H_2O analyzer system at three sampling durations at three sites representing a semiarid climate (THD & GYD) and a humid continental climate (MRD).

	Site*								
	------------THD-------------			-------------MRD-----------			--------------GYD------------		
	90 s	120 s	180 s	90 s	120 s	180 s	90 s	120 s	180 s
	--------------g of N_2O-N ha^{-1} d^{-1} --------------								
n	557	557	557	207	207	207	308	308	308
Mean	32.80	17.22	16.22	39.20	39.96	40.68	52.75	56.97	59.55
Median	2.22	1.00	1.00	25.26	25.87	26.81	11.07	11.39	11.24
Maximum	912.54	897.16	873.14	412.10	414.67	418.84	779.65	837.17	907.16
Minimum	0.92	-35.76	-30.16	-0.49	-0.38	-0.55	-8.47	-7.60	-4.90

*(MRD, Morris County, KS; GYD, Gray County, KS; THD, Thomas County, KS)

Table 2.2 Linear regression comparing 90-second sampling duration to 180-second sampling duration using LICOR 7820 N_2O/H_2O analyzer system at three sites representing a semiarid climate (THD & GYD) and a humid continental climate (MRD).

		Regression						Slope = 1 Test
Site*	n	r^2	RMSE	Slope	p-value	Intercept	p-value	p-value
MRD	207	0.9954	3.51	0.984	<0.0001	-0.815	0.0091	0.0006
GYD	308	0.9789	29.24	0.920	<0.0001	1.069	0.5455	<0.0001
THD	557	0.9977	3.40	1.042	<0.0001	0.022	0.8832	<0.0001

*(MRD, Morris County, KS; GYD, Gray County, KS; THD, Thomas County, KS)

Table 2.3 Comparison of different sampling durations used for measuring N_2O emissions with a LICOR 7820 N_2O/H_2O analyzer system across three sites combined.

		Regression						Slope = 1 Test
Comparison	n	r^2	RMSE	Slope	p-value	Intercept	p-value	p-value
90x120	1072	0.9976	6.08	0.990	<0.0001	-0.112	0.5620	<0.0001
90x180	1072	0.9813	16.89	0.939	<0.0001	0.960	0.0742	<0.0001
120x180	1072	0.9912	11.67	0.952	<0.0001	0.946	0.0110	<0.0001

Table 2.4 Linear regression comparing 120-second sampling duration to 180-second sampling duration using LICOR 7820 N_2O/H_2O analyzer system at three sites representing a semiarid climate (THD & GYD) and a humid continental climate (MRD).

		Regression						Slope = 1 Test
Site*	n	r^2	RMSE	Slope	p-value	Intercept	p-value	p-value
MRD	207	0.9986	1.94	0.998	<0.0001	-0.643	0.0002	0.4676
GYD	308	0.9904	19.92	0.938	<0.0001	1.250	0.2996	<0.0001
THD	557	0.9982	2.93	1.027	<0.0001	0.085	0.5038	<0.0001

Table 2.5 Linear regression comparing 90-second sampling duration to 120-second sampling duration using LICOR 7820 N_2O/H_2O analyzer system at three sites representing a semiarid climate (THD & GYD) and a humid continental climate (MRD).

		Regression						Slope = 1 Test
Site*	n	r^2	RMSE	Slope	p-value	Intercept	p-value	p-value
MRD	207	0.9973	2.69	0.986	<0.0001	-0.192	0.4183	0.0001
GYD	308	0.9971	10.75	0.985	<0.0001	-0.474	0.4662	<0.0001
THD	557	0.9998	0.91	1.015	<0.0001	-0.068	0.0889	<0.0001

*(MRD, Morris County, KS; GYD, Gray County, KS; THD, Thomas County, KS)

Figures

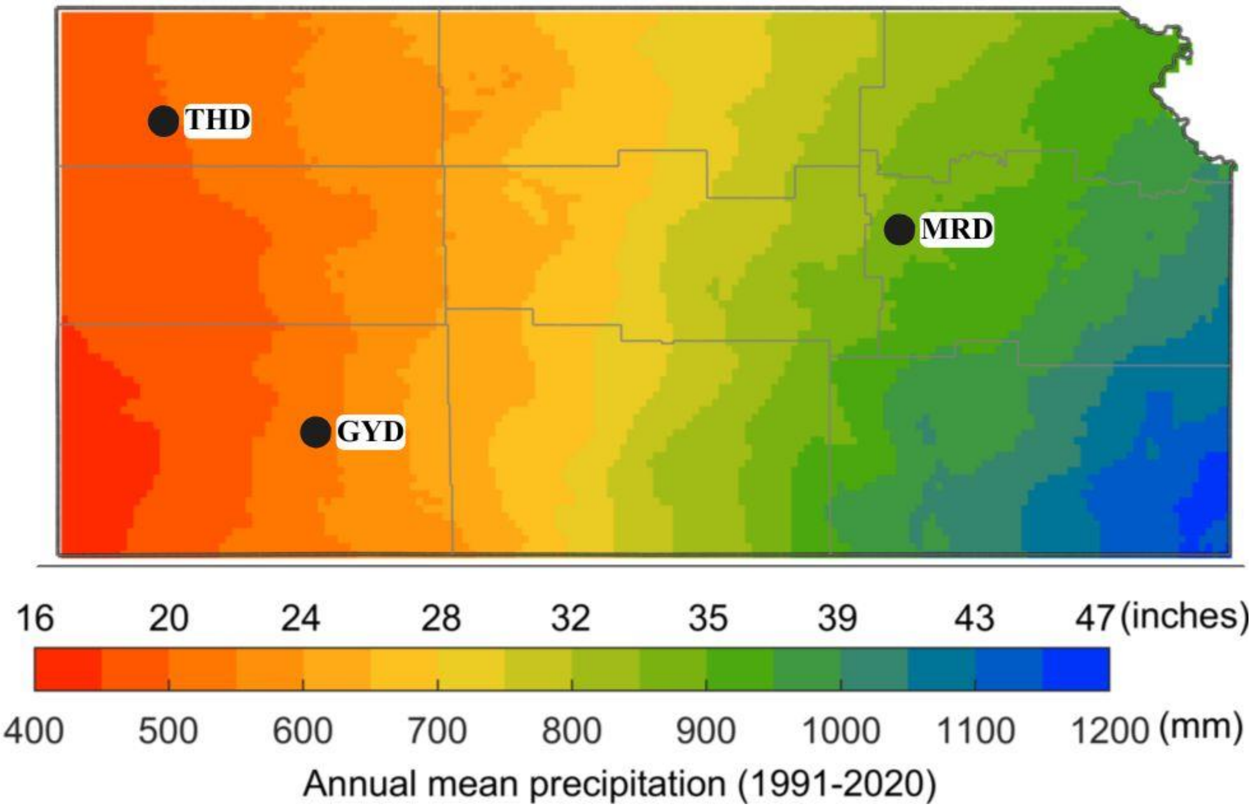

Figure 2.1 Thomas County, KS (THD), Gray County, KS (GYD), and Morris County, KS (MRD) field site locations across Kansas represent three distinct precipitation environments (adapted from the Office of the Kansas State Climatologist, 2020).

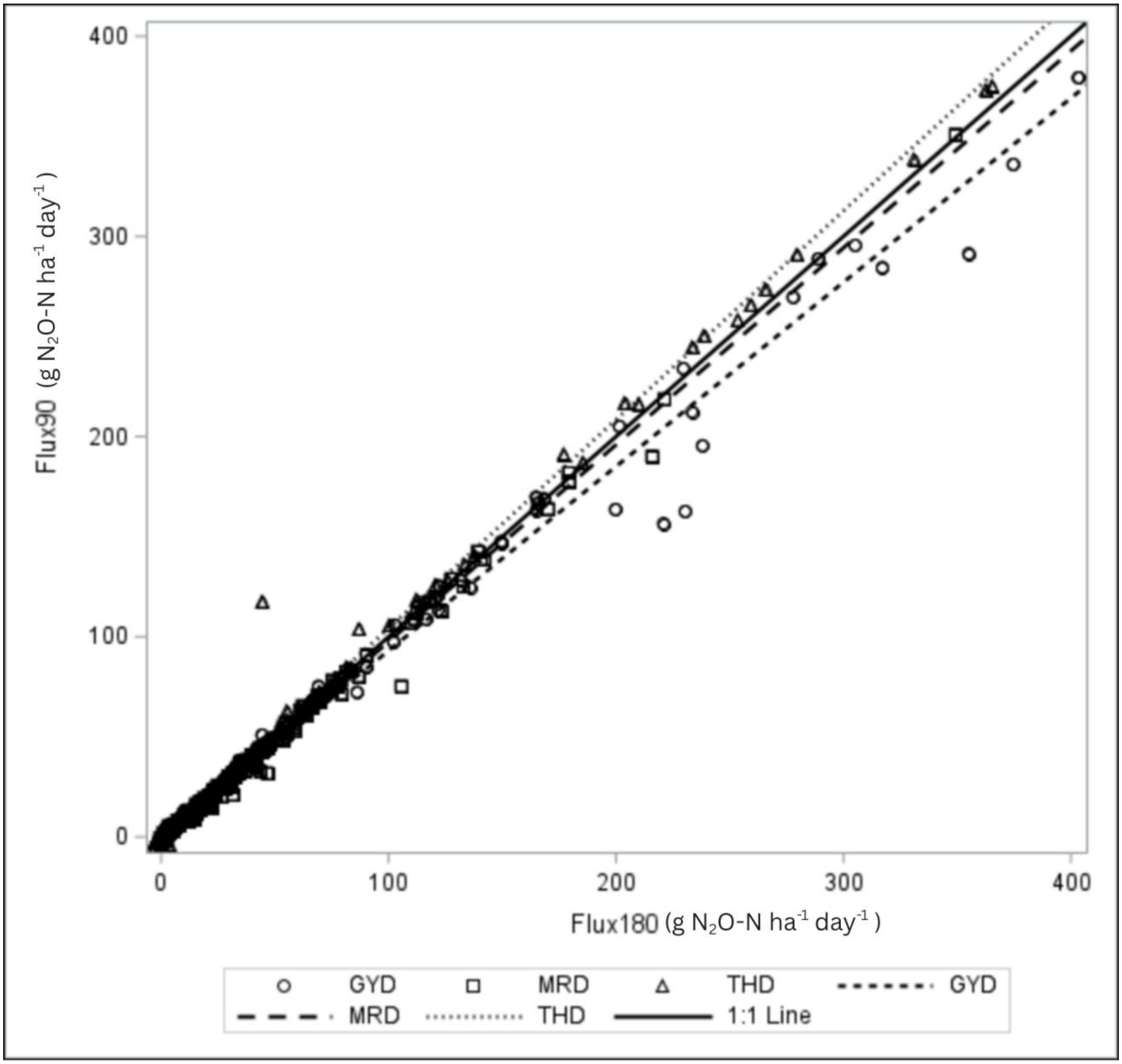

Figure 2.2 90-second sampling duration (g N_2O-N ha^{-1} day^{-1}) (Flux90) by 180-second sampling duration (g N_2O-N ha^{-1} day^{-1}) (Flux180) integration of all flux data at Thomas County (THD), Gray County (GYD), and Morris County (MRD).

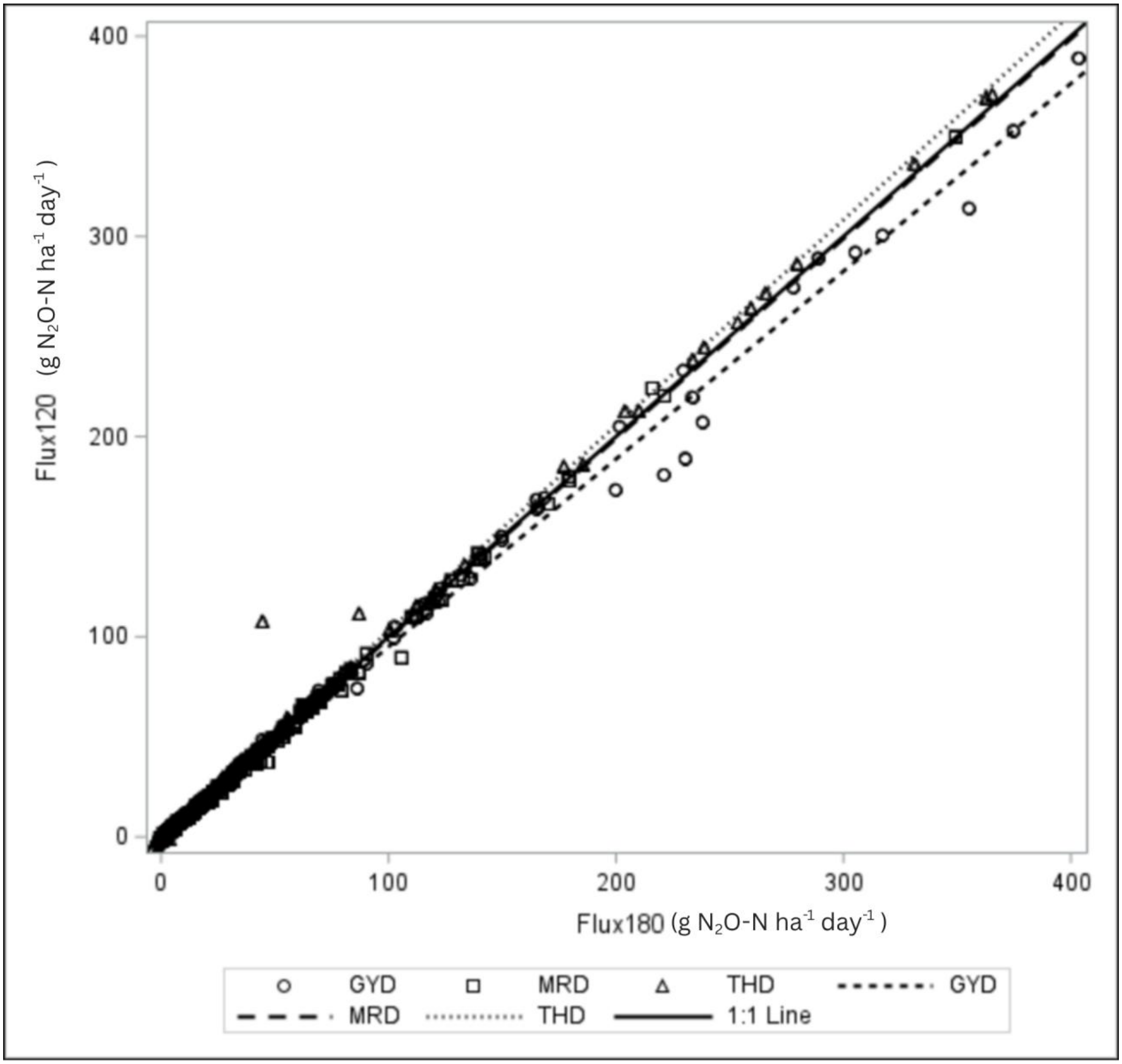

Figure 2.3 120-second sampling duration (g N_2O-N ha^{-1} day^{-1}) (Flux120) by 180-second sampling duration (g N_2O-N ha^{-1} day^{-1}) (Flux180) integration of all flux data at Thomas County (THD), Gray County (GYD), and Morris County (MRD).

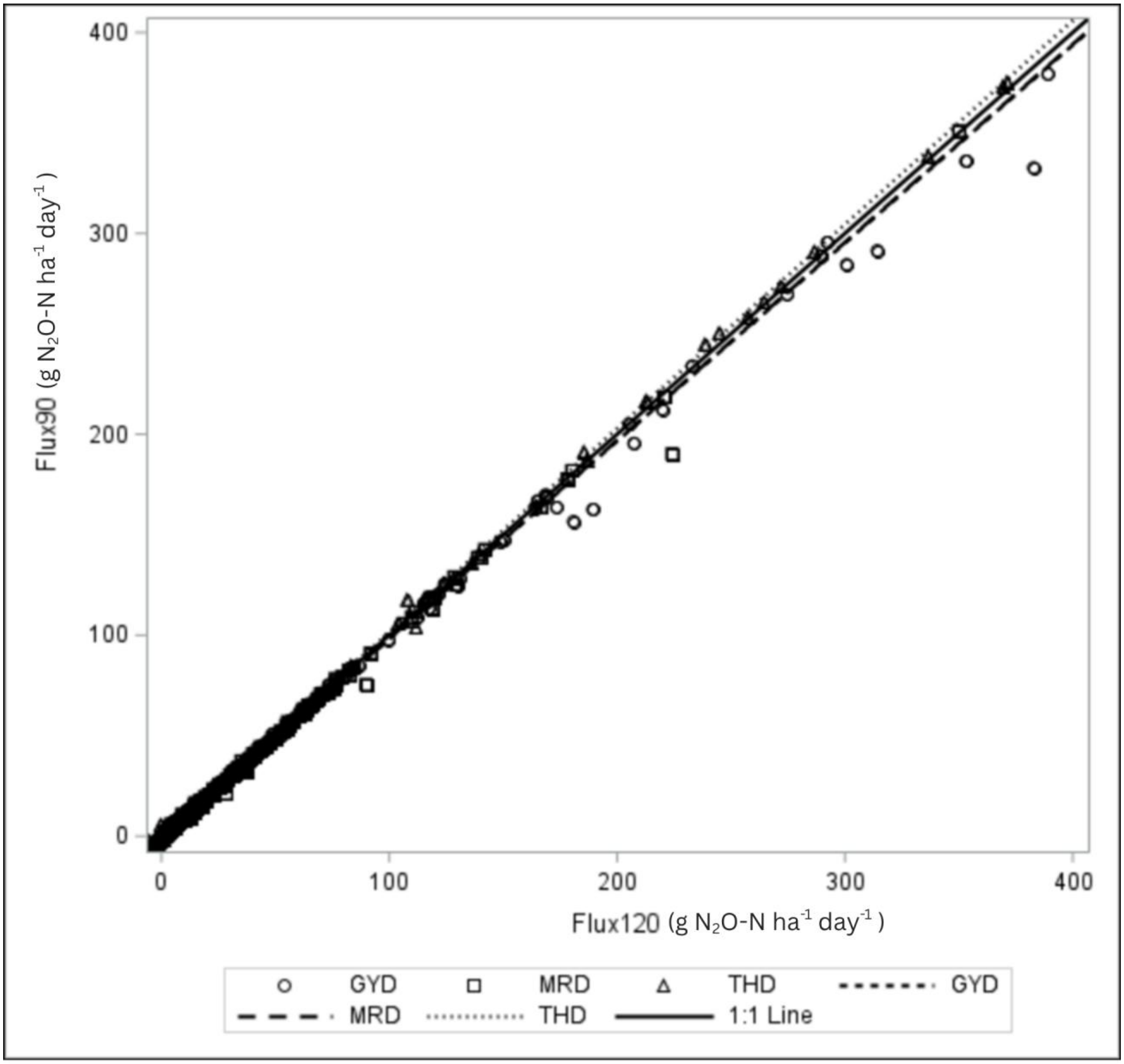

Figure 2.4 90-second sampling duration (g N_2O-N ha^{-1} day^{-1}) (Flux90) by 120-second sampling duration (g N_2O-N ha^{-1} day^{-1}) (Flux120) integration of all flux data at Thomas County (THD), Gray County (GYD), and Morris County (MRD).

Chapter 3 - Chamber Placement Effects on Nitrous Oxide Emission Estimation

Abstract

Nitrous oxide (N_2O) emissions have high spatial variability across the landscape, which can be difficult to quantify, especially in an agricultural setting with management using banded fertilizer applications. This study focused on the effects of chamber placement on N_2O flux in banded (38 cm centers) and non-banded nitrogen fertilizer treatments. Nitrous oxide emission measurements were collected using a trace gas analyzer system from grain sorghum fields with 76.2 cm rows at sites throughout central and western Kansas. Nitrogen fertilizer was applied at varying rates, placements, and timings. Rates of application were 0, 33.6, 67.3, 100.8, 134.5, 168.1, and 201.8 kg N ha^{-1}. Placement treatments were applied at planting at 67.3 kg N ha^{-1} and included broadcast urea treated with urease inhibitor – NBPT (N-(n-butyl) thiophosphoric triamide) (Agrotain, 1.05 L metric ton $urea^{-1}$), streamed UAN, and coultered UAN placed at approximately 7.6 cm deep on 38.1 cm spacing, placing the fertilizer band 19.1 cm from the plant on both sides (Model Generation III Fertilizer Coulter, Yetter Mfg. Co.). One site also included these placement treatments applied one month prior to planting. Emissions were collected from two chambers in each plot, one adjacent to the row and over the fertilizer band (on-band), and one centered in the inter-row area between the fertilizer bands (inter-row). In non-banded treatments, two chambers were placed in the same positions. Statistical analysis was conducted using SAS Version 9.4. PROC MIXED procedures. When evaluating rate treatments, there was an interaction between chamber position and nitrogen fertilizer rate ($p = 0.0043$). At high rates (>100.8 kg ha^{-1}), the on-band chambers had higher flux values than the inter-row

treatments ($p < 0.05$). On sampling days with high N_2O flux levels, differences between the two chamber placements were the largest. Since these two chamber placements had significant differences from one another, plots missing on-band chambers should be omitted from daily flux calculations to avoid underestimating or overestimating flux. Across all fertilizer placement treatments (broadcast urea with urease inhibitor - NBPT, streamed UAN, coultered UAN, and no nitrogen control) and at all sites, the interaction between fertilizer placement and chamber position was not significant at $\alpha = 0.05$ but was significant at $\alpha = 0.1$. Streamed UAN placements applied in a band at both application timings did show differences between flux values in the inter-row and on-band chambers ($p = 0.0768$). There was no statistical difference between the on-band and inter-row chambers in the broadcast urea with urease inhibitor - NBPT and no nitrogen control treatments. However, the mean flux for the on-band chamber overall was 0.45 nmol N_2O m^{-2} s^{-1} and the mean flux for the inter-row chamber overall was 0.29 nmol N_2O m^{-2} s^{-1} indicating a strong overriding influence of chamber position ($p = 0.0001$). Given the variability of collected results, plots with banded fertilizer application where either the on-band or inter-row chamber had missing data, should be omitted from analysis because of the potential of influence from the high concentration of fertilizer in one area. Chamber position as a main effect was highly significant when all sites were evaluated, meaning that regardless of fertilizer rate or placement relative to the chamber, there is enough inherent spatial variability that plots missing one of the two chambers should be omitted from the dataset.

Key Findings

- In banded treatments, chamber position resulted in a statistical difference between on-band and inter-row chambers at higher rates.

- In placement treatments, where a low rate of nitrogen was applied with different methods, on-band and inter-row were not statistically different from one another.

- As a best practice, in banded fertilizer studies, there is no suitable substitute replacement for the on-band chamber.

Introduction

Increased nitrogen fertilizer use accounted for 64% of the agricultural soil N_2O emissions increase since 1900 (Lu et al., 2022). N_2O emissions have been shown to vary greatly across a landscape (Ambus and Christensen, 1994). Landscape position, inorganic nitrogen concentration, and total organic carbon can influence the spatial variability of denitrification across a landscape (Johnson et al., 2022). Nitrous oxide is primarily derived from two parts of the global nitrogen cycle, nitrification, and denitrification (Gruber and Galloway, 2008). Nitrification and denitrification are processes that are driven by microbial activity and soil properties, which in turn influence N_2O emissions. Nitrification is the main N_2O producing pathway in low moisture conditions (Wang et al., 2023). Nitrification creates N_2O when ammonium oxidizers use NO_2^- as an alternate electron acceptor when oxygen is limited, causing natural N_2O emissions (Granli and Bøckman, 1994). The availability of NH_4^+ and NH_3 limits nitrification throughout the soil system (Norton, 2008). Therefore, locations on the field with higher concentrations of NH_4^+ or

NH_3, like a band of concentrated fertilizer, might have higher potential for increased N_2O loss through nitrification.

Denitrification becomes the main pathway of N_2O emission in high moisture conditions (Rudaz et al., 1990; Wang et al., 2023). One of the main factors contributing to denitrification's spatial variability is landscape position, with low spots having higher moisture accumulation, leading to increased levels of denitrification (Pennock et al., 1992). The relative size of an N_2O hot moment, a short period of time when N_2O flux is elevated, depends on how much water is added and how saturated the soil is (Barrat et al., 2020). The potential for denitrification losses of nitrogen as N_2O is high, particularly if high intensity rainfall occurs early in the growing season, when nitrogen has not yet been taken up by the crop (Schwenke and Haigh, 2016). Denitrification's association with moisture availability across a landscape could potentially contribute to spatial variability occurring without fertilizer influence. This moisture variability, combined with the concentrated application of fertilizer, may create the potential for N_2O production hot spots in the field.

There are recommendations and protocols used for sampling N_2O emissions using the static chamber method to ensure proper spatial representation. The USDA-ARS GRACEnet Project Protocol recommends that for N_2O flux measurements using chambers smaller than the row width, chambers be placed in both the row and inter-row areas of a plot to appropriately represent the space (Parkin and Venterea, 2010). Further, when large spatial variability is expected to exist, experiment structure, chamber number, and chamber placement may need to be adjusted to reduce variability (Chadwick et al., 2014). Experiments with nitrogen fertilizer placed in a narrow band may have some expected spatial variability. In which case, chamber placement should be adjusted to represent this expected variability (De Klien and Harvey, 2015). Multiple experiments across environments report influence of chamber placement on N_2O emission estimation when using a static chamber method. Cai et al. (2012) estimated daily N_2O emissions with the static chamber method and found that the chamber covering the row and interrow space had higher emissions than the chamber covering only the interrow space. Chadwick et al. (2014) evaluated five chambers per plot using the static chamber method, with large variability existing between all the chambers, especially on days with large flux. Additionally, fertilizer application method had an influence on the impact chamber placement made on N_2O emission estimation using the static chamber method (Liu et al., 2023). Literature does not yet describe the influence of chamber placement on estimation of N_2O emissions when using an automated trace gas analyzer system. The fixed size of such systems makes it difficult to adjust chamber size to cover a large, representative row area, since the volume and area are fixed in these systems.

The objective of this analysis was to assess how chamber placement relative to grain sorghum crop rows and nitrogen application bands influence cumulative N_2O emission measurements to inform assumptions about missing data. Hypotheses were (i) chamber position will impact N_2O emission estimates in banded treatments, with influence increasing at higher nitrogen application rates and (ii) chamber position will not have an impact on non-banded treatments.

Materials & Methods

Experimental Design

Individual chamber flux data were evaluated from chambers located in two positions. One was centered 19.1 cm off the planted row (on-band chamber). The second was centered 38.1 cm off the planted row, which corresponds to the center of the inter-row space (inter-row chamber). These chambers were installed in plots that received a range of fertilizer rates (0, 33.6, 67.3, 100.9, 134.5, 168.1, 201.8 kg N ha^{-1}) as streamed UAN and placements applied at 67.3 kg N ha^{-1} as broadcast urea treated with a urease inhibitor – NBPT (N-(n-butyl) thiophosphoric triamide) (Agrotain, 1.05 L metric ton $urea^{-1}$), streamed UAN, and coultered UAN. Treatments were evaluated at four site locations over the course of two years (2024 & 2025; Figure 3.1). The experiment was arranged in a randomized complete block design with four replications at each site. Nitrogen placement treatments were also established at each site. Applications were made at grain sorghum planting, and all nitrogen placement applications were made at 67.3 kg N ha^{-1}. Placement treatments included broadcast urea treated with urease inhibitor -NBPT, streamed UAN, and coultered UAN placed at approximately 7.6 cm deep on 38.1 cm spacing, placing the fertilizer band 19.1 cm from the plant on both sides (Model Generation III Fertilizer Coulter, Yetter Mfg. Co.). One site also included placement treatments that were applied one month prior to grain sorghum planting. These treatments also included broadcast urea treated with urease inhibitor -NBPT, streamed UAN, and coultered UAN placed at approximately 7.6 cm deep on 38.1 cm spacing, placing the fertilizer band 19.1 cm from the plant on both sides (Model Generation III Fertilizer Coulter, Yetter Mfg. Co.).

Soil Nitrous Oxide Emission Chamber Placement and Installation

Soil nitrous oxide (N_2O) emissions were collected from soil collars constructed from PVC (19.7 cm inner diameter x 11 cm long), inserted approximately 6 cm into the soil, leaving 5 cm of offset. N_2O flux measurements were collected from two collars in each plot. Collar A was centered 19.1 cm off the planted row. This location corresponds with the fertilizer band in streamed and coultered treatments (on-band chamber). Collar B was centered 38.1 cm off the planted row, which is directly between the two fertilizer bands in applicable treatments and corresponds to the center of the inter-row space (inter-row chamber). Collars were placed with 40 cm of space between them to allow for instrumentation space (Figure 3.2). When N_2O flux measurements were collected, collar A was read first, followed by collar B.

Soil Nitrous Oxide Emission Measurements

Measurements were collected using a N_2O/H_2O Trace Gas Analyzer (Model 7820, LI-COR) paired with a Portable Smart Chamber (Model 8200-01, LICOR). N_2O flux measurements were collected weekly at all site locations during the growing season. Measurements were generally taken between 6:00 and 14:00 (CST). On each sampling date, the portable smart chamber head was placed over the soil collar. N_2O flux measurements were then collected with a 120 second observation time, a 25 second deadband, and a 45 second post purge (LI-COR Biosciences, 2021). Realtime data viewing in the field was used to monitor analyzer performance. Data were collected and stored in the Portable Smart Chamber, including N_2O flux, diagnostic code values, total chamber volume, date, and time.

Flux data were downloaded and initially processed using Soil Flux Pro software (Version 5.3.1, LI-COR). This software was also used to input collar height information to adjust the total volume and evaluate each individual flux measurement to verify proper chamber and analyzer operation, omitting data collected when a diagnostic code was issued from the analyzer. Flux measurements that displayed irregular patterns or signs of analyzer malfunction, such as skips where N_2O concentration was not collected, major N_2O concentration jumps, or major N_2O concentration drops, indicating an issue with the chamber seal or analyzer pressure as identified in Soil Flux Pro, were reviewed and excluded from the dataset to ensure data quality.

N_2O fluxes were calculated by the LI-COR Portable Smart Chamber using one-second interval N_2O concentration data recorded by the N_2O/H_2O Trace Gas Analyzer over the 120-second sampling interval. Flux calculations were provided in nmol N_2O m^{-2} s^{-1}.

Statistical Analysis

Prior to statistical analysis, data were divided into two subsets, rate and placement. Each data set was analyzed as a randomized complete block design with four replications. Statistical analysis was conducted using SAS Version 9.4. (SAS Institute Inc.) PROC MIXED procedures were used to evaluate the effects of chamber position, nitrogen application rates or nitrogen application methods, and day of year on flux measurements. Within each site year, all main effects and interactions were evaluated. Across site years, PROC MIXED procedures were used to assess the effects of chamber position and nitrogen application rates or nitrogen application methods on flux measurements. Sites were selected intentionally based on climate conditions, so site year was evaluated as a fixed effect. Replication was included as a random effect. The subsets were evaluated for effects at all sites and at each individual site year. Alpha levels of 0.05 and 0.1 were used for statistical analyses.

Results & Discussion

Role of Chamber Placement in Assessing N_2O Emissions from Surface Banded UAN Rate Studies

There was an interaction between chamber position and rate ($p = 0.0043$, Table 3.2). The flux values from on-band chambers did increase with increasing nitrogen rate (Table 3.3, Figure 3.3). At higher nitrogen application rates, the effect of chamber placement was larger (Table 3.3, Figure 3.3). N_2O fluxes from the inter-row chambers numerically increase with increasing nitrogen fertilizer rate, while only statistically different from the control at the highest nitrogen application rate (201.8 kg ha^{-1}, Table 3.3, Figure 3.3). At fertilizer rates ≥ 134.5 kg ha^{-1}, the on-band chambers had higher flux values than the inter-row treatments ($p < 0.05$, Table 3.3, Figure 3.3). The main effect of chamber placement across all sites was significant, with the on-band chambers being higher than the inter-row chambers ($p < 0.0001$, Table 3.2). This corresponds with work done by De Klien and Harvey, (2015) in static chamber systems, where expected spatial variability, like fertilizer placement in a narrow band, necessitates the placement of multiple chambers to spatially represents and therefore weight this variability.

When evaluated further by site and site time, two sites showed strong support of the hypothesis that chamber placement impacts emission estimates in banded treatments. At GYD24, the inter-row chamber was different from the on-band chamber at a rate of 168.1 kg ha^{-1} and above (Table 3.4, Figure 3.4). At MRD24, the inter-row chamber was different from the on-band chamber at fertilizer application rates at or higher than 100.9 kg ha^{-1} (Table 3.5, Figure 3.5).

When evaluating effects from day of year (DOY) at GYD24, with all rates combined, only one sampling date, 173 (two weeks following fertilizer application), with exceptionally high fluxes (up to 12.14 nmol N_2O m^{-2} s^{-1}), resulted in a difference between the on-band and inter-row chambers (Table 3.6) All sampling dates besides DOY = 173 showed no differences between fluxes in the no nitrogen control and the inter-row chamber placement at all rates ($p < 0.05$). At MRD24, with all rates combined, only one sampling date, 228 (51 days following fertilizer application), with exceptionally high fluxes (up to 10.68 nmol N_2O m^{-2} s^{-1}), resulted in a difference between the on-band and inter-row chambers ($p < 0.05$; Table 3.7). All other sampling dates showed no differences between fluxes in the no nitrogen control and the inter-row chamber placement at all rates ($p > 0.05$). With the exception of DOY 173 at GYD24 and 228 at MRD24, recorded fluxes were relatively low and similar to recorded fluxes at other sites where differences were not observed. This difference in magnitude may have contributed to the differences observed between the control and the inter-row chamber placement on these specific dates. Days with conditions conducive to higher fluxes are when chamber positions are the most important for representing the space appropriately. Cai et al. (2012) reports N_2O flux values from the row plus interrow space to be greater than just the interrow space, indicating that if one of the chambers was missing, using the other chamber to substitute for the other would skew the results.

At THD and RND, the interaction between day of year and chamber position was not significant (Table 3.2). Most data from the site time analysis showed that there was no difference between fluxes in the no nitrogen control and the inter-row chamber placement at all rates ($p < 0.05$).

Since these collected flux values from the on-band and inter-row are different for the across site analysis ($p < 0.0001$) and for two of the four sites (MRD24, $p = 0.0471$; GYD24, 0.0306) (Table 3.2), if one chamber value is missing, the other chamber value cannot be substituted as the average for the entire plot area. This is supported by protocols from the static chamber method, which support the use of smaller chambers in both the row area and the inter-row area to represent the entire area of the plot (Parkin and Venterea, 2010). Even though the relationship is dependent on rate, having a consistent protocol for dealing with plots that are missing flux data from either the inter-row or on-band chamber will require that these plots be omitted from calculation. This work is consistent with protocols for use of the static chamber method developed by De Klien and Harvey (2015), which indicated that chambers placed in plots with expected spatial variability, like the stream banded fertilizer in our study, should be placed to represent this variability. With chamber placement having such clear effects on estimated daily flux, plots that do not have both chambers represented will likely be skewed by this spatial variability that requires both chambers to capture.

Role of Chamber Placement in Assessing N_2O Emissions from Broadcast, Surface Banded, and Subsurface Banded Nitrogen Fertilizer Placement Studies

Across all treatments (broadcast urea with urease inhibitor - NBPT, streamed UAN, coultered UAN, and no nitrogen control) and at all sites, the interaction between fertilizer placement and chamber position was not significant at $\alpha = 0.05$ but was significant at $\alpha = 0.1$ (Table 3.8). Main effects of chamber position and fertilizer placement method were both significant when all sites were analyzed together. The mean flux for the on-band chamber was 0.45 nmol N_2O m^{-2} s^{-1} and the mean flux for the inter-row chamber was 0.29 nmol N_2O m^{-2} s^{-1} indicating a strong overriding influence of chamber position ($p = 0.0001$, Table 3.8). The interaction of chamber position and placement, when evaluated at $\alpha = 0.1$, the on-band and inter-row chambers in the at-planting broadcasted treatment and the no nitrogen control did not show differences at any site (Table 3.9). In contrast to the broadcast treatments, when compared across all sites streamed UAN placements applied in a band at both application timings did show differences between flux values in the inter-row and on-band chambers ($p = 0.0768$, Table 3.9). However, coultered treatments applied in a band at planting did not show differences between the on-band and inter-row chambers, while coultered treatments applied in a band in the early treatment at MRD24 did result in difference (Table 3.9).

When evaluated by site, the hypothesis that non-banded treatments will not have a relationship with chamber position was partially supported. At MRD24, while there was no interaction between chamber position and fertilizer placement, chamber position as a main effect was significant (Table 3.8), suggesting that in addition to the influence of fertilizer, spatial variability potentially from other processes such as plant uptake support that the on-band and inter-row chambers are different from one another. Cai et al. (2012) reports N_2O flux values from the row plus interrow space to be greater than just the interrow space, indicating that if one of the chambers was missing, using the other chamber to substitute for the other would skew the results.

At GYD24, THD24, and RND25 no differences were detected between the two chambers in the broadcast urea with urease inhibitor - NBPT and no nitrogen control treatments ($p > 0.05$). Streamed and coultered UAN treatments applied in bands also did not show statistical differences between the on-band and inter-row chambers (Table 3.8).

Overall, these results conclusively show that there was no statistical difference between the on-band and inter-row chambers in the broadcast urea with urease inhibitor - NBPT and no nitrogen control treatments. This is supported by work from Folorunso and Rolston (1984), where chamber placement was investigated using the static chamber method and found that N_2O flux values were spatially independent of one another under broadcast organic fertilizer treatments. However, this spatial independence contrasts with work from Ambus and Christensen (1994) and Chadwick et al. (2014) that both report high N_2O emission variability over very short distances. Like broadcast and no nitrogen control treatments, coultered placements that were applied in bands at planting did not show a difference between the on-band and inter-row chambers (Table 3.9). However, coultered placement applied early did result in a difference between the two chambers (Table 3.9). This difference between the early and at-planting treatment suggests that there is potential for spatial dependence, even if not consistently observed in this work. This spatial independence shown from the coultered treatment at planting contrasts with work from Liu et al. (2023), that reports correlation between nitrogen fertilizer placement and chamber placement, though this study used a much higher rate of nitrogen fertilizer (285 kg ha^{-1}) than was applied in our work (67.3 kg ha^{-1}). The observed spatial independence in our study is likely due to this relatively low rate of nitrogen application (67.3 kg ha^{-1}), since we began observing differences between the on-band and inter-row chambers at rates higher than 100.9 kg ha^{-1} (Table 3.3).

These findings inform the decision to continue to use data from plots with either broadcast or no nitrogen control treatments where either the on-band or inter-row chamber had missing data, since the remaining chamber would represent a statistically similar flux level (Table 3.9). However, given the variability of collected results, plots with banded fertilizer application where either the on-band or inter-row chamber had missing data, should be omitted from analysis because of the potential of influence from the high concentration of fertilizer in one area.

Conclusion

In rate treatments applied as streamed UAN in a narrow band, chamber position resulted in a statistical difference between on-band and inter-row chambers at higher rates (> 100.9 kg ha^{-1}). The chambers located between fertilizer bands generally did not produce a flux that was statistically different from the daily no nitrogen control flux value. At lower nitrogen rates, chamber position had a much smaller effect on overall flux values. Chamber position as a main effect was highly significant when all sites were evaluated, meaning that regardless of fertilizer rate or placement relative to the chamber, there is enough inherent spatial variability from the added fertilizer in the evaluated area that these values should not be substituted for one another and that plots missing one of the two chambers should be omitted from the dataset. Overall, chamber position relative to fertilizer placement plays a major role, which informs the need to place chambers to represent expected spatial variability. These results also support omitting plots where the entire row area was not spatially represented, ensuring that the calculated mean flux represents expected or unexpected spatial variability.

References

Ambus, P., and S. Christensen. 1994. Measurement of N_2O emission from a fertilized grassland: An analysis of spatial variability. Journal of Geophysical Research 99(D8): 16549. doi: https://doi.org/10.1029/94jd00267.

Barrat, H.A., J. Evans, D.R. Chadwick, I.M. Clark, K. Le Cocq, et al. 2020. The impact of drought and rewetting on N_2O emissions from soil in temperate and Mediterranean climates. European Journal of Soil Science 72(6): 2504–2516. doi: https://doi.org/10.1111/ejss.13015.

Cai, Y., W. Ding, and J. Luo. 2012. Spatial variation of nitrous oxide emission between interrow soil and interrow plus row soil in a long-term maize cultivated sandy loam soil. Geoderma 181-182: 2–10. doi: https://doi.org/10.1016/j.geoderma.2012.03.005.

Chadwick, D.R., L. Cardenas, T.H. Misselbrook, K.A. Smith, R.M. Rees, et al. 2014. Optimizing chamber methods for measuring nitrous oxide emissions from plot-based agricultural experiments. European Journal of Soil Science 65(2): 295–307. doi: https://doi.org/10.1111/ejss.12117.

Climate Change & Infectious Diseases Group, and K. Brugger. 2017. World Maps of Köppen-Geiger Climate Classification. Vu-wien.ac.at. https://koeppen-geiger.vu-wien.ac.at/usa.htm.

Clough, T.J., P. Rochette, S.M. Thomas, M. Pihlatie, J.R. Christiansen, et al. 2020. Global Research Alliance N_2O chamber methodology guidelines: Design considerations. Journal of Environmental Quality 49(5): 1081–1091. doi: https://doi.org/10.1002/jeq2.20117.

De Klien, C., and M. Harvey. 2015. Nitrous Oxide Chamber Methodology Guidelines Version 1.1. https://www.ars.usda.gov/ARSUserFiles/31831/2012%20Chamber_Methodology_Guidelines_Chapter6.pdf

Granli, T., and O. Bøckman. 1994. Nitrous Oxide from Agriculture. Norwegian Journal of Agricultural Sciences. https://www.cabidigitallibrary.org/doi/full/10.5555/19941906345

Gruber, N., and J.N. Galloway. 2008. An Earth-system perspective of the global nitrogen cycle. Nature 451(7176): 293–296. doi: https://doi.org/10.1038/nature06592.

IPCC, 2007: Climate Change 2007: The Physical Science Basis. Contribution of Working Group I to the Fourth Assessment Report of the Intergovernmental Panel on Climate Change [Solomon, S., D. Qin, M. Manning, Z. Chen, M. Marquis, K.B. Averyt, M. Tignor and H.L. Miller (eds.)]. Cambridge University Press, Cambridge, United Kingdom and New York, NY, USA. https://www.ipcc.ch/site/assets/uploads/2020/02/ar4-wg1-sum_vol_en.pdf

IPCC, 2021: Climate Change 2021: The Physical Science Basis. Contribution of Working Group I to the Sixth Assessment Report of the Intergovernmental Panel on Climate Change [Masson-Delmotte, V., P. Zhai, A. Pirani, S.L. Connors, C. Péan, S. Berger, N. Caud, Y. Chen, L. Goldfarb, M.I. Gomis, M. Huang, K. Leitzell, E. Lonnoy, J.B.R. Matthews, T.K. Maycock, T. Waterfield, O. Yelekçi, R. Yu, and B. Zhou (eds.)]. Cambridge University Press, Cambridge, United Kingdom and New York, NY, USA, 2391 pp. doi:10.1017/9781009157896. https://www.ipcc.ch/report/ar6/wg1/

Johnson, F.E., R.N. Lerch, P.P. Motavalli, K.S. Veum, and P.C. Scharf. 2022. Spatial variability of denitrification enzyme activity and actual denitrification emissions on Missouri claypan soils. Soil Science Society of America Journal 86(6): 1582–1596. doi: https://doi.org/10.1002/saj2.20457.

LI-COR Biosciences. 2021. Using the Smart Chamber - Soil Gas Flux Survey Chamber. LI-COR Biosciences. https://www.licor.com/support/Smart-Chamber/topics/the-measurement-cycle.html

Liu, C., Y. Liu, W. Gao, K. Gao, J. Li, et al. 2023. The effect of chamber placement site on N_2O emission under different fertilizer regimes from maize field. Agriculture, Ecosystems & Environment 341: 108210. doi: https://doi.org/10.1016/j.agee.2022.108210.

Lu, C., Z. Yu, J. Zhang, P. Cao, H. Tian, et al. 2022. Century-long Changes and Drivers of Soil Nitrous Oxide (N_2O) Emissions across the Contiguous United States. Global Change Biology 28(7): 2505–2524. doi: https://doi.org/10.1111/gcb.16061.

Norton, J.M. 2008. Nitrification in Agricultural Soils. Agronomy Monographs: 173–199. doi: https://doi.org/10.2134/agronmonogr49.c6.

Parkin, T., and R. Venterea. 2010. USDA-ARS GRACEnet Project Protocols - Chamber-Based Trace Gas Flux Measurements. https://www.ars.usda.gov/ARSUserFiles/31831/2003GRACEnetTraceGasProtocol.pdf

Pennock, D.J., C. van Kessel, R.E. Farrell, and R.A. Sutherland. 1992. Landscape-Scale Variations in Denitrification. Soil Science Society of America Journal 56(3): 770–776. doi: https://doi.org/10.2136/sssaj1992.03615995005600030016x.

Ravishankara, A.R., J.S. Daniel, and R.W. Portmann. 2009. Nitrous Oxide (N_2O): the Dominant Ozone-Depleting Substance Emitted in the 21st Century. Science 326(5949): 123–125. doi: https://doi.org/10.1126/science.1176985.

Rudaz, A., E. Davidson, and M. Firestone. 1990. Source of Nitrous Oxide Production following Wetting of Dry Soil. https://www.sciencedirect.com/science/article/abs/pii/0378109791905077

Schwenke, G.D., and B.M. Haigh. 2016. The Interaction of Seasonal Rainfall and Nitrogen Fertiliser Rate on Soil N_2O Emission, Total N Loss and Crop Yield of Dryland Sorghum and Sunflower Grown on sub-tropical Vertosols. Soil Research 54(5): 604. doi: https://doi.org/10.1071/sr15286.

Tallec, T., A. Brut, L. Joly, N. Dumelié, D. Serça, et al. 2019. N_2O flux measurements over an irrigated maize crop: A comparison of three methods. Agricultural and Forest Meteorology 264: 56–72. doi: https://doi.org/10.1016/j.agrformet.2018.09.017.

Tian, H., R. Xu, J.G. Canadell, R.L. Thompson, W. Winiwarter, et al. 2020. A Comprehensive Quantification of Global Nitrous Oxide Sources and Sinks. Nature 586(7828): 248–256. doi: https://doi.org/10.1038/s41586-020-2780-0.

US Environmental Protection Agency. 2024. Inventory of U.S. Greenhouse Gas Emissions and Sinks: 1990-2022. www.epa.gov. https://www.epa.gov/ghgemissions/inventory-us-greenhouse-gas-emissions-and-sinks-1990-2022.

USDA NRCS. 2019. Web Soil Survey. usda.gov. https://websoilsurvey.nrcs.usda.gov/app/.

Wang, H., Z. Yan, X. Ju, X. Song, J. Zhang, et al. 2023. Quantifying Nitrous Oxide Production Rates from Nitrification and Denitrification under Various Moisture Conditions in Agricultural Soils: Laboratory Study and Literature Synthesis. Frontiers in Microbiology 13. doi: https://doi.org/10.3389/fmicb.2022.1110151.

Tables

Table 3.1 Descriptions of evaluated site years including 30-year average annual precipitation and temperature (Office of the State Climatologist, 2020), Köppen Climate Classification, elevation, and soil type (USDA NRCS, 2019).**

Site*	30-Year Average Annual Precipitation	30-Year Average Annual Temperature	Köppen Climate Classification**	Elevation	Soil Type
	mm	°C		m	
MRD24	860	12.5	Cfa	416	Irwin silty clay loam
GYD24	550	12.8	Bsk	851	Richfield silt loam
THD24	500	11.2	Bsk	1005	Keith silt loam
RND25	770	13.5	Cfa	467	Shellabarger sandy loam

*(MRD24, Morris County, KS in 2024; GYD24, Gray County, KS in 2024; THD24, Thomas County, KS in 2024; RND25, Reno County, KS in 2025)
** Köppen Climate Classification (Cfa, humid sub-tropical climate; Bsk, cold semi-arid climate) obtained from Climate Change & Infectious Diseases Group and Brugger, (2017) based on the data of Kotteck et al. (2006)

Table 3.2 Analysis of Variance (ANOVA) table for four site years*, MRD24, GYD24, THD24, and RND25 evaluating relationships between chamber position, nitrogen fertilizer application rate (Rate), and day of year (DOY). Bolded values represent statistical significance at $p < 0.05$.

	All Sites	MRD24	GYD24	THD24	RND25
Chamber Position**	**<0.0001**	**<0.0001**	**0.0059**	0.6719	0.1413
Rate	**<0.0001**	**<0.0001**	**<0.0001**	**0.0063**	**<0.0001**
Chamber Position*Rate	**0.0043**	**0.0471**	**0.0306**	0.2553	0.3375
DOY	.	**<0.0001**	**<0.0001**	**<0.0001**	**<0.0001**
DOY*Chamber Position	.	**<0.0001**	**<0.0001**	0.9966	0.2753
DOY*Rate	.	**<0.0001**	**<0.0001**	**<0.0001**	**<0.0001**
DOY*Chamber Position*Rate	.	0.1427	0.1898	0.9366	0.9947

*(MRD24, Morris County, KS in 2024; GYD24, Gray County, KS in 2024; THD24, Thomas County, KS in 2024; RND25, Reno County, KS in 2025)

****p values presented represent comparisons of least square means between the inter-row chamber and the on-band chamber within each nitrogen rate.

Table 3.3 Comparison of estimate values for all evaluated site years*, evaluating relationships between chamber position and nitrogen fertilizer application rate (Rate) applied as a stream over the on-band chamber position. Letters indicate statistical significance at $p < 0.05$.

	Chamber Position	
Rate	On-Band	Inter-Row
kg ha^{-1}	---------------------------- nmol N_2O m^{-2} s^{-1}	-------------------------------
0	0.22 E	0.23 DE
33.6	0.28 CDE	0.36 BCDE
67.3	0.53 BCDE	0.43 BCDE
100.9	0.73 B	0.37 BCDE
134.5	1.27 A	0.55 BCDE
168.1	1.44 A	0.62 BCD
201.8	1.20 A	0.65 BC

*(MRD24, Morris County, KS in 2024; GYD24, Gray County, KS in 2024; THD24, Thomas County, KS in 2024; RND25, Reno County, KS in 2025)

Table 3.4 Comparison of estimate values for GYD24*, evaluating relationships between chamber position and nitrogen fertilizer application rate (Rate) applied as a stream over the on-band chamber position. Letters indicate statistical significance at $p < 0.05$.

	Chamber Position	
Rate	On-Band	Inter-Row
kg ha^{-1}	---------------------------- nmol N_2O m^{-2} s^{-1}	----------------------------
0	0.21 D	0.10 D
33.6	0.43 D	0.86 CD
67.3	0.43 D	0.50 D
100.9	0.66 D	0.61 D
134.5	2.39 AB	0.93 BCD
168.1	3.09 A	1.04 BCD
201.8	2.32 ABC	0.64 D

*(MRD24, Morris County, KS in 2024; GYD24, Gray County, KS in 2024; THD24, Thomas County, KS in 2024; RND25, Reno County, KS in 2025)

Table 3.5 Comparison of estimate values for MRD24*, evaluating relationships between chamber position and nitrogen fertilizer application rate (Rate) applied as a stream over the on-band chamber position. Letters indicate statistical significance at $p < 0.05$.

	Chamber Position	
Rate	On-Band	Inter-Row
kg ha^{-1}	---------------------------- nmol N_2O m^{-2} s^{-1}	----------------------------
0	0.35 C	0.40 C
33.6	0.35 C	0.24 C
67.3	0.88 BC	0.58 C
100.9	1.65 A	0.46 C
134.5	1.27 AB	0.60 BC
168.1	1.78 A	0.72 BC
201.8	1.66 A	0.59 BC

*(MRD24, Morris County, KS in 2024; GYD24, Gray County, KS in 2024; THD24, Thomas County, KS in 2024; RND25, Reno County, KS in 2025)

Table 3.6 Comparison of estimate values for GYD24*, evaluating relationships between chamber position and day of year (DOY) applied as a stream over the on-band chamber position. Letters indicate statistical significance at $p < 0.05$.

	Chamber Position	
DOY	On-Band	Inter-Row
	---------------------------- nmol N_2O m^{-2} s^{-1} ----------------------------	
166	1.19 CD	1.32 CD
173	12.14 A	4.04 B
180	0.88 CD	0.18 D
193	2.70 BC	0.66 CD
200	0.42 D	0.06 D
207	0.07 D	0.04 D
215	0.23 D	0.07 D
227	-0.06 D	0.97 CD
236	0.01 D	-0.01 D
243	0.30 D	0.03 D
250	0.07 D	-0.01 D
257	-0.01 D	-0.01 D
285	-0.12 D	-0.07 D

*(MRD24, Morris County, KS in 2024; GYD24, Gray County, KS in 2024; THD24, Thomas County, KS in 2024; RND25, Reno County, KS in 2025)

Table 3.7 Comparison of estimate values for MRD24*, evaluating relationships between chamber position and day of year (DOY) applied as a stream over the on-band chamber position. Letters indicate statistical significance at $p < 0.05$.

	Chamber Position	
DOY	On-Band	Inter-Row
	--------------------------- nmol N_2O m^{-2} s^{-1} ---------------------------	
185	1.72 C	1.47 CD
192	1.48 C	0.89 CDEFG
199	0.23 EFG	0.17 FG
205	0.19 FG	0.19 FG
215	1.03 CDEF	0.56 CDEFG
219	0.26 EFG	0.09 FG
228	10.68 A	3.56 B
235	1.28 CDE	0.34 DEFG
240	0.39 DEFG	0.04 FG
247	0.06 FG	0.04 FG
254	0.03 FG	-0.01 FG
261	0.02 FG	-0.01 FG
269	0.71 CDEFG	0.29 DEFG
276	0.05 FG	-0.03 FG
283	-0.04 FG	-0.05 G
290	-0.03 FG	-0.03 FG
297	-0.05 G	-0.06 G

*(MRD24, Morris County, KS in 2024; GYD24, Gray County, KS in 2024; THD24, Thomas County, KS in 2024; RND25, Reno County, KS in 2025)

Table 3.8 Analysis of Variance (ANOVA) table for four site years*, MRD24, GYD24, THD24, and RND25 evaluating relationships between chamber position and nitrogen fertilizer application placement (Placement). Bolded values represent statistical significance at $p < 0.05$.

	All Sites	**MRD24**	**GYD24**	**THD24**	**RND25**
Chamber Position**	**0.0001**	**0.0039**	0.5057	0.2773	0.9554
Placement	**0.0009**	**0.0087**	0.3642	**0.0482**	**<0.0001**
Placement*Chamber Position	0.0768	0.2028	0.3152	0.8834	0.6374

*(MRD24, Morris County, KS in 2024; GYD24, Gray County, KS in 2024; THD24, Thomas County, KS in 2024; RND25, Reno County, KS in 2025)

******p values presented represent comparisons of least square means between the inter-row chamber and the on-band chamber within each nitrogen placement.

Table 3.9 Comparison of estimate values for all sites*, evaluating relationships between chamber position and nitrogen fertilizer application method (Placement) including treatments applied at planting and early (one month prior to planting). Letters indicate statistical significance at $p < 0.1$.

	Chamber Position	
Placement	On-Band	Inter-Row
	------------------- nmol N_2O m^{-2} s^{-1} ----------------------	
Control	0.25 FG	0.22 G
Early – Broadcast Treated Urea	0.47 ABCD	0.28 DEFG
Early – Streamed UAN	0.61 AB	0.18 FG
Early – Coultered UAN	0.55 ABC	0.26 EFG
At Planting – Broadcast Urea with Urease Inhibitor - NBPT	0.37 CDEF	0.37 CDEF
At Planting – Streamed UAN	0.59 A	0.41 BCDE
At Planting – Coultered UAN	0.30 DEFG	0.30 DEFG

*(MRD24, Morris County, KS in 2024; GYD24, Gray County, KS in 2024; THD24, Thomas County, KS in 2024; RND25, Reno County, KS in 2025)

Figures

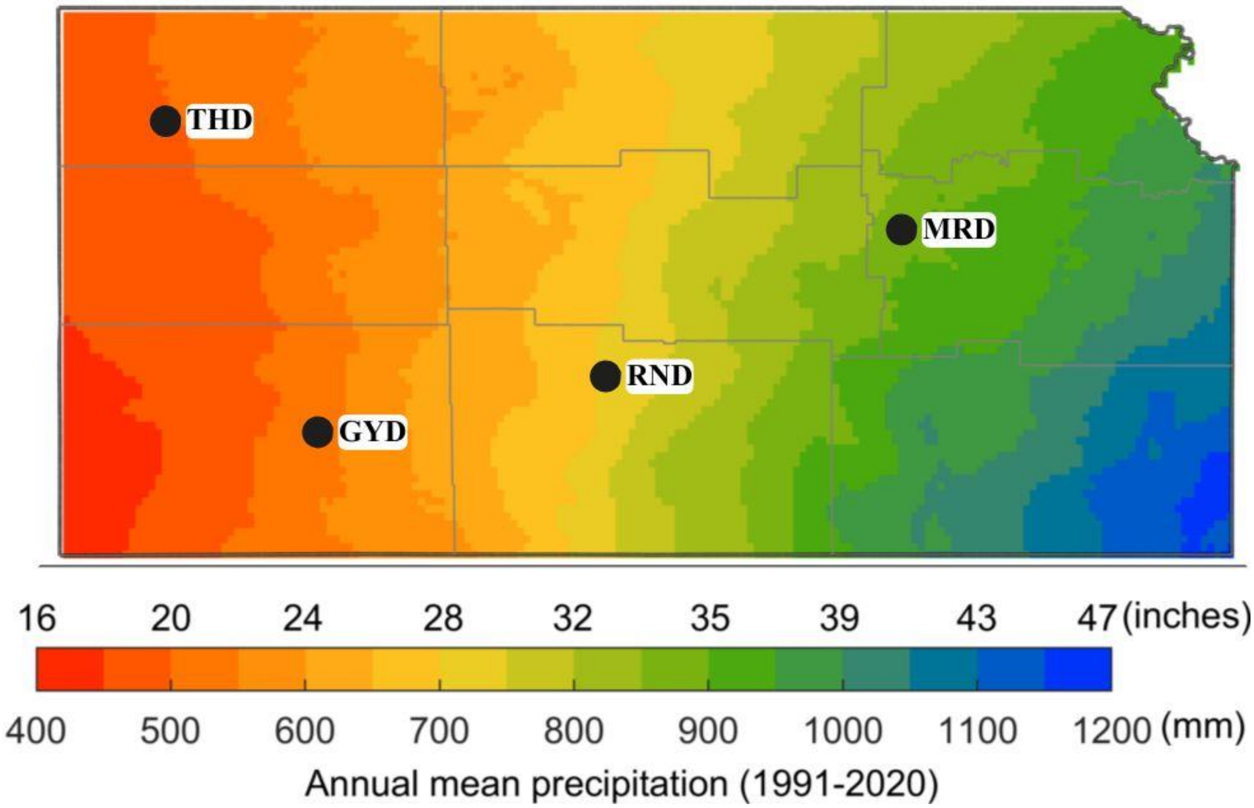

Figure 3.1 Thomas County, KS (THD), Gray County, KS (GYD), Reno County, KS (RND), and Morris County, KS (MRD) field site locations across Kansas represent three distinct precipitation environments (adapted from the Office of the Kansas State Climatologist, 2020).

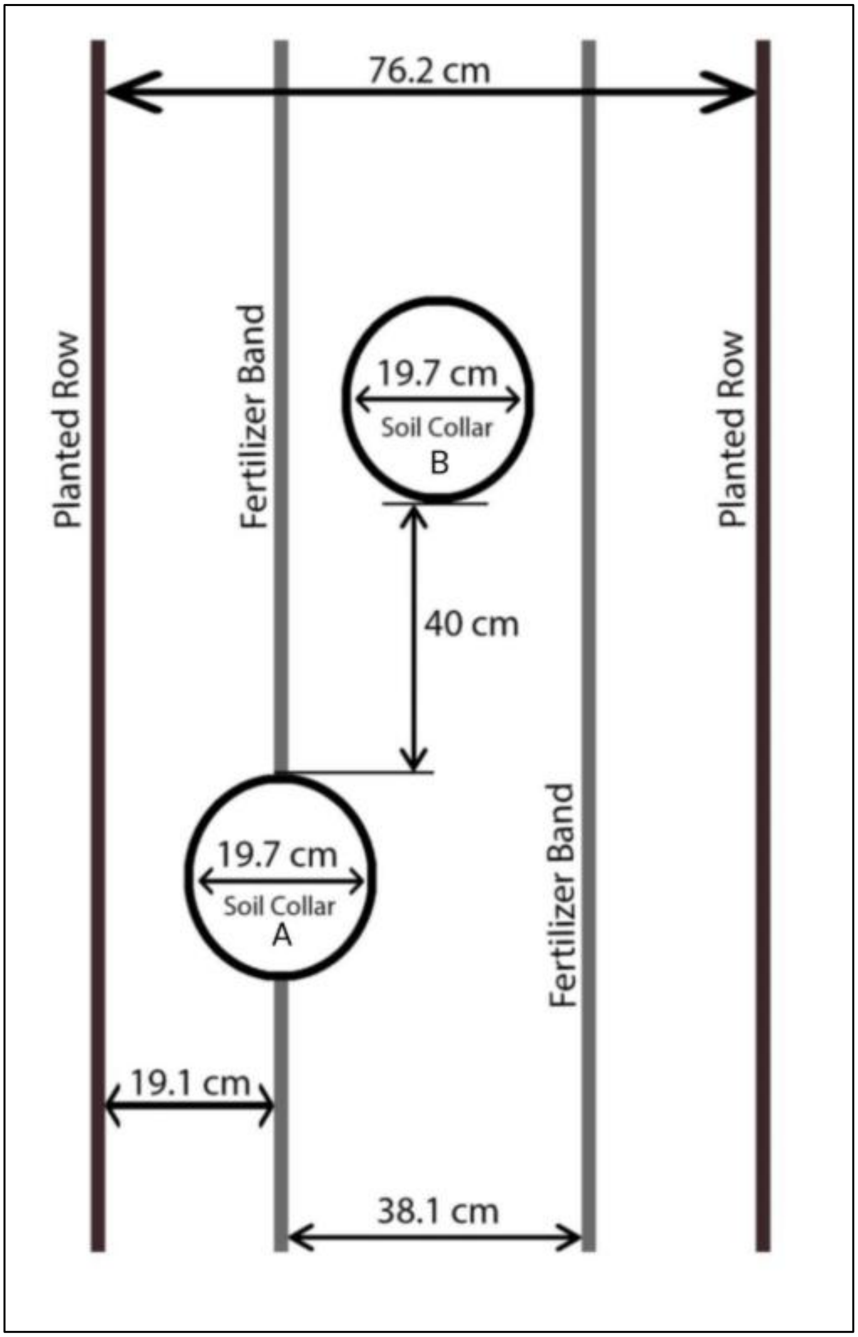

Figure 3.2 In-season soil collar placement for nitrous oxide (N_2O) sample collection to spatially represent both on-band and between-band treatments.

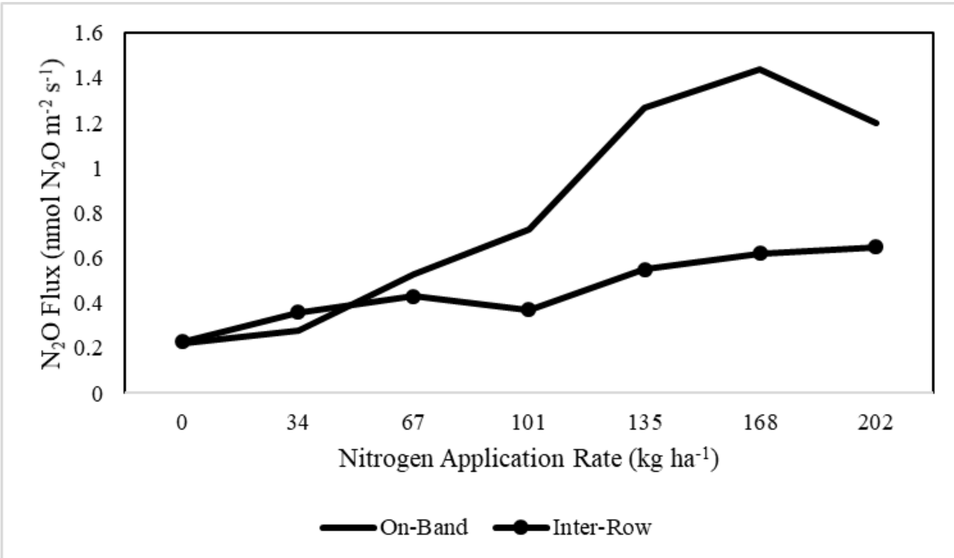

Figure 3.3 Comparison of estimate values for all evaluated site years, evaluating relationships between chamber position and nitrogen fertilizer application rate (Rate) applied as a stream over the on-band chamber position.

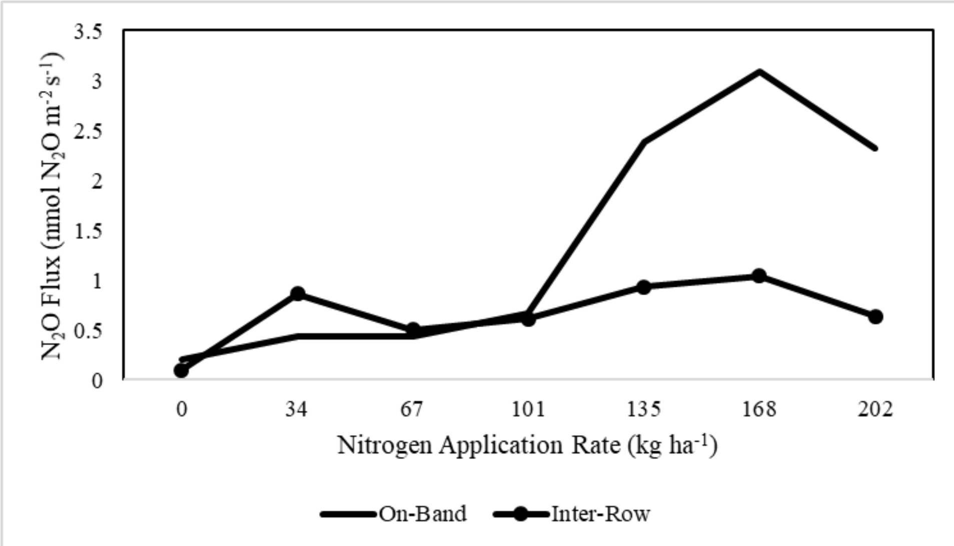

Figure 3.4 Comparison of estimate values for GYD24, Gray County in 2024, evaluating relationships between chamber position and nitrogen fertilizer application rate (Rate) applied as a stream over the on-band chamber position.

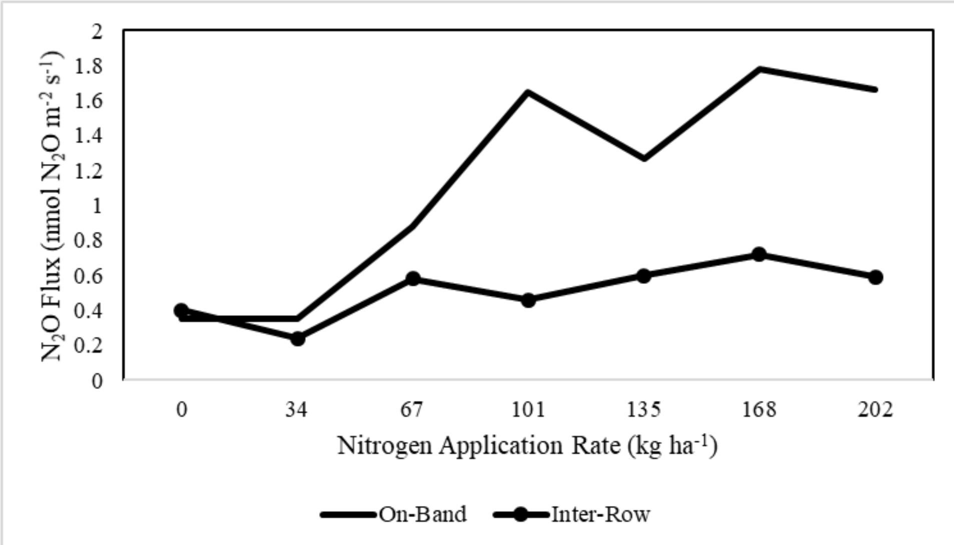

Figure 3.5 Comparison of estimate values for MRD24, Morris County in 2024, evaluating relationships between chamber position and nitrogen fertilizer application rate (Rate) applied as a stream over the on-band chamber position.

Chapter 4 - Nitrous Oxide Emissions from Grain Sorghum Production

Abstract

The Intergovernmental Panel on Climate Change (IPCC) approximates the global warming potential of N_2O at 300 times that of carbon dioxide. More than one third of all N_2O emissions are anthropogenic and are primarily due to agriculture. This study aims to compare N_2O emissions from sorghum fields under varying precipitation regimes and fertilizer management, to assess whether the IPCC default emissions factor of 1% overestimates these emissions and to evaluate how disaggregating this factor based on environmental and management factors could improve its accuracy. Field trials were conducted over six site years with a range of annual precipitation (350 mm -700 mm). The study evaluated six nitrogen application rates of streamed UAN (including a control), along with three additional product & placement combinations, evaluated both at planting and one month prior to planting. N_2O fluxes were measured using an N_2O/H_2O trace gas flux analyzer (Model 7820, LI-COR) and portable Smart Chamber system (Model 8200-01, LI-COR) and processed using Soil Flux Pro software (Version 5.3.1, LI-COR). Analysis of cumulative N_2O emissions data show an influence of nitrogen application rate on cumulative N_2O flux at all evaluated site years ($p < 0.0001$). Increasing nitrogen fertilizer application rates resulted in higher cumulative N_2O emissions ($p < 0.05$). Overall, nitrogen fertilizer applied one month prior to planting did not show any differences between nitrogen fertilizer application methods. Sorghum grown in dryer environments generally did result in lower cumulative N_2O emissions compared to sorghum grown in wetter environments with similar nitrogen treatments. N_2O emissions from grain

sorghum did not always peak within the first two weeks following nitrogen application, but a peak was observed within the first month following nitrogen application, typically following a rainfall event. Overall, increasing nitrogen rate did not result in increased N_2O emission factors and subsurface placement with a coulter or addition of the urease inhibitor – NBPT (N-(n-butyl) thiophosphoric triamide) did not clearly reflect a reduction in emissions factors in evaluated environments. The EF values calculated, specifically those from the more characteristic rainfall year, 2025, are largely in-line with IPCC's disaggregated EF value for arid and semiarid environments of 0.5 percent (IPCC, 2019).

Key Findings

- Increasing nitrogen fertilizer application rates resulted in higher cumulative N_2O emissions.

- Overall, increasing nitrogen rate did not result in increased N_2O emission factors and subsurface placement with a coulter or addition of a urease inhibitor did not clearly reflect a reduction in emissions factors in evaluated environments.

- EF values, specifically those from the more characteristic rainfall year, 2025, are largely in-line with IPCC's disaggregated EF value for arid and semiarid environments of 0.5 percent (IPCC, 2019).

Introduction

Greenhouse gases result from both natural and anthropogenic sources that absorb and emit radiation at specific wavelengths which result in the greenhouse effect (IPCC, 2012). Water vapor (H_2O), carbon dioxide (CO_2), nitrous oxide (N_2O), methane (CH_4), and ozone (O_3) are the primary greenhouse gases in the Earth's atmosphere (IPCC, 2012). Of these gases, agricultural production mainly contributes to the emission of methane, carbon dioxide, and nitrous oxide (Adegbeye et al., 2020; IPCC 2007).

Of these greenhouse gases, N_2O has very powerful effects in the atmosphere. N_2O contributes to ozone depletion and requires 114 years to decay in the atmosphere, compared to methane's 12 years (IPCC, 2007; Ravishankara et al., 2009). Over a 100-year timeline, N_2O has a global warming potential that is approximately 300 times that of carbon dioxide (IPCC, 2007; US Environmental Protection Agency, 2024). The global atmospheric N_2O concentration has increased from a pre-industrial level of approximately 270 ppb to 319 ppb in 2005 (IPCC, 2007). In 2019, the concentration of N_2O in the atmosphere was 332 ppb (IPCC, 2021). This increase in atmospheric concentration is, in part, due to the increased use of nitrogen fertilizers during the same period. Increased nitrogen fertilizer use accounted for 64% of the agricultural soil N_2O emissions increase since 1900 (Lu et al., 2022).

Agricultural practices can be used to decrease N_2O emissions from cropping systems. Most N_2O emissions occur during periods when the soil is moist. N_2O production in all soils increases with increasing soil moisture, with little N_2O emitted from dry soils (Barton et al., 2007; Pihlatie et al., 2004; Storlien et al., 2014; Storlien et al., 2013). Daily N_2O emissions are best correlated with precipitation and water filled pore space (Barton et al., 2007; Malhi and Lemke, 2007). With these emissions increasing when soil is moist, crops like sorghum, that are grown in areas with lower rainfall, could show less N_2O emissions over time. In grain sorghum experiments, dry weather resulted in lower N_2O emissions and fewer detectable fluxes (Barton et al., 2007; Storlien et al., 2013). The Intergovernmental Panel on Climate Change (IPCC) uses a default emissions factor of 1% for modeling N_2O emissions from managed soils receiving nitrogen additions (IPCC, 2006). This means that 1% of applied nitrogen is assumed to be lost as N_2O to the atmosphere. In 2019, the IPCC revised default emissions factors based on environment. In wet environments, synthetic nitrogen fertilizer application has a default emission factor of 1.6 %. In dry climates, the default emission factor for synthetic nitrogen fertilizer was adjusted to 0.5% (IPCC, 2019). The default emission factor synthetic nitrogen fertilizer for all other environments remains at 1.0% (IPCC, 2019). With emissions decreasing when soil is dry, crops like sorghum, that are grown in areas with lower rainfall, are expected to show less N_2O emissions overall.

Nitrogen management practices like fertilizer rate and placement can impact the N_2O emissions from agricultural soils. Consistently, deeper placement of nitrogen fertilizer within the soil results in lower N_2O emissions in sorghum systems (Fertitta-Roberts et al., 2017; Van Kessel et al., 2012). Shallow and surface placement result in higher N_2O emissions across multiple studies (Fertitta-Roberts et al., 2017; Halvorson and Del Grosso, 2013; Rychel et al., 2020). Fertilizer rates have had varied effects on N_2O emissions. Higher rates of nitrogen fertilizer application have increased N_2O emissions across many studies and cropping systems (Malhi and

Lemke, 2007; Preza-Fontes et al., 2020; Schwenke and Haigh, 2016). In Tribune, Kansas, the recommended nitrogen application rate providing optimum economic return is approximately 135kg N ha^{-1} (Schlegel and Havlin, 2020). Conversely, increased fertilizer rates did not increase N_2O emissions according to Barton et al. (2007) and Gehl et al. (2020). Given these mixed results, further research is needed to understand how fertilizer rate, placement, timing and product impact N_2O emissions across different precipitation regimes.

The objective of this study was to quantify N_2O emissions during grain sorghum growing seasons across a rainfall gradient under various nitrogen management practices. The hypotheses were: (i) sorghum grown in drier environments will exhibit lower cumulative N_2O emissions than sorghum grown in wetter environments with similar nitrogen treatments; (ii) daily N_2O emissions from grain sorghum crop fields will peak in the first two weeks following nitrogen application; (iii) nitrogen management practices involving lower application rates, the use of a urease inhibitor - NBPT, and deeper placement will result in reduced N_2O emissions over the growing season.

Materials and Methods

Site Descriptions

Over the course of two growing seasons (2024 and 2025), experiments were conducted at six different site locations across a precipitation gradient in Kansas. The first and easternmost location (MRD24) for the 2024 growing season was in Morris County (Lat/Long: 38° 47' 35.5914", -96° 48' 53.8554") at an approximate elevation of 416 meters. The soil type is classified as Irwin silty clay loam, with a taxonomic classification of fine, mixed, superactive, mesic Pachic Argiustoll (USDA NRCS, 2019). The region has a humid subtropical climate (Köppen Climate Classification: Cfa), obtained from Climate Change & Infectious Diseases Group and Brugger, (2017) based on the data of Kotteck et al. (2006). The region has an average annual precipitation of 860 mm and an average annual temperature of 13 °C (30-year average) (Office of the Kansas State Climatologist, 2020).

For the 2025 growing season, the first and easternmost location (RND25) was in Reno County (Lat/Long: 37° 53' 18.456", -98° 2' 49.092") at an approximate elevation of 467 meters. The soil type is mainly classified as Shellabarger sandy loam, with a taxonomic classification of fine-loamy, mixed, superactive, mesic Udic Argiustoll (USDA NRCS, 2019). The region has a humid subtropical climate (Köppen Climate Classification: Cfa), obtained from Climate Change & Infectious Diseases Group and Brugger, (2017) based on the data of Kotteck et al. (2006). The region has an average annual precipitation of 770 mm and an average annual temperature of 13 °C (30-year average) (Office of the Kansas State Climatologist, 2020).

The second location (GYD24) for the 2024 growing season was in Gray County (Lat/Long: 37° 34' 32.412", -100° 24' 32.2554") at an approximate elevation of 851 meters. The soil type is classified as mainly Richfield silt loam, with a taxonomic classification of fine, smectitic, mesic Aridic Argiustoll (USDA NRCS, 2019). The region has a cold semi-arid climate (Köppen Climate Classification: Bsk), obtained from Climate Change & Infectious Diseases Group and Brugger, (2017) based on the data of Kotteck et al. (2006). The region has an average annual precipitation of 550 mm and an average annual temperature of 13 °C (30-year average) (Office of the Kansas State Climatologist, 2020).

The second location (GYD25) for the 2025 growing season was in Gray County (Lat/Long: 37° 38' 40.308", -100° 25' 58.1874") at an approximate elevation of 850 meters. The soil type is classified as mainly Harney silt loam, with a taxonomic classification of fine, smectitic, mesic Typic Argiustoll (USDA NRCS, 2019). The region has a cold semi-arid climate (Köppen Climate Classification: Bsk), obtained from Climate Change & Infectious Diseases Group and Brugger, (2017) based on the data of Kotteck et al. (2006). The region has an average annual precipitation of 540 mm and an average annual temperature of 13 °C (30-year average) (Office of the Kansas State Climatologist, 2020).

The third and westernmost location (THD24) for the 2024 growing season was in Thomas County (Lat/Long: 39° 14' 5.4954", -101° 12' 11.8434"°) at an approximate elevation of 1005 meters. The soil type is classified as mainly Keith silt loam, with a taxonomic classification of fine-silty, mixed, superactive, mesic Aridic Argiustoll (USDA NRCS, 2019). The region has a cold semi-arid climate (Köppen Climate Classification: Bsk) obtained from Climate Change & Infectious Diseases Group and Brugger, (2017) based on the data of Kotteck et al. (2006). The region has an average annual precipitation of 500 mm and an average annual temperature of 11 °C (30-year average) (Office of the Kansas State Climatologist, 2020).

The third and westernmost location (THD25) for the 2025 growing season was in Thomas County (Lat/Long: 39° 18' 0.612", -101° 12' 21.276") at an approximate elevation of

1010 meters. The soil type is classified as mainly Ulysses silt loam, with a taxonomic classification of Fine-silty, mixed, superactive, mesic Aridic Haplustoll (USDA NRCS, 2019). The region has a cold semi-arid climate (Köppen Climate Classification: Bsk), obtained from Climate Change & Infectious Diseases Group and Brugger, (2017) based on the data of Kotteck et al. (2006). The region has an average annual precipitation of 500 mm and an average annual temperature of 11 °C (30-year average) (Office of the Kansas State Climatologist, 2020).

Experimental Design

At each study location, twenty-six treatments were assigned to 4 blocks using a spatial optimization procedure (Coombes, 2009). The plot size at all locations was 3.05 meters by 12.20 meters. Treatments consist of a factorial of six application methods by two timings at a common nitrogen rate, 6 nitrogen rates applied as streamed UAN, and a zero applied nitrogen control. This arrangement allows for quantification of both nitrogen use efficiency as affected by method and time of nitrogen application as well as quantification of the overall nitrogen response characteristics of that particular site-year from the array of nitrogen rates. Treatment levels in the factorial include 6 application methods: dry broadcast urea, dry broadcast urea treated with urease inhibitor - NBPT (N-(n-butyl) thiophosphoric triamide) (Agrotain, 1.05 L metric ton urea^{-1}), streamed UAN (offset 19.1 cm on either side of the planted row), streamed UAN treated with a urease inhibitor – NBPT (Agrotain, 2.1 L metric ton urea^{-1}; offset 19.1 cm on either side of the planted row), coultered UAN (offset 19.1 cm on either side of the planted row, placed at approximately 7.6 cm deep), and sprayed UAN, and at two timings of nitrogen application. Application timings are all prior to planting grain sorghum and include an at planting application and an application one month (4 weeks) prior to planting (Table 4.1). In the method x timing factorial plots, nitrogen was applied at a reduced rate of 67.3 kg N ha^{-1}. The 6 nitrogen rate treatments, applied as streamed UAN, offset 19.1 cm on either side of the planted row, were 33.6, 67.3, 100.9, 134.5, 168.1, and 201.8 kg N ha^{-1} applied at planting for each location (Table 4.1). Grain sorghum was planted in June in 76.2 cm rows at 123,500 seeds ha^{-1} and was harvested in October or November (Table 4.1).

Soil Nitrous Oxide Emission Measurements and Calculations

Soil nitrous oxide (N_2O) emissions were measured using an N_2O/H_2O trace gas analyzer (Model 7820, LI-COR) paired with a portable Smart Chamber system (Model 8200-01, LI-COR). Measurements were collected from four replicate plots at each site for the following fertilizer rates (0, 33.6, 67.3, 100.9, 134.5, 168.1, 201.8 kg N ha^{-1}) as streamed UAN and placements applied at 67.3 kg N ha^{-1} as broadcast urea treated with a urease inhibitor – NBPT (Agrotain, 1.05 L metric ton $urea^{-1}$), streamed UAN, and coultered UAN. Additionally, N_2O fluxes were collected, at MRD24, GYD25, and THD25 from placement treatments applied one month prior to planting at 67.3 kg N ha^{-1} as broadcast urea treated with a urease inhibitor – NBPT (Agrotain, 1.05 L metric ton $urea^{-1}$), streamed UAN, and coultered UAN.

Two PVC collars (19.7 cm inner diameter x 11 cm long) were inserted approximately 6 cm into the soil, leaving 5 cm exposed above the soil surface were installed in the interrow between the second and third rows of each plot, to represent half of the row width, 38.1 cm, with placement resulting in less than 2.2% overlap between chambers. The collars were installed after planting/fertilization and remained in place throughout the duration of the growing season. Since the collars were identical in size and installed under the same conditions, N_2O fluxes from each collar were averaged to estimate a representative flux across the row. N_2O flux measurements were collected weekly at all site locations during the growing season. Measurements were generally taken between 6:00 and 14:00 (CST). On each sampling date, the portable smart chamber head was placed over the soil collar. N_2O flux measurements were then collected with a 120 second observation time, a 25 second deadband, and a 45 second post purge (LI-COR Biosciences, 2021). Realtime data viewing in the field was used to monitor analyzer performance. Data were collected and stored in the Portable Smart Chamber, including N_2O flux, diagnostic code values, total chamber volume, date, and time.

Data were downloaded and initially processed using Soil Flux Pro software (Version 5.3.1, LI-COR). This software was also used to input collar height information to adjust the total volume, calculate the flux (nmol N_2O m^{-2} s^{-1}), and evaluate each individual flux measurement to verify proper chamber and analyzer operation, omitting data collected when a diagnostic code was issued from the analyzer. Flux measurements that displayed irregular patterns or signs of analyzer malfunction, such as skips where N_2O concentration was not collected, major N_2O concentration jumps, or major N_2O concentration drops, indicating an issue with the chamber seal or analyzer pressure as identified in Soil Flux Pro software, were reviewed and excluded from the dataset to ensure data quality. Additionally, plots missing measurements from either the on-band or inter-row chamber were excluded from flux calculations.

Appropriate unit conversion and the molar mass of the nitrogen molecule (28.0134 g mol^{-1}) were used to adjust the flux to a nitrogen mass per area-time basis (g N_2O-N ha^{-1} day^{-1}) (Equation 4.1). Daily N_2O flux for each treatment was calculated by averaging two chambers per row within each plot, and negative, near-zero flux values were set to 0. Data representing plots missing one or both chamber measurements at a given sampling time were omitted and replaced with an average of the other evaluated reps. Cumulative N_2O emissions were estimated using daily flux values and the trapezoidal integration method, following the approach of Venterea et al. (2011), which assumes linear flux changes between measurement dates (Equation 4.2). Nitrogen-induced emissions were calculated to estimate N_2O emissions from nitrogen fertilizer application by subtracting background emissions measured from unfertilized control plots (Equation 4.3). The emissions factor (EF) was calculated as a percentage of nitrogen fertilizer applied that was lost as N_2O during the entire growing season (Equation 4.4).

$$\text{Daily Flux (g N}_2\text{O-N ha}^{-1}) = \frac{nmol\ N_2O}{m^2 \cdot s} \cdot \frac{mol\ N_2O}{(1 \cdot 10^9)nmol\ N_2O} \cdot \frac{3600\ s}{h} \cdot \frac{24\ h}{d} \cdot \frac{28.0134\ g\ of\ N}{mol\ N_2O} \cdot \frac{10,000\ m^2}{ha}$$

Equation 4.1 Daily flux calculation where m is meters, s is seconds, h is hours, d is days, g is grams, and ha is hectare.

$$\text{Cumulative flux (kg N}_2\text{O-N ha}^{-1}) = \sum_{i=1}^{n} \left[\frac{X_i\ + X_{(i+1)}}{2}\right] \cdot \left(T_{(i+1)}\ - T_i\right)$$

Equation 4.2 Cumulative flux calculation, where X_i is daily flux at initial time, $X_{(i+1)}$ is daily flux at final time, T_i is time of initial flux, and $T_{(i+1)}$ is time of final flux.

$$\underset{(\text{g N}_2\text{O-N ha}^{-1})}{\text{Nitrogen induced emissions}} = \underset{(\text{g N}_2\text{O-N ha}^{-1})}{\textit{Cumulative flux of treatment}} - \underset{(\text{g N}_2\text{O-N ha}^{-1})}{\textit{Cumulative flux of control}}$$

Equation 4.3 Nitrogen-induced emissions (NIE) calculation.

$$\text{Emissions factor } (\%) = \frac{Nitrogen\ induced\ emissions\ \left(g\ N_2O - N\ ha^{-1}\right)}{Nitrogen\ \ fertilizer\ applied\ (g\ N\ ha^{-1})}$$

Equation 4.4 Emissions factor (EF) calculation.

Statistical Analysis

Prior to statistical analysis, data were divided into two subsets, rate treatments and placement treatments. Each data set was analyzed as a randomized complete block design with four replications. Statistical analysis was conducted using SAS Version 9.4. (SAS Institute Inc.) PROC MIXED procedures were used to assess relationships between nitrogen application rates or nitrogen application methods and cumulative N_2O emissions. Plots were located at a new location each year, so site year could be considered random, but sites were selected intentionally based on climate conditions, so site year is evaluated as a fixed effect. Replication was included as a random effect. An alpha level of 0.05 was used for all statistical analyses.

Results

Precipitation

During the 2024 growing season, the easternmost site, MRD24 (June-October), received 231.8 mm of precipitation, 258.8 mm less than the 30-year normal precipitation for the county (Table 4.2). This precipitation was concentrated during the beginning of the season (Table 4.3). During the 2025 growing season, the easternmost site, RND25 (June-October), received 422.7

mm of precipitation, 82.3 mm more than the 30-year normal precipitation for the county (Table 4.2). This precipitation was well distributed throughout the growing season (Table 4.3).

In the 2024 growing season, GYD24 (June-October), received 451.6 mm of precipitation, 131.2 mm more than the 30-year normal precipitation for the county (Table 4.2). This precipitation was concentrated during the beginning of the growing season (Table 4.3). During the 2025 growing season, GYD25 (June-September), received 258.1 mm of precipitation, 17.2 mm less than the 30-year normal precipitation for the county (Table 4.2). This precipitation was concentrated at the end of the growing season (Table 4.3).

The westernmost site in 2024, THD24 (June-October), received 265.8 mm of precipitation, 52.7 mm less than the 30-year normal precipitation for the county (Table 4.2). This precipitation was concentrated towards the beginning and end of the growing season (Table 4.3). The westernmost site in 2025, THD25 (June-September), received 249.9 mm of precipitation, 30.3 mm less than the 30-year normal precipitation for the county (Table 4.2). This precipitation was concentrated towards the middle of the growing season (Table 4.3).

Rate Treatments

Since the dataset containing the 201.8 kg ha^{-1} rate of nitrogen application was incomplete, it was dropped from the dataset for initial evaluation. Following this omission, nitrogen fertilizer rate and site year had a significant interaction ($p < 0.0001$). Therefore, analysis by site year was conducted, including the 201.8 kg ha^{-1} nitrogen application rate, where available. Nitrogen fertilizer rate had effects on cumulative N_2O emissions at all evaluated site years (Table 4.4). Cumulative N_2O emissions generally increase with an increasing nitrogen application rate at all sites (Figures 4.3 - 4.8). Additionally, large fluxes of N_2O emissions from treatments receiving recommended fertilizer rates at the given site years were temporally related to large rainfall events following planting (Figure 4.2). In four of six site years, 67.3 kg ha^{-1} and 33.6 kg ha^{-1} application rates were not statistically different from the zero-nitrogen control (Table 4.4). Nitrogen application rates at and above 168.1 kg ha^{-1} were always statistically different from the zero-nitrogen control (Table 4.4).

Overall, 2024 had higher EF values, compared to values from similar treatments in 2025 (Table 4.5). In 2024, 13 of 17 evaluated rate treatments across all sites had EF values greater than 0.5%. In 2025, 1 of 18 evaluated rate treatments across all sites had EF values greater than 0.5%. When analyzing rate treatments, none of the evaluated sites had EF values that clearly increased with increasing nitrogen rate (Table 4.5).

Early Placement Treatments

Since the dataset containing the streamed UAN with urease inhibitor - NBPT fertilizer placement was incomplete, it was dropped from the dataset for initial evaluation. Following this omission, nitrogen fertilizer placement and site year had a significant interaction ($p < 0.0001$). Therefore, analysis by site year was conducted, including the streamed UAN with urease inhibitor - NBPT fertilizer placement, where available. In placement treatments applied one month prior to planting, nitrogen fertilizer placement influenced cumulative N_2O emissions in two of three evaluated site years (Table 4.6) (Figures 4.9 - 4.11). In 2024, at MRD, following two weeks after application, there were no differences in cumulative flux between any of the applied treatments (Figure 4.9). At GYD in 2025, all treatments that received nitrogen additions did not have different fluxes from one another (Table 4.6). THD in 2025 showed no differences between treatments receiving nitrogen (Table 4.6).

When evaluating EF values from placement treatments applied one month prior to planting, coulter placement of UAN did not result in lower EF values at any site (Table 4.7). At MRD in 2024, broadcast urea with urease inhibitor - NBPT (0.68%) did result in lower EF values compared to the streamed UAN alternative (0.89%). All EF values from MRD were greater than 0.5%. At GYD in 2025, broadcast urea with urease inhibitor - NBPT (1.05%) and coultered UAN (0.97%) had the highest EF values. All calculated EF values at GYD were greater than 0.5%. At THD in 2025, streamed UAN with urease inhibitor - NBPT (0.82%) and coultered UAN (0.87%) had the highest EF values, both greater than 0.5%, but less than 1%. Broadcast urea with urease inhibitor - NBPT (0.40%) and streamed UAN (0.34%) at THD both had EF values less than 0.5%.

At Planting Placement Treatments

Since the dataset containing the streamed UAN with urease inhibitor - NBPT, coultered UAN, and broadcast urea with urease inhibitor - NBPT fertilizer placements were incomplete, it was dropped from the dataset for initial evaluation. Following this omission, nitrogen fertilizer placement and site year had a significant interaction ($p < 0.0001$). Therefore, analysis by site year was conducted, including the streamed UAN with urease inhibitor - NBPT fertilizer placement, where available. Nitrogen fertilizer placement had an effect on cumulative N_2O emissions at four of the six evaluated site years (Table 4.8). Individually, placement treatments resulted in highly variable cumulative fluxes that were different across sites (Figures 4.12 - 4.17). In 2024, at MRD and in 2025 at THD, there was no difference between any of the evaluated nitrogen fertilizer placement treatments, including the no nitrogen control (Table 4.8). At THD in 2024, contrasting to the results at MRD24 and THD25, the broadcast urea with urease inhibitor - NBPT resulted in the highest overall cumulative emissions (758 g N_2O-N ha^{-1}), higher than the coultered (354 g N_2O-N ha^{-1}) and zero-nitrogen control treatments (388 g N_2O-N ha^{-1}) ($p = 0.269$; Table 4.8). The cumulative flux from the streamed UAN placement (685 g N_2O-N ha^{-1}) was not different from the broadcast urea with urease inhibitor - NBPT. The cumulative fluxes from the coulter and zero-nitrogen control were not different from one another. At GYD in 2024, all treatments receiving nitrogen applications had higher cumulative flux values (1166 - 1569 g N_2O-N ha^{-1}) than the zero-nitrogen control (390 g N_2O-N ha^{-1}) ($p = 0.0001$; Table 4.8). The coultered treatment had higher cumulative emissions than all other treatments (1569 g N_2O-N ha^{-1}) (Table 4.8). The cumulative flux from the broadcast urea with urease inhibitor - NBPT and streamed UAN treatments were not different from each other. In 2025, cumulative flux at RND had no differences between placements, but all treatments receiving nitrogen (353 - 447 g N_2O-N ha^{-1}) were higher than the zero-nitrogen control (125 g N_2O-N ha^{-1}) ($p = 0.0015$; Table 4.8). At GYD in 2025, coultered and streamed UAN treatments did not have different cumulative fluxes from the zero-nitrogen control (288 g N_2O-N ha^{-1}), while the streamed UAN with urease inhibitor - NBPT placement showed higher emissions compared to all other treatments (1145 g N_2O-N ha^{-1}) ($p = 0.0151$; Table 4.8).

For placement treatments applied at planting, EF values were highly variable. At GYD in 2024, coultered UAN had the highest EF value (1.75%) (Table 4.9), with all the calculated values greater than 1%. At THD in 2024, the broadcast urea with urease inhibitor - NBPT had the highest EF (0.55%). Two of three evaluated treatments at THD24 had EF values under 0.5%, but all values were less than 1%. At MRD in 2024, streamed UAN had the highest EF value (1.81%), which was greater than 1%. In 2025 at GYD, streamed UAN with urease inhibitor - NBPT had the highest EF value (1.27%), which was greater than 1%, but all other treatments were less than 0.5%. At THD in 2025, streamed UAN had the highest EF (0.15%), which was still less than 0.5%. At RND in 2025, streamed UAN had the highest EF (0.48%), which was still lower than 0.5%.

Discussion

Rate Treatments

Nitrogen fertilizer application rate has been well documented as a major contributor to cumulative N_2O emissions in grain sorghum by Preza-Fontes et al. (2020), Schwenke and Haigh (2016), and Zebarth et al. (2008). Our work supports this hypothesis that cumulative N_2O emissions are responsive to nitrogen fertilizer rate, since nitrogen application rate had a relationship with cumulative N_2O flux at all evaluated site locations ($p < 0.05$). As expected, treatments with higher nitrogen fertilizer rates resulted in higher cumulative N_2O emissions. Higher nitrogen fertilizer rates likely resulted in higher available NO_3^- in the soil, as described by Mosier et al. (1998). Higher rates of NO_3^- in the soil likely denitrified following rainfall events after planting (Schwenke and Haigh, 2016). Since large increases in cumulative flux at recommended fertilizer rates correspond well with precipitation events early in the growing season across all site years (Figure 4.2), this denitrification process, and therefore N_2O emissions, were likely more prevalent early in the growing season since the young crop had not yet reached peak nitrogen uptake, as supported by work from Barton et al. (2007).

Early Placement Treatments

In nitrogen fertilizer treatments applied one month prior to planting, placement was related to cumulative N_2O flux. Of placements evaluated, we expected the coulter treatment and the fertilizer treated with urease inhibitors to result in lower emissions than surface applied UAN. This hypothesis was supported by a study conducted in a similar semi-arid environment by Halvorson and Del Grosso (2013), where N_2O emissions were decreased with the use of urease inhibitors in urea. However, work done in a humid continental climate (Köppen Climate Classification: Dfb), based on the data of Kotteck et al. (2006), by Wood et al. (2023) showed that urease inhibitors used with urea did not impact N_2O emissions. Deeper placement of nitrogen fertilizer within the soil consistently resulted in lower N_2O emissions in sorghum systems (Fertitta-Roberts et al., 2017; Van Kessel et al., 2012). Shallow and surface placement result in higher N_2O emissions across multiple studies (Fertitta-Roberts et al., 2017; Halvorson and Del Grosso, 2013; Rychel et al., 2020). Contrastingly, our results show that there were no differences between any of the applied fertilizer placements when applied one month prior to planting, apart from the zero-nitrogen control. Our observed results could be caused by consistent low precipitation in the later portion of the season at MRD24 (Table 4.3) and the semi-arid environments assessed in GYD25 and THD25 (Table 4.2). If there was not sufficient rainfall to promote the denitrification process prior to crop planting and uptake, it may mean that the crop was able to successfully uptake nitrogen before it was lost through pathways driven by moisture, like leaching and denitrification.

At Planting Placement Treatments

In nitrogen fertilizer treatments applied at planting, placement had an association with cumulative flux in four of six site years evaluated. One site that did not have a response to nitrogen fertilizer placement (THD25) was also the site that had the lowest cumulative N_2O emissions overall, which could be the result of the lower than average in-season precipitation (Table 4.2). Malhi and Lemke (2007) found that the magnitude of cumulative N_2O emissions largely reflected precipitation levels, which could reflect the cause of these lower fluxes. In the easternmost site in 2025, RND, there were no differences between any of the plots that received nitrogen fertilizers. At both GYD25 and THD24, treatments with a urease inhibitor resulted in high N_2O emissions, with streamed UAN with urease inhibitor - NBPT higher than other treatments at GYD25 (p 0.0151) and broadcast urea with urease inhibitor - NBPT higher than other treatments at THD24 ($p = 0.0269$).

Urea hydrolysis is the process that converts urea ($CO(NH_2)_2$) to NH_4^+, a form of nitrogen available for plant uptake (Perin et al., 2020). When urea hydrolysis is incomplete, NH_3 can be lost to the atmosphere, resulting in less nitrogen being available for the plant. Urease is the enzyme that drives the conversion of urea to NH_4^+. A urease inhibitor results in less nitrogen loss to the atmosphere as NH_3, since the process of conversion from urea to NH_4^+ is delayed, and more nitrogen in the form of urea is able to move into the soil. This urea-nitrogen can then be moved into the soil by rainfall as urea, where it is then converted to NH_4^+ (Perin et al., 2020). Increased NH_4^+ in the soil could lead to increased nitrification and denitrification, resulting in more N_2O emissions. This, with literature from Wood et al. (2023) and Zhengping et al. (1991), that also have observed increases in N_2O emissions in treatments using urease inhibitors, supports the observed increase in N_2O emissions from treatments with the urease inhibitor at GYD25 and THD24.

At GYD24, the coultered treatment was higher than all other treatments ($p = 0.0001$). This is similar to results found by Bastos et al. (2021) and Drury et al. (2006) that reflect elevated cumulative N_2O emissions from subsurface placed nitrogen fertilizer. However, these findings contradict the findings of Fertitta-Roberts et al. (2017), and Van Kessel et al. (2012), that reflect decreased cumulative N_2O emissions from subsurface nitrogen placement. A couple possible explanations for these different findings may relate to poor closure of the channel following fertilizer placement and/or, subsurface placement may disrupt the soil structure, potentially causing preferential cracks to form along the injection band as the soil dries, creating the potential for loss from this application area. This could also promote water infiltration into the fertilizer band, which would result in increased N_2O emissions.

Emission Factors (EF)

Overall, increasing nitrogen rate did not result in increased N_2O emission factors, in agreement with previous work done in this area by Gehl et al. (2020). However, this lack of response to nitrogen rate contrasts with results from Schwenke and Haigh (2016), which did show a response of EF values to nitrogen application rate. In addition to rate response, subsurface placement in a coulter or addition of a urease inhibitor did not clearly reflect a reduction in emissions factors in evaluated environments. Emission factors ranged from –0.14 to 2.25 percent in 2024 and –0.02 to 1.27 percent in 2025. This year-to-year variability emphasizes the influence of annual and seasonal precipitation effects on EF values.

Considering the evaluated environments, a recommended nitrogen application rate for a yield goal of 6275.86 kg ha^{-1}, Kansas State University (2026) recommends applying 145.7-156.9 kg N ha^{-1}, with higher application recommended at sites with higher rainfall potential. At these recommended rates, the average EF value for site years in 2024 is 1.06 percent and for site years in 2025 is 0.27 percent for 2025. The EF values calculated here (Tables 4.5, 4.7, 4.9), specifically those from the more characteristic rainfall year, 2025 (Table 4.2), are largely in-line with IPCC's disaggregated EF value for arid and semiarid environments of 0.5 percent (IPCC, 2019).

Conclusion

Analysis of cumulative N_2O emissions data show an interaction between nitrogen application rates and site year at all evaluated sites. Increasing nitrogen fertilizer application rates resulted in higher cumulative N_2O emissions ($p < 0.05$). Overall, nitrogen fertilizer applied one month prior to planting did not show any differences between nitrogen fertilizer application methods. Sorghum grown in dryer environments generally did result in lower cumulative N_2O emissions compared to sorghum grown in wetter environments with similar nitrogen treatments. As shown in figures (4.3-4.17), N_2O emissions from grain sorghum did not always peak within the first two weeks following nitrogen application, but a peak was observed within the first month following nitrogen application, typically following a rainfall event. Overall, increasing nitrogen rate did not result in increased N_2O emission factors and subsurface placement with a coulter or addition of a urease inhibitor did not clearly reflect a reduction in emissions factors in evaluated environments. The EF values calculated, specifically those from the more characteristic rainfall year, 2025, are largely in-line with IPCC's disaggregated EF value for arid and semiarid environments of 0.5 percent (IPCC, 2019).

References

Adegbeye, M.J., P. Ravi Kanth Reddy, A.I. Obaisi, M.M.M.Y. Elghandour, K.J. Oyebamiji, et al. 2020. Sustainable agriculture options for production, greenhouse gasses and pollution alleviation, and nutrient recycling in emerging and transitional nations - An overview. Journal of Cleaner Production 242: 118319. doi: https://doi.org/10.1016/j.jclepro.2019.118319.

Barton, L., R. Kiese, D. Gatter, K. Butterbach-Bahl, R. Buck, et al. 2007. Nitrous Oxide Emissions from a Cropped Soil in a Semi-arid Climate. Global Change Biology 14(1): 177–192. doi: https://doi.org/10.1111/j.1365-2486.2007.01474.x.

Bastos, L.M., C.W. Rice, P.J. Tomlinson, and D. Mengel. 2021. Untangling soil-weather drivers of daily N_2O emissions and fertilizer management mitigation strategies in no-till corn. Soil Science Society of America Journal 85(5): 1437–1447. doi: https://doi.org/10.1002/saj2.20292.

Climate Change & Infectious Diseases Group, and K. Brugger. 2017. World Maps of Köppen-Geiger Climate Classification. Vu-wien.ac.at. https://koeppen-geiger.vu-wien.ac.at/usa.htm.

Coombes, N. 2018. DiGGer: DiGGer design generator under correlation and blocking. R package version 1.0.3. http://nswdpibiom.org/austatgen/software

Drury, C.F., W.D. Reynolds, C.S. Tan, T.W. Welacky, W. Calder, et al. 2006. Emissions of Nitrous Oxide and Carbon Dioxide. Soil Science Society of America Journal 70(2): 570–581. doi: https://doi.org/10.2136/sssaj2005.0042.

Fertitta-Roberts, C., S. Spatari, D.A. Grantz, and G.D. Jenerette. 2017. Trade-offs across productivity, GHG intensity, and Pollutant Loads from Second-generation Sorghum Bioenergy. GCB Bioenergy: 1764–1779. doi: https://doi.org/10.1111/gcbb.12471.

Gehl, K.A., L. Haag, J. Warren, S. Sharma, and P.J. Tomlinson. 2020. Dryland Sorghum Nitrogen Management: Implications for Utilization as Ethanol Feedstock. Kansas

Agricultural Experiment Station Research Reports 6(5). doi: https://doi.org/10.4148/2378-5977.7926.

Halvorson, A.D., and S.J. Del Grosso. 2013. Nitrogen Placement and Source Effects on Nitrous Oxide Emissions and Yields of Irrigated Corn. Journal of Environmental Quality 42(2): 312–322. doi: https://doi.org/10.2134/jeq2012.0315.

IPCC, 2006: 2006 IPCC Guidelines for National Greenhouse Gas Inventories, Prepared by the National Greenhouse Gas Inventories Programme [Eggleston H.S., Buendia L., Miwa K., Ngara T. and Tanabe K. (eds)]. IGES, Japan. https://www.ipcc-nggip.iges.or.jp/public/2006gl/

IPCC, 2007: Climate Change 2007: The Physical Science Basis. Contribution of Working Group I to the Fourth Assessment Report of the Intergovernmental Panel on Climate Change [Solomon, S., D. Qin, M. Manning, Z. Chen, M. Marquis, K.B. Averyt, M. Tignor and H.L. Miller (eds.)]. Cambridge University Press, Cambridge, United Kingdom and New York, NY, USA. https://www.ipcc.ch/site/assets/uploads/2020/02/ar4-wg1-sum_vol_en.pdf

IPCC, 2012: Glossary of terms. In: Managing the Risks of Extreme Events and Disasters to Advance Climate Change Adaptation [Field, C.B., V. Barros, T.F. Stocker, D. Qin, D.J. Dokken, K.L. Ebi, M.D. Mastrandrea, K.J. Mach, G.-K. Plattner, S.K. Allen, M. Tignor, and P.M. Midgley (eds.)]. A Special Report of Working Groups I and II of the Intergovernmental Panel on Climate Change (IPCC). Cambridge University Press, Cambridge, UK, and New York, NY, USA, pp. 555-564. https://archive.ipcc.ch/pdf/special-reports/srex/SREX-Annex_Glossary.pdf

IPCC, 2019: 2019 Refinement to the 2006 IPCC Guidelines for National Greenhouse Gas Inventories [Calvo Buendia, E., Tanabe, K., Kranjc, A., Baasansuren, J., Fukuda, M., Ngarize, S., Osako, A., Pyrozhenko, Y., Shermanau, P. and Federici, S. (eds)]. IPCC, Switzerland. https://www.ipcc-nggip.iges.or.jp/public/2019rf/index.html

IPCC, 2021: Climate Change 2021: The Physical Science Basis. Contribution of Working Group I to the Sixth Assessment Report of the Intergovernmental Panel on Climate Change

[Masson-Delmotte, V., P. Zhai, A. Pirani, S.L. Connors, C. Péan, S. Berger, N. Caud, Y. Chen, L. Goldfarb, M.I. Gomis, M. Huang, K. Leitzell, E. Lonnoy, J.B.R. Matthews, T.K. Maycock, T. Waterfield, O. Yelekçi, R. Yu, and B. Zhou (eds.)]. Cambridge University Press, Cambridge, United Kingdom and New York, NY, USA, 2391 pp. doi:10.1017/9781009157896. https://www.ipcc.ch/report/ar6/wg1/

Kansas State University. 2026. Nutrient Recommendations. Department of Agronomy. https://www.agronomy.k-state.edu/outreach-and-services/soil-testing-lab/recommendations.html.

Kansas State University Soil Testing Lab. 2025. Soil Analysis for Researchers. Department of Agronomy. https://www.agronomy.k-state.edu/outreach-and-services/soil-testing-lab/soil-analysis/researchers.html.

Koch. 2026. AGROTAIN™ Nitrogen Stabilizer. kochagronomicservices.com. https://kochagronomicservices.com/agrotain.

Lam, S.K., H. Suter, A.R. Mosier, and D. Chen. 2016. Using nitrification inhibitors to mitigate agricultural N2 O emission: a double-edged sword? Global Change Biology 23(2): 485–489. doi: https://doi.org/10.1111/gcb.13338.

LI-COR Biosciences. 2021. Using the Smart Chamber - Soil Gas Flux Survey Chamber. LI-COR Biosciences. https://www.licor.com/support/Smart-Chamber/topics/the-measurement-cycle.html

Lu, C., Z. Yu, J. Zhang, P. Cao, H. Tian, et al. 2022. Century-long Changes and Drivers of Soil Nitrous Oxide (N_2O) Emissions across the Contiguous United States. Global Change Biology 28(7): 2505–2524. doi: https://doi.org/10.1111/gcb.16061.

Malhi, S.S., and R. Lemke. 2007. Tillage, Crop Residue and N Fertilizer Effects on Crop yield, Nutrient uptake, Soil Quality and Nitrous Oxide Gas Emissions in a Second 4-yr Rotation Cycle. Soil and Tillage Research 96(1-2): 269–283. doi: https://doi.org/10.1016/j.still.2007.06.011.

Mosier, A., C. Kroeze, C. Nevison, O. Oenema, S. Seitzinger, et al. 1998. Closing the global N_2O budget: nitrous oxide emissions through the agricultural nitrogen cycle. Nutrient Cycling in Agroecosystems 52: 225–248. doi: https://doi.org/10.1023/A:1009740530221.

Northwest Alliance for Computational Science and Engineering. PRISM Climate Group, Oregon State University. PRISM. https://prism.oregonstate.edu/.

Office of the Kansas State Climatologist. 2020. Office of the Kansas State Climatologist. ksu.edu. https://climate.ksu.edu/products/climatology/ (accessed 27 February 2026).

Perin, V., E.A. Santos, R. Lollato, D. Ruiz-Diaz, and G.J. Kluitenberg. 2020. Impacts of Ammonia Volatilization from Broadcast Urea on Winter Wheat Production. Agronomy Journal 112(5): 3758–3772. doi: https://doi.org/10.1002/agj2.20371.

Pihlatie, M., E. Syväsalo, A. Simojoki, M. Esala, and K. Regina. 2004. Contribution of Nitrification and Denitrification to N_2O Production in peat, Clay and Loamy Sand Soils under Different Soil Moisture Conditions. Nutrient Cycling in Agroecosystems 70(2): 135–141. doi: https://doi.org/10.1023/b:fres.0000048475.81211.3c.

Preza-Fontes, G., P.J. Tomlinson, K.L. Roozeboom, J. Warren, and D.A. Ruiz Diaz. 2020. Nitrogen Fertilization Offsets the N2O Mitigating Effects of Cover-Crops and Double-Crop Soybean in a Wheat–Sorghum System. Agronomy Journal 112(2): 772–785. doi: https://doi.org/10.1002/agj2.20095.

Ravishankara, A.R., J.S. Daniel, and R.W. Portmann. 2009. Nitrous Oxide (N_2O): the Dominant Ozone-Depleting Substance Emitted in the 21st Century. Science 326(5949): 123–125. doi: https://doi.org/10.1126/science.1176985.

Rychel, K., K. Meurer, G. Börjesson, M. Strömgren, G. Tarekegn Getahun, et al. 2020. Deep N Fertilizer Placement Mitigated N_2O Emissions in a Swedish Field Trial with Cereals. Nutrient Cycling in Agroecosystems 118. doi: https://doi.org/10.1007/s10705-020-10089-3.

Schlegel, A.J., and J.L. Havlin. 2020. Irrigated grain sorghum response to 55 years of nitrogen, phosphorus, and potassium fertilization. Agronomy Journal 113(1): 464–477. doi: https://doi.org/10.1002/agj2.20453.

Schwenke, G.D., and B.M. Haigh. 2016. The interaction of seasonal rainfall and nitrogen fertiliser rate on soil N_2O emission, total N loss and crop yield of dryland sorghum and sunflower grown on sub-tropical Vertosols. Soil Research 54(5): 604–618. doi: https://doi.org/10.1071/sr15286.

Storlien, J., J. Heilman, T. Boutton, and D. Baltensperger. 2013. The Carbon Footprint of Bioenergy Sorghum Production in Central Texas: Production Implications on Greenhouse Gas Emissions, Carbon cycling, and Life Cycle Analysis. https://www.proquest.com/docview/1497271563?parentSessionId=OSIo8JsdRSgxwWbXws1JUpZMOeVwFm1J3votyHfGFCs%3D&pq-origsite=primo&accountid=11789&sourcetype=Dissertations%20&%20Theses

Storlien, J., F.M. Hons, J.P. Wight, and J.L. Heilman. 2014. Carbon Dioxide and Nitrous Oxide Emissions Impacted by Bioenergy Sorghum Management. Soil Science Society of America Journal 78(5): 1694–1706. doi: https://doi.org/10.2136/sssaj2014.04.0176.

University of Missouri Agricultural Experiment Station. 1998. Recommended Chemical Soil Test Procedures for the North Central Region North Central Regional Publication No. 221(Revised). Columbia, MO. https://extension.missouri.edu/sites/default/files/legacy_media/wysiwyg/Extensiondata/Pub/pdf/specialb/sb1001.pdf

US Environmental Protection Agency. 2024. Inventory of U.S. Greenhouse Gas Emissions and Sinks: 1990-2022. www.epa.gov. https://www.epa.gov/ghgemissions/inventory-us-greenhouse-gas-emissions-and-sinks-1990-2022.

USDA NRCS. 2019. Web Soil Survey. usda.gov. https://websoilsurvey.nrcs.usda.gov/app/.

Van Kessel, C., R. Venterea, J. Six, M.A. Adviento-Borbe, B. Linquist, et al. 2012. Climate, Duration, and N Placement Determine N_2O Emissions in Reduced Tillage systems: A

Meta-Analysis. Global Change Biology 19(1): 33–44. doi: https://doi.org/10.1111/j.1365-2486.2012.02779.x.

Venterea, R.T., B. Maharjan, and M.S. Dolan. 2011. Fertilizer Source and Tillage Effects on Yield-Scaled Nitrous Oxide Emissions in a Corn Cropping System. Journal of Environmental Quality 40(5): 1521–1531. doi: https://doi.org/10.2134/jeq2011.0039.

Wallace, A., R. Armstrong, R. Harris, O. Belyaeva, P. Grace, et al. 2018. Fertiliser timing and use of inhibitors to reduce N2O emissions of rainfed wheat in a semi-arid environment. Nutrient Cycling Agroecosystems 112: 231–252. doi: https://doi.org/10.1007/s10705-018-9941-7.

Wood, M.D., X. Gao, K.H.D. Tiessen, M. Tenuta, and D.N. Flaten. 2023. Enhanced efficiency urea fertilizers and timing effects on N_2O emissions from spring wheat production in Manitoba. Agronomy Journal 116(1): 51–72. doi: https://doi.org/10.1002/agj2.21448.

Zebarth, B.J., P. Rochette, D.L. Burton, and M. Price. 2008. Effect of fertilizer nitrogen management on N_2O emissions in commercial corn fields. Canadian Journal of Soil Science 88(2): 189–195. doi: https://doi.org/10.4141/cjss06010.

Zhengping, W., L. Liantie, O. Cleemput, and L. Baert. 1991. Effect of urease inhibitors on denitrification in soil. Soil use and management 7(4): 230–233. doi: https://doi.org/10.1111/j.1475-2743.1991.tb00879.x.

Tables

Table 4.1 Summary of field operations for all evaluated site years*.

	Site Year*					
Operation	GYD24	THD24	MRD24	GYD25	THD25	RND25
Early Fertilizer Application	April 30, 2024	April 22, 2024	May 10, 2024	May 15, 2025	May 14, 2025	.
Planting	June 7, 2024	June 29, 2024**	June 25, 2024	June 19, 2025	June 18, 2025	June 23, 2025
Hybrid	58M58DT	30A30DT**	58M58DT	30A30DT	30A30DT	59C30 DT2
Population (seeds ha^{-1})	123,500	165,490**	123,500	123,500	123,500	123,500
Grain Harvest	October 18, 2024	November 3, 2024	November 11, 2024	November 12-14, 2025	November 19, 2025	November 3, 2025

* (GYD24, Gray County, KS in 2024; THD24, Thomas County, KS in 2024; MRD24, Morris County, KS in 2024; GYD25, Gray County, KS in 2025; THD25, Thomas County, KS in 2025; RND25, Reno County, KS in 2025)

**THD24 required a replant due to environmental conditions. First planting occurred June 6, 2024, with hybrid 58M58DT at 123,500 seeds ha^{-1}. Replant information is shown in the table.

Table 4.2 Measured precipitation during grain sorghum growing season for all site-years*.

Site Year*	Measured Season Precipitation	30-Year Normal Season Precipitation	Departure from Normal
	---------- mm ----------		
GYD24	451.6	320.8	131.2
THD24	265.8	318.5	-52.7
MRD24	231.8	490.7	-258.8
GYD25	262.3	275.3	-12.9
THD25	249.9	280.2	-30.3
RND25	422.7	340.4	82.3

* (GYD24, Gray County, KS in 2024; THD24, Thomas County, KS in 2024; MRD24, Morris County, KS in 2024; GYD25, Gray County, KS in 2025; THD25, Thomas County, KS in 2025; RND25, Reno County, KS in 2025)

Table 4.3 Measured precipitation during grain sorghum growing season for all site-years*, evaluated in 15-day increments.

	Days Since Planting										
Site Year*	15	30	45	60	75	90	105	120	135	150	165
	--- mm ---										
GYD24	117.6	112.8	81.5	35.3	37.3	9.4	45	12.7	0.0	.	.
THD24	17.0	52.9	60.8	14.3	12.8	18.9	9.0	6.7	1.2	7.2	65.0
MRD24	63.1	6.2	67.3	32.5	24.3	24.5	8.2	5.7	.	.	.
GYD25	22.4	33.3	9.1	30.5	35.8	45.5	85.9	.	.	.	.
THD25	25.9	13.0	79.0	28.4	96.3	4.8	2.5	.	.	.	.
RND25	17.8	15.2	55.9	33.0	86.4	43.2	58.4	30.5	.	.	.

* (GYD24, Gray County, KS in 2024; THD24, Thomas County, KS in 2024; MRD24, Morris County, KS in 2024; GYD25, Gray County, KS in 2025; THD25, Thomas County, KS in 2025; RND25, Reno County, KS in 2025)

Table 4.4 Comparisons of estimates of cumulative N_2O flux for nitrogen fertilizer rates at all evaluated site-years*. Letters within the same column indicate statistical significance at $p < 0.05$.

	Site Year*					
Nitrogen Fertilizer Application Rate	GYD24	THD24	MRD24	GYD25	THD25	RND25
kg N ha^{-1}	-- g N_2O-N ha^{-1} ---------------------------------					
0	390 E	388 C	788 C	288 C	143 D	125 D
34	2753 B	412 C	684 C	280 C	154 D	258 CD
67	1166 DE	685 BC	2004 BC	417 BC	247 CD	447 AB
101	1694 CD	523 C	3064 AB	309 C	404 BC	297 BCD
135	918 DE	1981 A	2621 AB	649 ABC	551 AB	303 BC
168	3884 A	1504 AB	3520 A	847AB	500 B	547 A
202	2555 BC	.	3111 AB	913 A	745 A	488 A
p-value	<0.0001	0.0055	0.0014	0.0443	0.0001	0.0011
LSD	1007.2	872.4	1387.8	487.0	218.0	176.5

* (GYD24, Gray County, KS in 2024; THD24, Thomas County, KS in 2024; MRD24, Morris County, KS in 2024; GYD25, Gray County, KS in 2025; THD25, Thomas County, KS in 2025; RND25, Reno County, KS in 2025)

Table 4.5 Emission Factor (EF) for nitrogen fertilizer applied at variable rates at planting for all site-years.

	Site Year*					
Nitrogen Fertilizer Application Rate	GYD24	THD24	MRD24	GYD25	THD25	RND25
kg ha^{-1}	---------------------------------- % ----------------------------------					
34	7.03	0.07	-0.31	-0.02	0.03	0.40
67	1.14	0.44	1.81	0.19	0.15	0.48
101	1.29	-0.14	2.25	0.02	0.26	0.17
135	0.39	1.18	1.36	0.27	0.30	0.13
168	2.08	0.66	1.62	0.53	0.21	0.25
202	1.07	.	1.15	0.31	0.30	0.18

* (GYD24, Gray County, KS in 2024; THD24, Thomas County, KS in 2024; MRD24, Morris County, KS in 2024; GYD25, Gray County, KS in 2025; THD25, Thomas County, KS in 2025; RND25, Reno County, KS in 2025)

Table 4.6 Comparisons of estimates of cumulative N_2O flux for nitrogen fertilizer placement methods applied one month prior to planting at all evaluated site-years*. Letters within the same column indicate statistical significance at $p < 0.05$.

Nitrogen Fertilizer Placement	Site Years* MRD24	GYD25	THD25
	------------------------- g N_2O-N ha^{-1}	------------------------	
Control	788 B	288 B	143
Broadcast Urea with Urease Inhibitor - NBPT	2115 A	1287 A	475
Streamed UAN	2300 A	946 A	434
Streamed UAN with Urease Inhibitor - NBPT	.	917 A	344
Coultered UAN	2352 A	1229 A	788
p-value	0.0103	0.0150	0.1982
LSD	908.4	557.1	542.3

*(MRD24, Morris County, KS in 2024; GYD25, Gray County, KS in 2025; THD25, Thomas County, KS in 2025)

Table 4.7 Emission Factor (EF) for nitrogen fertilizer applied with variable placement one month prior to planting for all site-years*.

Nitrogen Fertilizer Placement	Site Year* MRD24	GYD25	THD25
	----------------------------	**%**	------------------------------
Broadcast Urea with Urease Inhibitor - NBPT	0.68	1.05	0.40
Streamed UAN	0.89	0.55	0.34
Streamed UAN with Urease Inhibitor - NBPT	.	0.51	0.82
Coultered UAN	1.03	0.97	0.87

* (GYD24, Gray County, KS in 2024; THD24, Thomas County, KS in 2024; MRD24, Morris County, KS in 2024; GYD25, Gray County, KS in 2025; THD25, Thomas County, KS in 2025; RND25, Reno County, KS in 2025)

Table 4.8 Comparisons of estimates of cumulative N_2O flux for nitrogen fertilizer placement methods at all evaluated site-years*. Letters within the same column indicate statistical significance at $p < 0.05$.

Nitrogen Fertilizer Placement	Site Years*					
	GYD24	THD24	MRD24	GYD25	THD25	RND25
Control	390 C	388 B	788	288 B	143	125 B
Broadcast Urea with Urease Inhibitor - NBPT	1204 B	758 A	871	.	.	360 A
Streamed UAN	1166 B	685 A	2004	417 B	247	447 A
Streamed UAN with Urease Inhibitor - NBPT	.	.	.	1144 A	.	.
Coultered UAN	1569 A	354 B	.	566 B	186	353 A
p-value	0.0001	0.0269	0.0615	0.0151	0.3466	0.0015
LSD	318.3	295.5	1096.1	490.6	160.6	124.7

* (GYD24, Gray County, KS in 2024; THD24, Thomas County, KS in 2024; MRD24, Morris County, KS in 2024; GYD25, Gray County, KS in 2025; THD25, Thomas County, KS in 2025; RND25, Reno County, KS in 2025)

Table 4.9 Emission Factor (EF) for nitrogen fertilizer applied with variable placement at planting for all site-years*.

	Site Year*					
Nitrogen Fertilizer Placement	GYD24	THD24	MRD24	GYD25	THD25	RND25
	---------------------------------- % ----------------------------------					
Broadcast Urea with Urease Inhibitor - NBPT	1.20	0.55	0.12	.	.	0.35
Streamed UAN	1.14	0.44	1.81	0.19	0.15	0.48
Streamed UAN with Urease Inhibitor - NBPT	.	.	.	1.27	.	.
Coultered UAN	1.75	-0.05	.	0.41	0.06	0.34

*(GYD24, Gray County, KS in 2024; THD24, Thomas County, KS in 2024; MRD24, Morris County, KS in 2024; GYD25, Gray County, KS in 2025; THD25, Thomas County, KS in 2025; RND25, Reno County, KS in 2025)

Figures

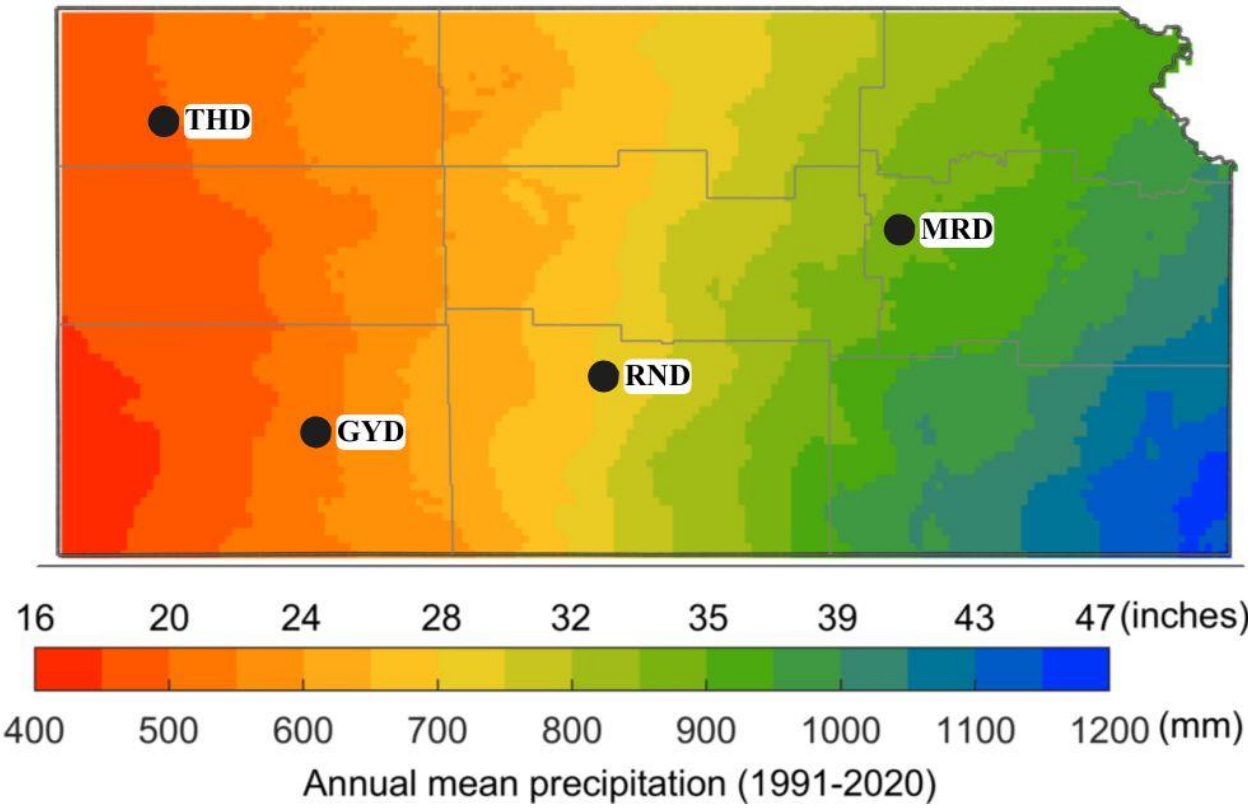

Figure 4.1 Thomas County, KS (THD), Gray County, KS (GYD), Reno County, KS (RND) and Morris County, KS (MRD) field site locations across Kansas represent three distinct precipitation environments (adapted from the Office of the Kansas State Climatologist, 2020).

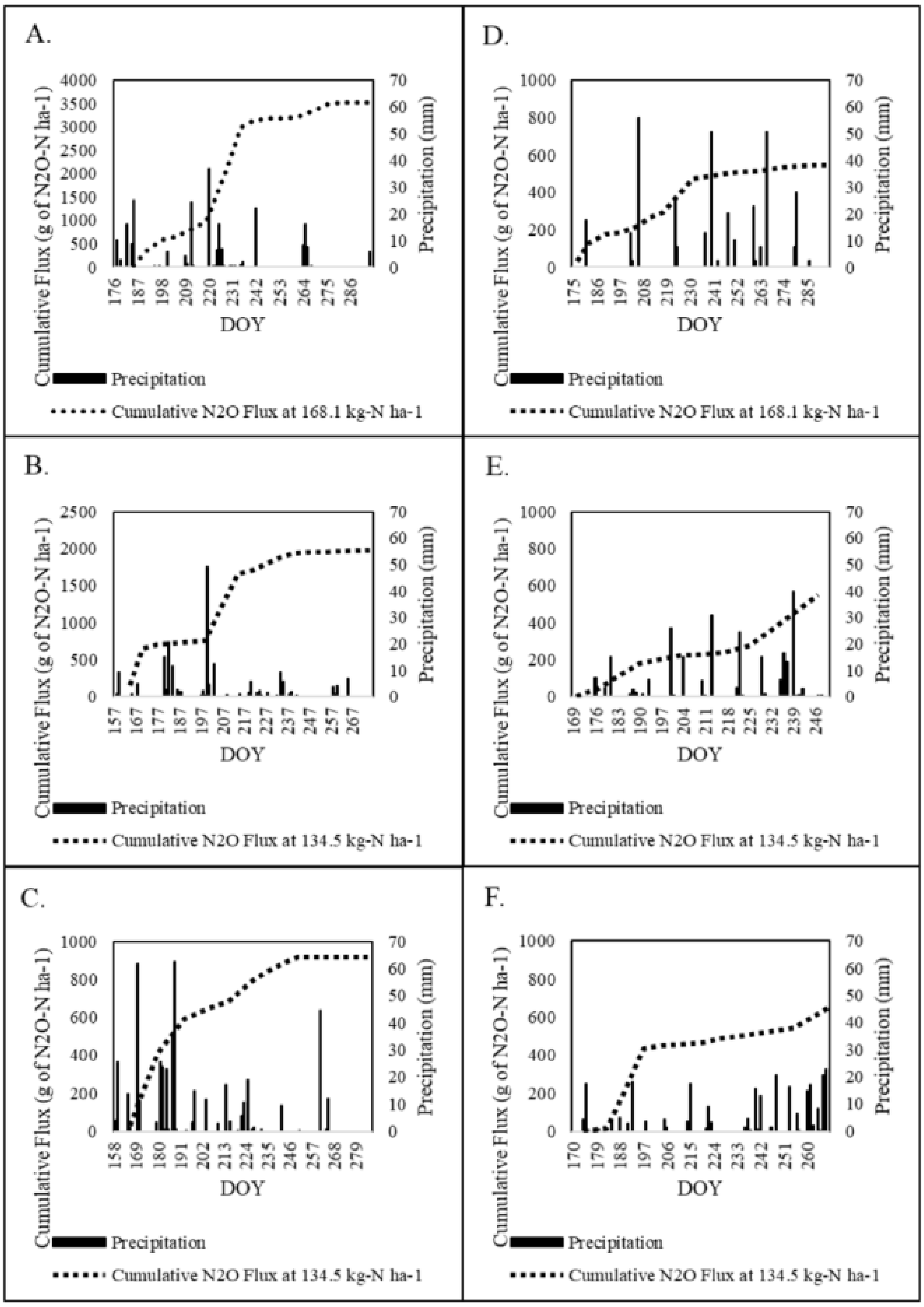

Figure 4.2 Mean total cumulative nitrous oxide (N_2O) emissions during grain sorghum growing season as effected by optimum nitrogen fertilizer application rate and precipitation at six site locations including Morris County in 2024 (MRD24) (A), Thomas County in 2024 (THD24) (B), Gray County in 2024 (GYD24) (C), Reno County in 2025 (RND25) (D), Thomas County in 2025 (THD25) (E), and Gray County in 2025 (GYD25) (F). (DOY, Day of Year)

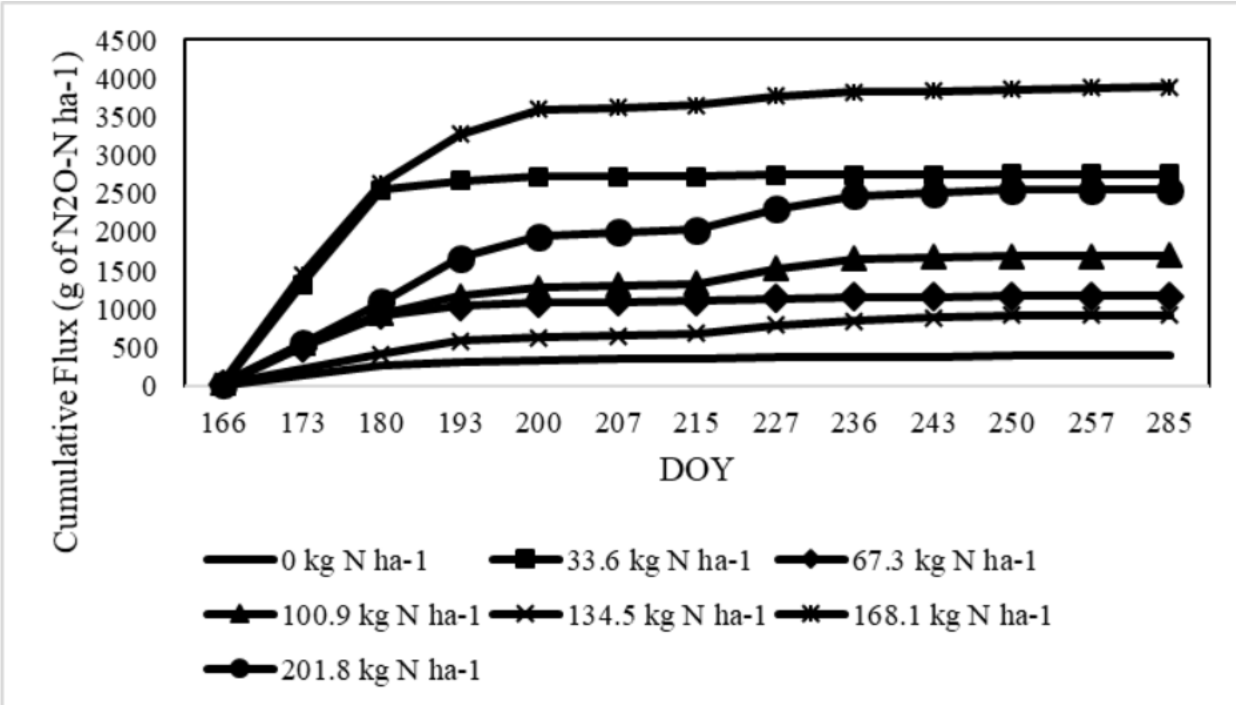

Figure 4.3 Mean cumulative nitrous oxide (N_2O) emissions during grain sorghum growing season as effected by nitrogen fertilizer application rate at Gray County in 2024 (GYD24). (DOY, Day of Year)

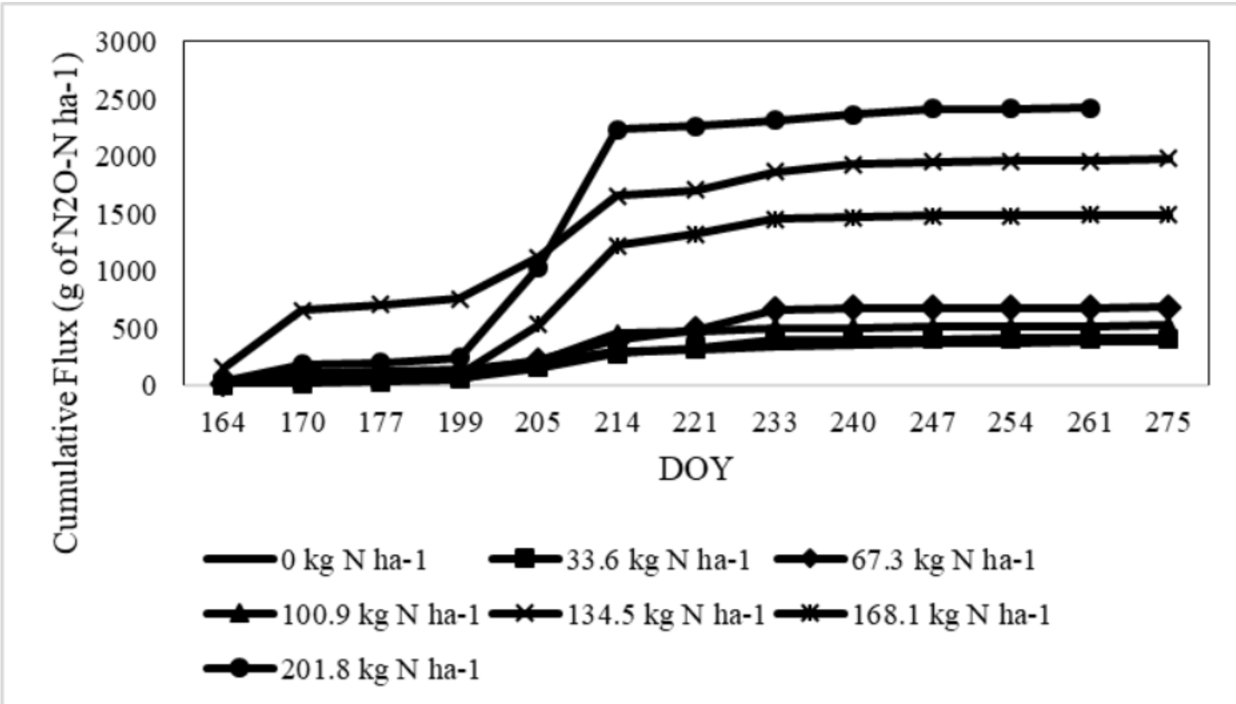

Figure 4.4 Mean cumulative nitrous oxide (N_2O) emissions during grain sorghum growing season as effected by nitrogen fertilizer application rate at Thomas County in 2024 (THD24). (DOY, Day of Year)

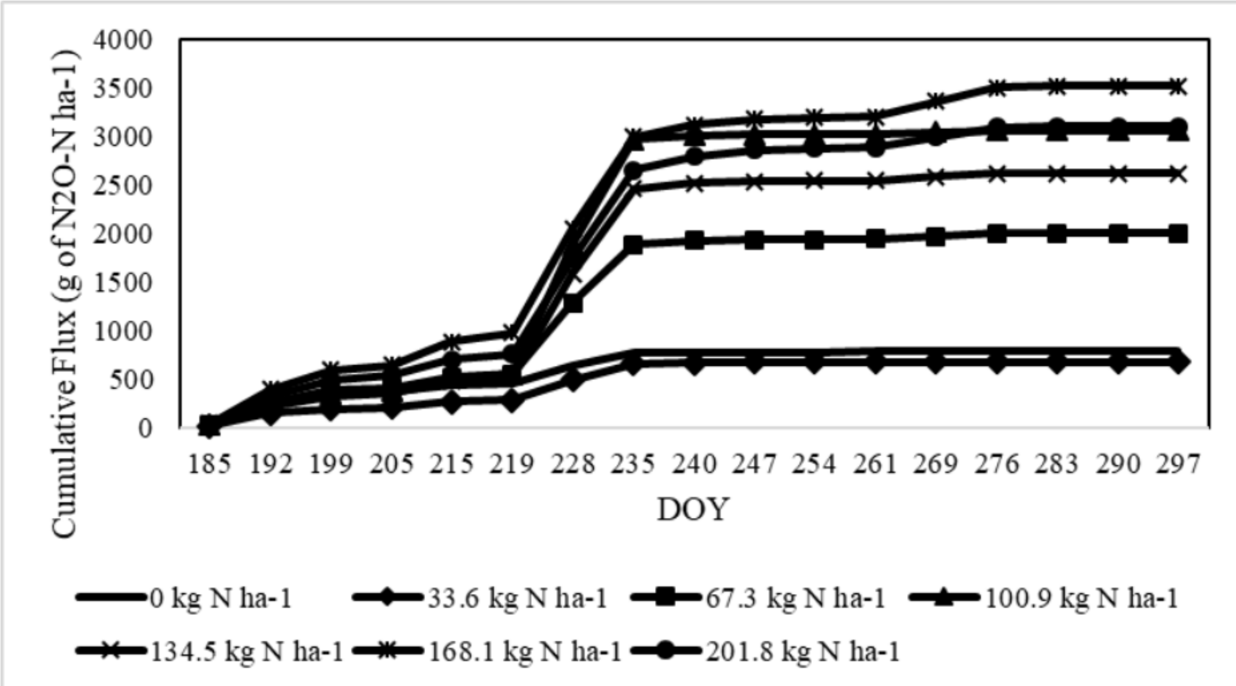

Figure 4.5 Mean cumulative nitrous oxide (N_2O) emissions during grain sorghum growing season as effected by nitrogen fertilizer application rate at Morris County in 2024 (MRD24). (DOY, Day of Year)

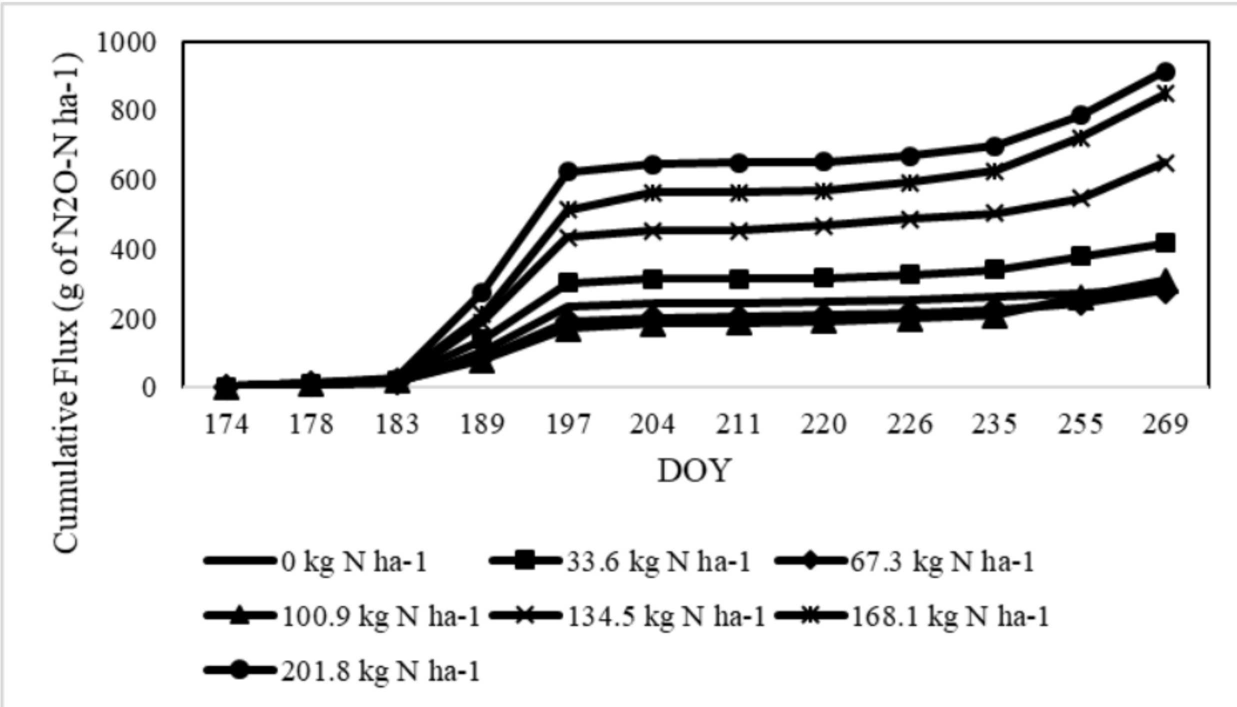

Figure 4.6 Mean cumulative nitrous oxide (N_2O) emissions during grain sorghum growing season as effected by nitrogen fertilizer application rate at Gray County in 2025 (GYD25). (DOY, Day of Year)

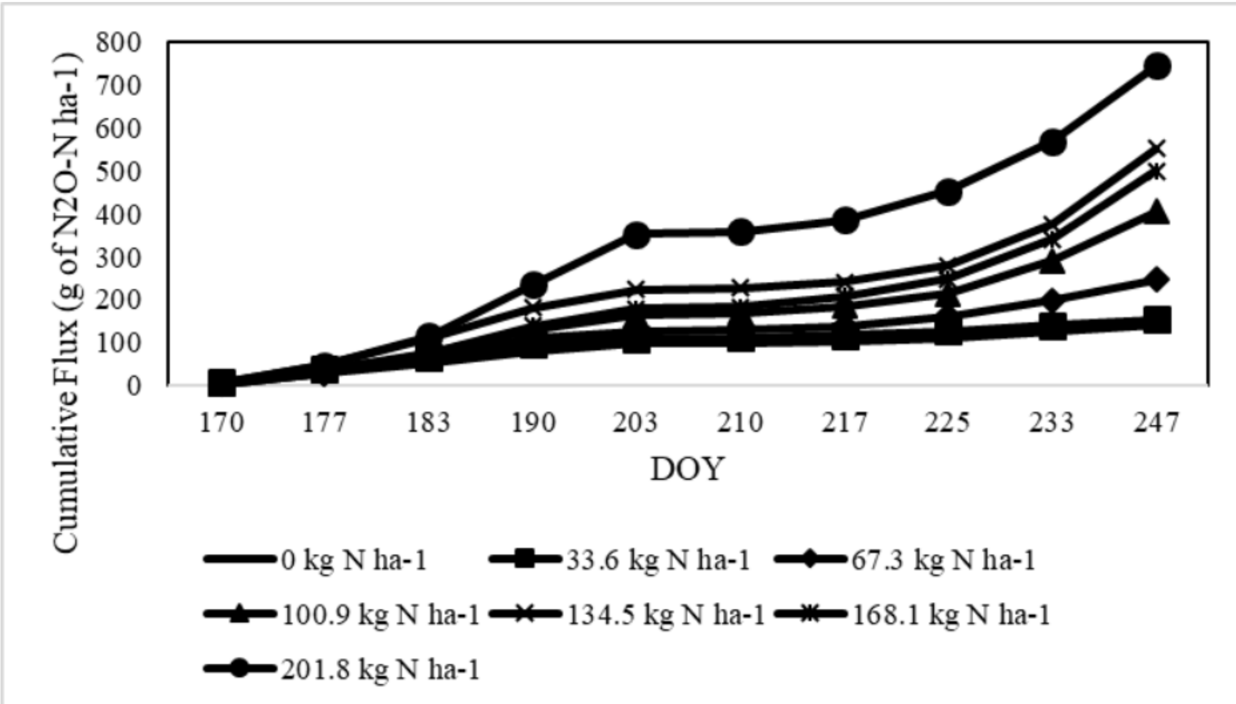

Figure 4.7 Mean cumulative nitrous oxide (N_2O) emissions during grain sorghum growing season as effected by nitrogen fertilizer application rate at Thomas County in 2025 (THD25). (DOY, Day of Year)

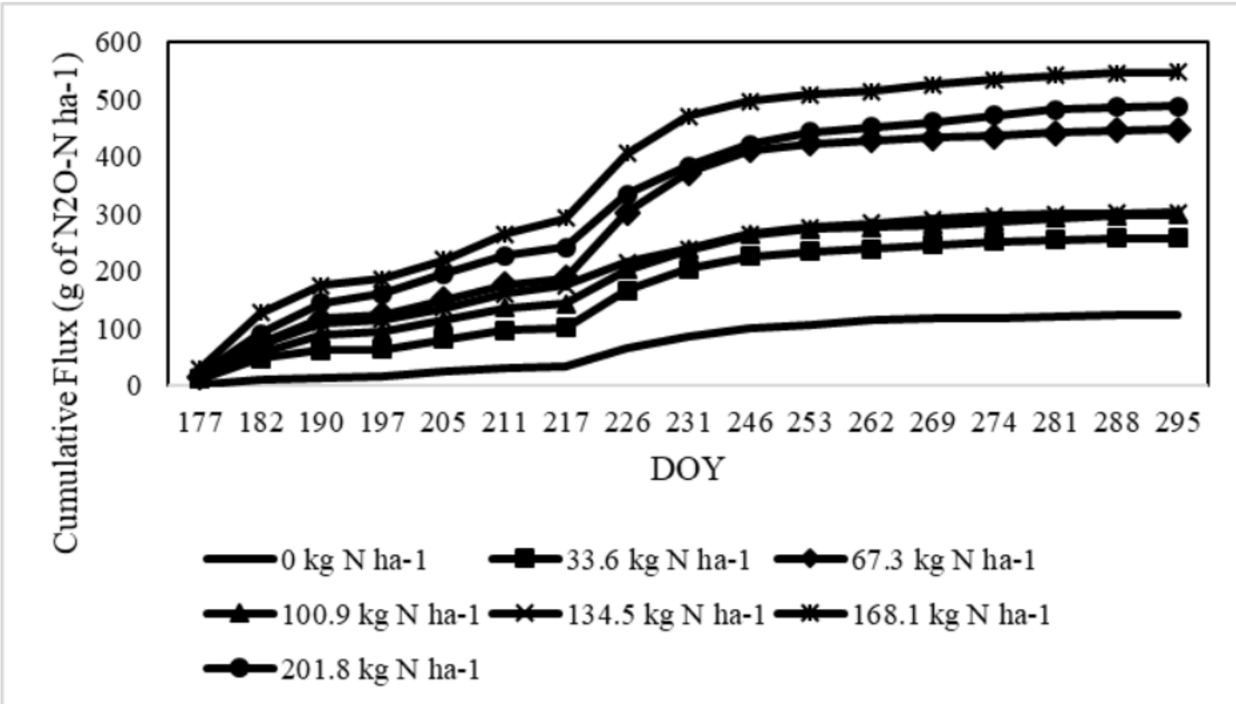

Figure 4.8 Mean cumulative nitrous oxide (N_2O) emissions during grain sorghum growing season as effected by nitrogen fertilizer application rate at Reno County in 2025 (RND25). (DOY, Day of Year)

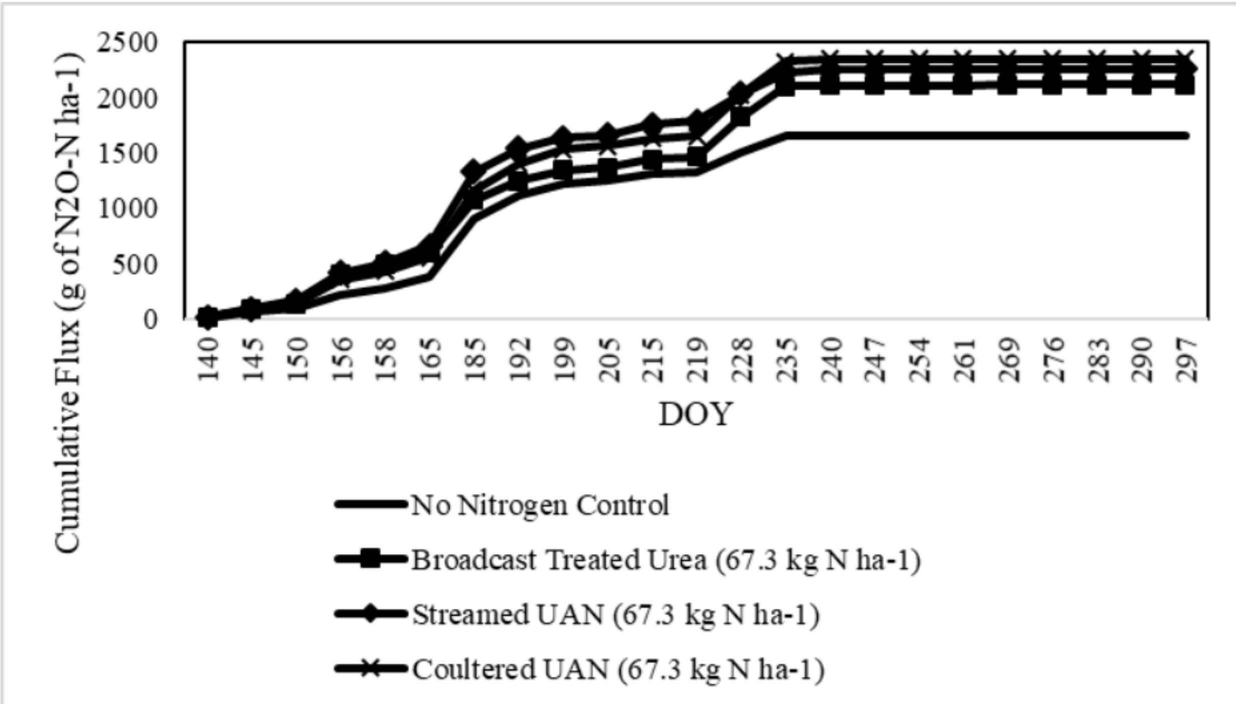

Figure 4.9 Mean cumulative nitrous oxide (N_2O) emissions during grain sorghum growing season as effected by nitrogen fertilizer application placement applied one month prior to planting at Morris County in 2024 (MRD24). (DOY, Day of Year)

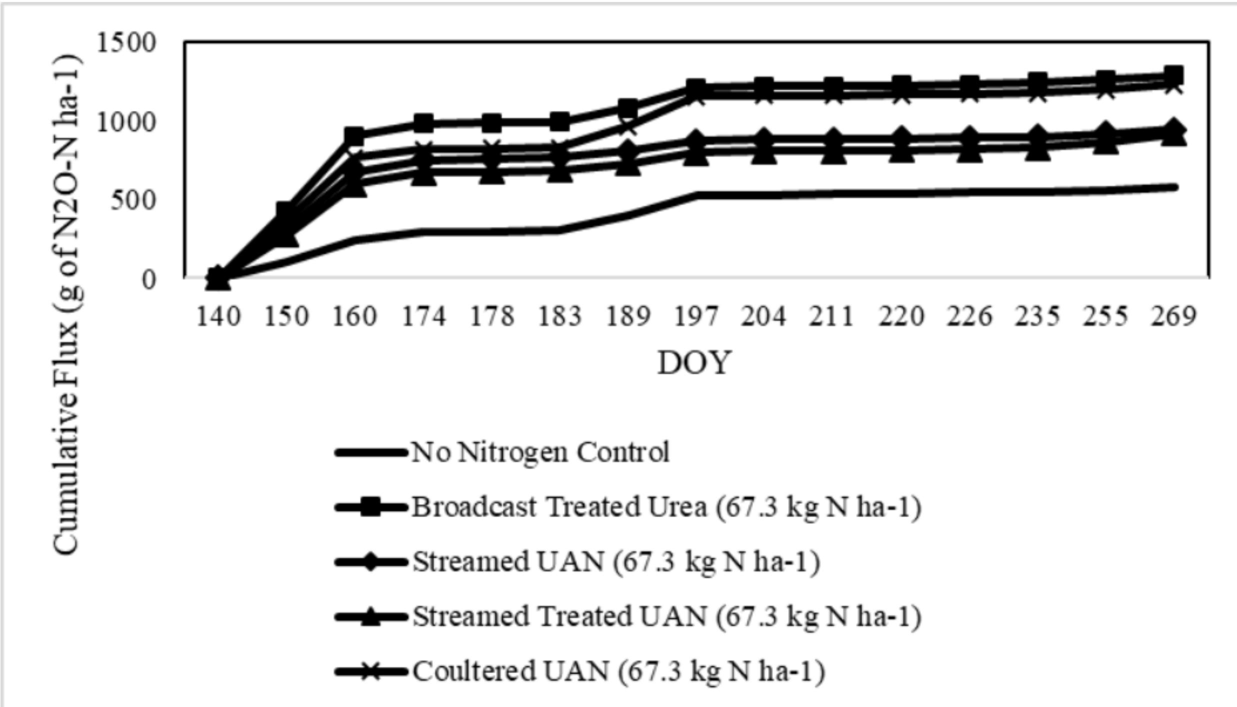

Figure 4.10 Mean cumulative nitrous oxide (N_2O) emissions during grain sorghum growing season as effected by nitrogen fertilizer application placement applied one month prior to planting at Gray County in 2025 (GYD25). (DOY, Day of Year)

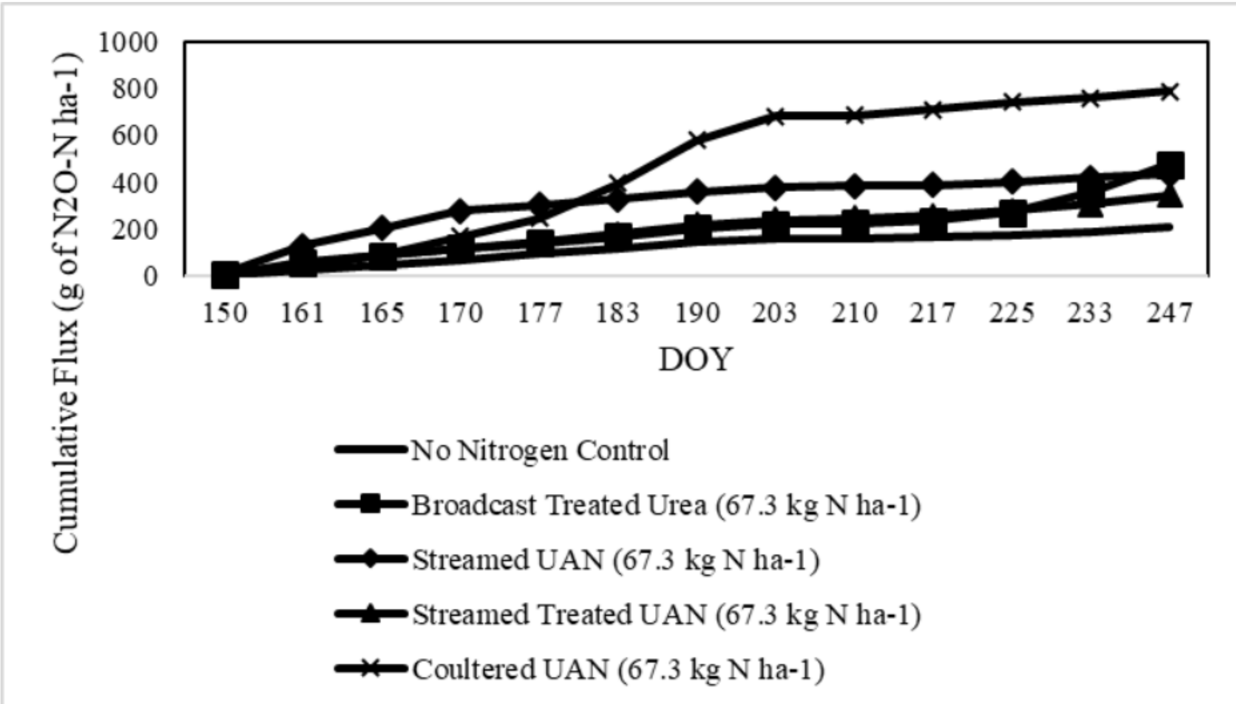

Figure 4.11 Mean cumulative nitrous oxide (N_2O) emissions during grain sorghum growing season as effected by nitrogen fertilizer application placement applied one month prior to planting at Thomas County in 2025 (THD25). (DOY, Day of Year)

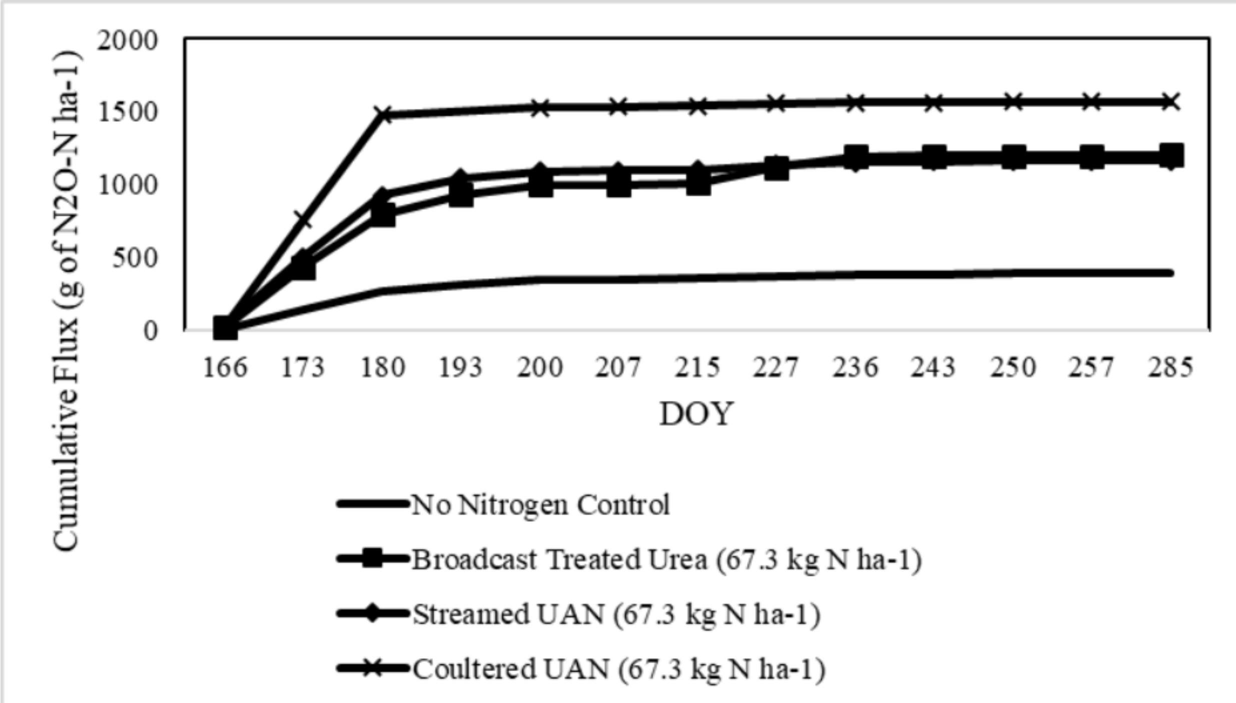

Figure 4.12 Mean cumulative nitrous oxide (N_2O) emissions during grain sorghum growing season as effected by nitrogen fertilizer application placement applied at planting at Gray County in 2024 (GYD24). (DOY, Day of Year)

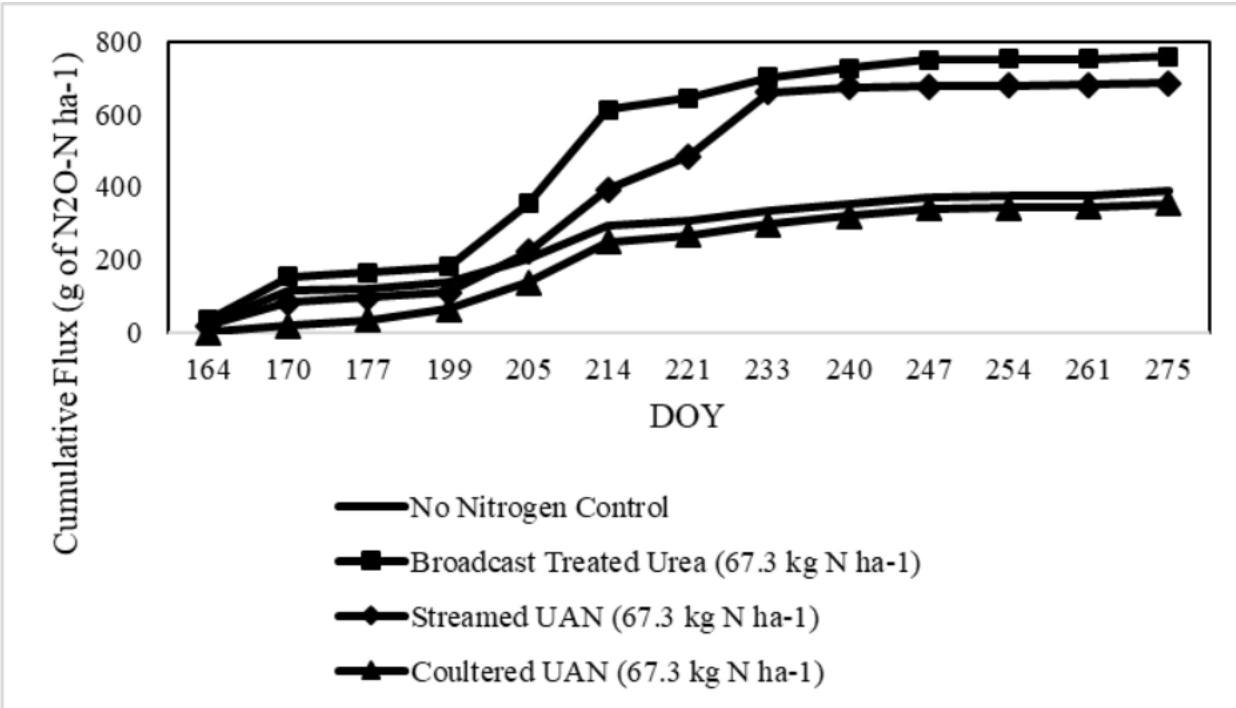

Figure 4.13 Mean cumulative nitrous oxide (N_2O) emissions during grain sorghum growing season as effected by nitrogen fertilizer application placement applied at planting at Thomas County in 2024 (THD24). (DOY, Day of Year)

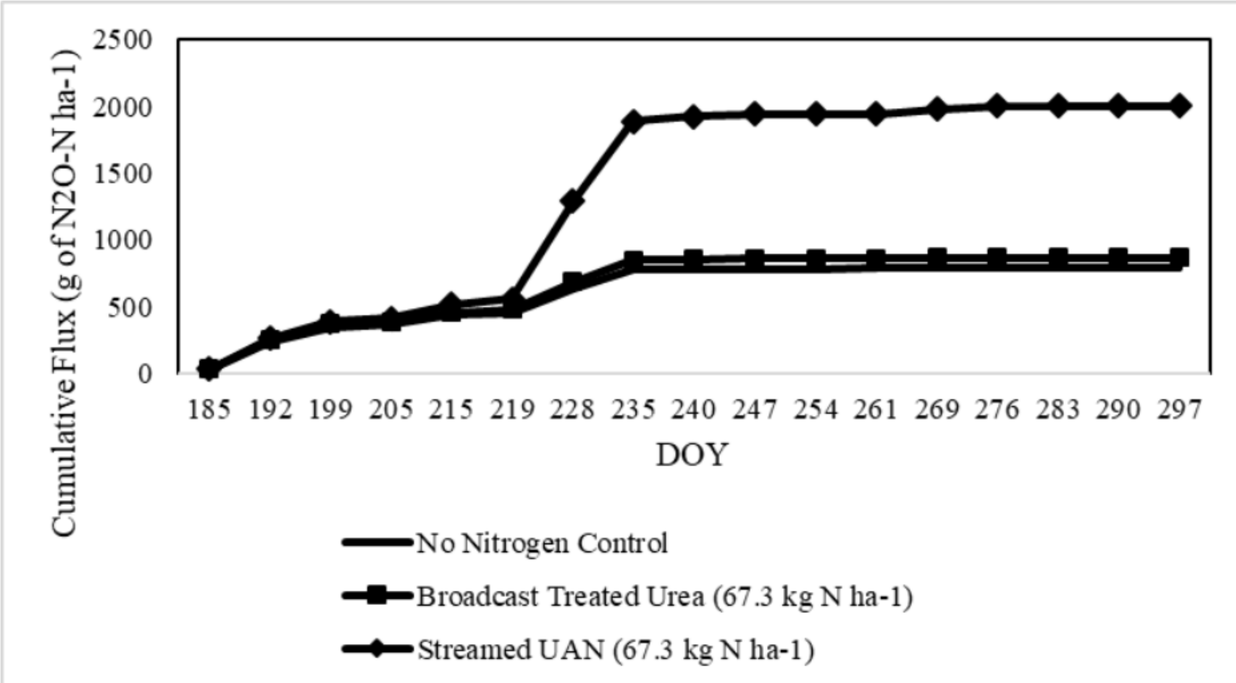

Figure 4.14 Mean cumulative nitrous oxide (N_2O) emissions during grain sorghum growing season as effected by nitrogen fertilizer application placement applied at planting at Morris County in 2024 (MRD24). (DOY, Day of Year)

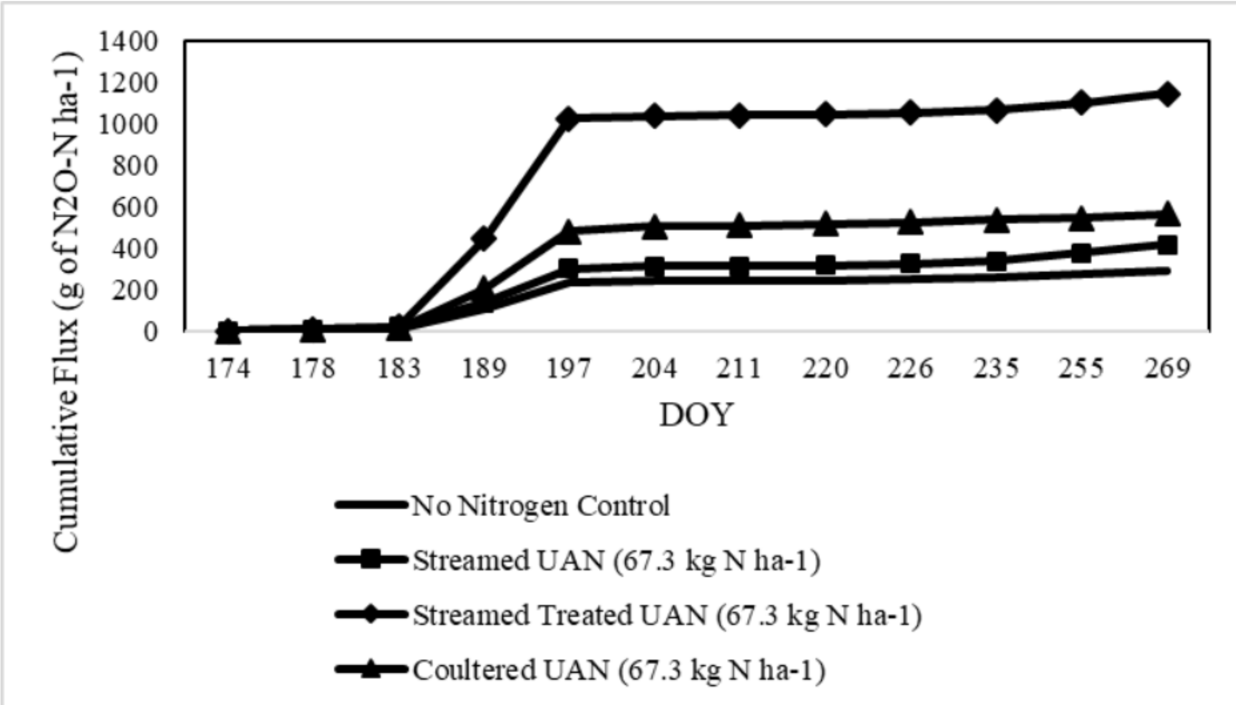

Figure 4.15 Mean cumulative nitrous oxide (N_2O) emissions during grain sorghum growing season as effected by nitrogen fertilizer application placement applied at planting at Gray County in 2025 (GYD25). (DOY, Day of Year)

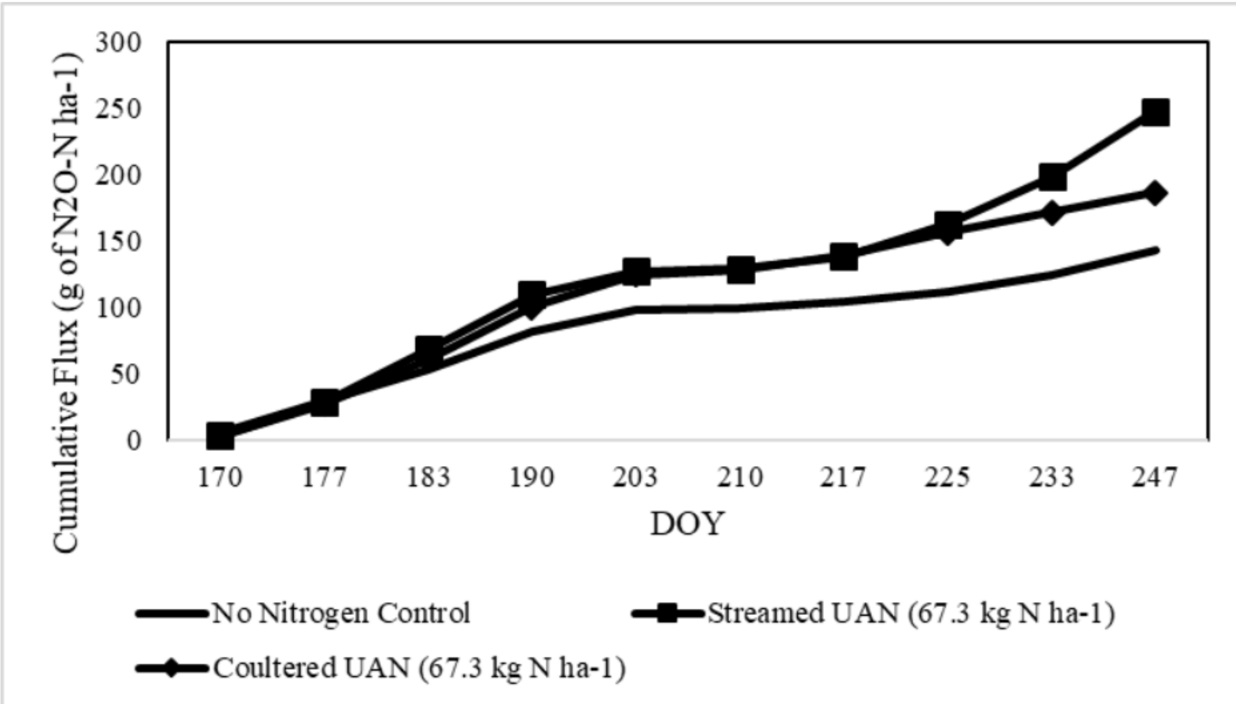

Figure 4.16 Mean cumulative nitrous oxide (N_2O) emissions during grain sorghum growing season as effected by nitrogen fertilizer application placement applied at planting at Thomas County in 2025 (THD25). (DOY, Day of Year)

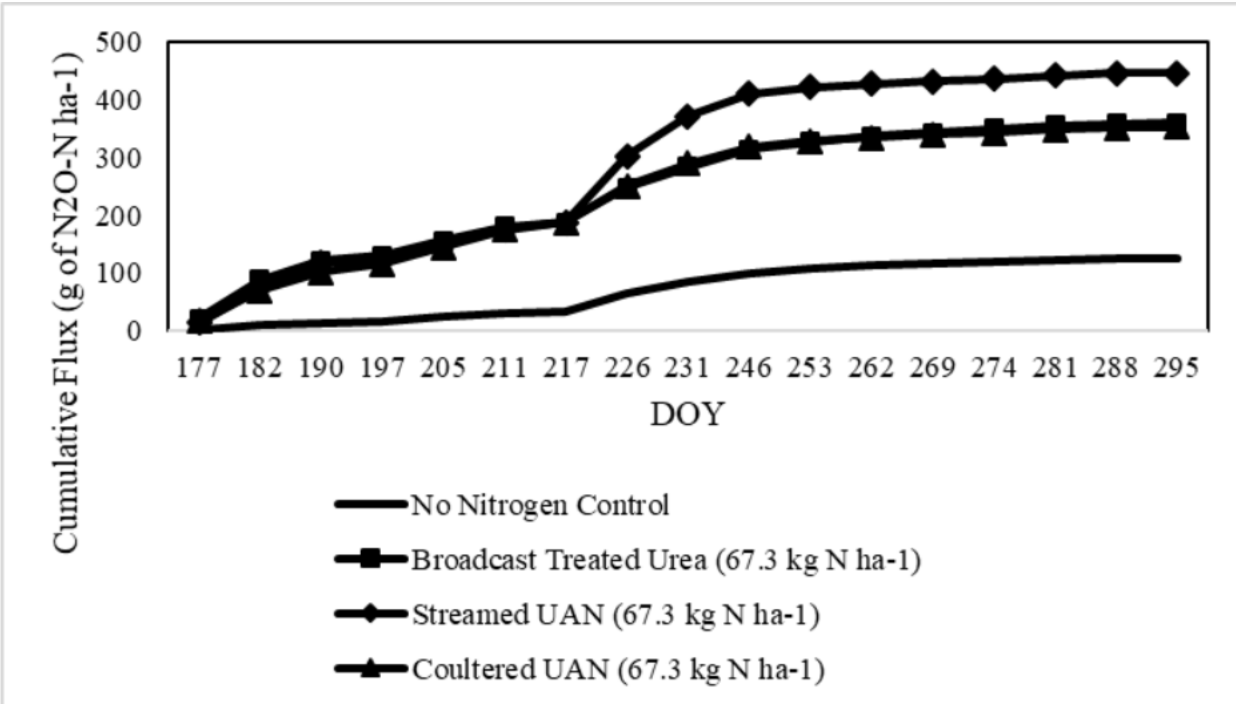

Figure 4.17 Mean cumulative nitrous oxide (N_2O) emissions during grain sorghum growing season as effected by nitrogen fertilizer application placement applied at planting at Reno County in 2025 (RND25). (DOY, Day of Year)

Appendix A - SAS Codes

Comparison of Sampling Duration – Regression Analysis

```
Data FFAR;
length SiteTimeKey $ 16;
Input LOC $ SiteTimeKey $ Plot $ Flux180Raw Flux180 Flux120Raw Flux120
FluxDiff Flux90Raw Flux90;
Cards;
;
run;
Proc Sort data=FFAR; by SiteTimeKey Plot;
run;
* Run the 90 vs. 120';
*By SiteTimeKey;
Title '90 vs. 120 by SiteTimeKey';
Proc Reg data=FFAR; by SiteTimeKey;
Model Flux90=Flux120;
IsSlope1: test Flux120=1;
ods output ParameterEstimates=Reg90v120bySiteTime;
ods output TestANOVA=Slope1Test90v120bySiteTime;
run;
*All Data;
Title '90 vs. 120 AllData';
Proc Reg data=FFAR;
Model Flux90=Flux120;
IsSlope1: test Flux120=1;
ods output ParameterEstimates=Reg90v120_ALL;
ods output TestANOVA=Slope1Test90v120_ALL;
run;
*All Data by LOC;
Title '90 vs. 120 AllDataByLOC';
Proc Reg data=FFAR; by LOC;
Model Flux90=Flux120;
IsSlope1: test Flux120=1;
ods output ParameterEstimates=Reg90v120_ALL_BYLOC;
ods output TestANOVA=Slope1Test90v120_ALL_BYLOC;
run;
* Run the 90 vs. 180';
*By SiteTimeKey;
Title '90 vs. 180 by SiteTimeKey';
Proc Reg data=FFAR; by SiteTimeKey;
Model Flux90=Flux180;
IsSlope1: test Flux180=1;
ods output ParameterEstimates=Reg90v180bySiteTime;
ods output TestANOVA=Slope1Test90v180bySiteTime;
run;
*All Data;
Title '90 vs. 180 AllData';
Proc Reg data=FFAR;
Model Flux90=Flux180;
IsSlope1: test Flux180=1;
ods output ParameterEstimates=Reg90v180_ALL;
ods output TestANOVA=Slope1Test90v180_ALL;
run;
```

```
*All Data by LOC;
Title '90 vs. 180 AllDataByLOC';
Proc Reg data=FFAR; by LOC;
Model Flux90=Flux180;
IsSlope1: test Flux180=1;
ods output ParameterEstimates=Reg90v180_ALL_BYLOC;
ods output TestANOVA=Slope1Test90v180_ALL_BYLOC;
run;
* Run the 120 vs. 180';
*By SiteTimeKey;
Title '120 vs. 180 by SiteTimeKey';
Proc Reg data=FFAR; by SiteTimeKey;
Model Flux120=Flux180;
IsSlope1: test Flux180=1;
ods output ParameterEstimates=Reg120v180bySiteTime;
ods output TestANOVA=Slope1Test120v180bySiteTime;
run;
*All Data;
Title '120 vs. 180 AllData';
Proc Reg data=FFAR;
Model Flux120=Flux180;
IsSlope1: test Flux180=1;
ods output ParameterEstimates=Reg120v180_ALL;
ods output TestANOVA=Slope1Test120v180_ALL;
run;
*All Data by LOC;
Title '120 vs. 180 AllDataByLOC';
Proc Reg data=FFAR; by LOC;
Model Flux120=Flux180;
IsSlope1: test Flux180=1;
ods output ParameterEstimates=Reg120v180_ALL_BYLOC;
ods output TestANOVA=Slope1Test120v180_ALL_BYLOC;
run;
```

Chamber Placement Analysis

```
Data Chamber;
Input Site $ DOY SiteTime $ Rep TRT Rate Plot Flux FluxType QAQC;

*For QAQC Code:
*QAQC 0 denotes both chambers bad;
*QAQC 1 denotes good;
*QAQC 2 denotes A chamber good;
*QAQC 3 denotes B chamber good;

If QAQC=0 then delete;
If QAQC=2 then delete;
If QAQC=3 then delete;

* For flux types:
1 = Chamber A
2 = Chamber B
3 = Average of A & B;
```

```
cards;
;
run;
proc print data=chamber;
run;
ods listing;
data ChamberRate;
set chamber;
where FluxType in (1,2)and TRT in (1,16,20,21,22,23,24);
run;
data ChamberApp;
set chamber;
where FluxType in (1,2)and TRT in (1,3,4,6,15,16,18);
run;
Proc Sort data=ChamberRate; by SiteTime Plot;
run;
Proc Sort data=ChamberApp; by SiteTime Plot;
run;
*This will evaluate are there differences between flux types when analyized
across all data;
Proc Mixed data=ChamberRate;
Class SiteTime Rep TRT FluxType;
Model Flux=FluxType /residual OUTP=RateFlux_pred_out;
Random SiteTime Rep(SiteTime);
LSMEANS FluxType /pdiff alpha=0.05;
ods output diffs=RateFluxppp lsmeans=RateFluxmmm tests3=RateFluxType3;
ods listing exclude diffs lsmeans;
run;
%include 'c:\sas\pdmix800.sas';
*%pdmix800(CumuFluxppp,CumuFluxmmm,alpha=0.10,sort=yes,mixfmt=no);
%pdmix800(RateFluxppp,RateFluxmmm,alpha=0.05,sort=yes,mixfmt=no);
*%pdmix800(CumuFluxppp,CumuFluxmmm,alpha=0.01,sort=yes,mixfmt=no);
run;
*This will evaluate if there is a flux type x rate interaction when analyized
across all data;
Proc Mixed data=ChamberRate;
Class SiteTime Rep TRT FluxType Rate;
Model Flux=FluxType|Rate /residual OUTP=Rate2Flux_pred_out;
Random SiteTime Rep(SiteTime);
LSMEANS FluxType|Rate /pdiff alpha=0.05;
ods output diffs=Rate2Fluxppp lsmeans=Rate2Fluxmmm tests3=Rate2FluxType3;
ods listing exclude diffs lsmeans;
run;

%include 'c:\sas\pdmix800.sas';
*%pdmix800(CumuFluxppp,CumuFluxmmm,alpha=0.10,sort=yes,mixfmt=no);
%pdmix800(Rate2Fluxppp,Rate2Fluxmmm,alpha=0.05,sort=yes,mixfmt=no);
*%pdmix800(CumuFluxppp,CumuFluxmmm,alpha=0.01,sort=yes,mixfmt=no);
Run;
*This will evaluate if there is a flux type x time x rate interaction when
analyized for each site-year;
Proc Mixed data=ChamberRate; by site;
Class Site DOY Rep TRT FluxType Rate;
Model Flux=FluxType|Rate|DOY /residual OUTP=Rate3Flux_pred_out;
Random Rep;
LSMEANS FluxType|Rate /pdiff alpha=0.05;
ods output diffs=Rate3Fluxppp lsmeans=Rate3Fluxmmm tests3=Rate3FluxType3;
```

```
ods listing exclude diffs lsmeans;
run;
%include 'c:\sas\pdmix800.sas';
*%pdmix800(CumuFluxppp,CumuFluxmmm,alpha=0.10,sort=yes,mixfmt=no);
%pdmix800(Rate3Fluxppp,Rate3Fluxmmm,alpha=0.05,sort=yes,mixfmt=no);
*%pdmix800(CumuFluxppp,CumuFluxmmm,alpha=0.01,sort=yes,mixfmt=no);
run;
*This will evaluate if there is a flux type x rate interaction for each
SiteTime;
Proc Mixed data=ChamberRate; by SiteTime;
Class SiteTime Rep TRT FluxType Rate;
Model Flux=FluxType|Rate /residual OUTP=CumuFlux_pred_out;
Random Rep;
LSMEANS FluxType|Rate /pdiff alpha=0.05;
ods output diffs=CumuFluxppp lsmeans=CumuFluxmmm tests3=CumuFluxType3;
ods listing exclude diffs lsmeans;
run;
%include 'c:\sas\pdmix800.sas';
*%pdmix800(CumuFluxppp,CumuFluxmmm,alpha=0.10,sort=yes,mixfmt=no);
%pdmix800(CumuFluxppp,CumuFluxmmm,alpha=0.05,sort=yes,mixfmt=no);
*%pdmix800(CumuFluxppp,CumuFluxmmm,alpha=0.01,sort=yes,mixfmt=no);
run;
Application Analysis
Proc Mixed data=ChamberApp;
Class SiteTime Rep FluxType;
Model Flux=FluxType /residual OUTP=AppFlux_pred_out;
Random SiteTime Rep(SiteTime);
LSMEANS FluxType /pdiff alpha=0.05;
ods output diffs=AppFluxppp lsmeans=AppFluxmmm tests3=AppFluxType3;
ods listing exclude diffs lsmeans;
run;
%include 'c:\sas\pdmix800.sas';
*%pdmix800(CumuFluxppp,CumuFluxmmm,alpha=0.10,sort=yes,mixfmt=no);
%pdmix800(AppFluxppp,AppFluxmmm,alpha=0.05,sort=yes,mixfmt=no);
*%pdmix800(CumuFluxppp,CumuFluxmmm,alpha=0.01,sort=yes,mixfmt=no);
run;
proc sort data=chamberApp;
by Site;
run;
Proc Mixed data=ChamberApp;By Site;
Class SiteTime Rep TRT FluxType;
Model Flux=FluxType|TRT /residual OUTP=App2Flux_pred_out;
Random SiteTime Rep(SiteTime);
LSMEANS FluxType|TRT /pdiff alpha=0.05;
ods output diffs=App2Fluxppp lsmeans=App2Fluxmmm tests3=App2FluxType3;
ods listing exclude diffs lsmeans;
run;
%include 'c:\sas\pdmix800.sas';
*%pdmix800(CumuFluxppp,CumuFluxmmm,alpha=0.10,sort=yes,mixfmt=no);
%pdmix800(App2Fluxppp,App2Fluxmmm,alpha=0.05,sort=yes,mixfmt=no);
*%pdmix800(CumuFluxppp,CumuFluxmmm,alpha=0.01,sort=yes,mixfmt=no);
run;
Proc Mixed data=ChamberApp;
Class SiteTime Rep TRT FluxType;
Model Flux=FluxType|TRT /residual OUTP=App2Flux_pred_out;
Random SiteTime Rep(SiteTime);
LSMEANS FluxType|TRT /pdiff alpha=0.05;
```

```
ods output diffs=App2Fluxppp lsmeans=App2Fluxmmm tests3=App2FluxType3;
ods listing exclude diffs lsmeans;
run;
%include 'c:\sas\pdmix800.sas';
*%pdmix800(CumuFluxppp,CumuFluxmmm,alpha=0.10,sort=yes,mixfmt=no);
%pdmix800(App2Fluxppp,App2Fluxmmm,alpha=0.05,sort=yes,mixfmt=no);
*%pdmix800(CumuFluxppp,CumuFluxmmm,alpha=0.01,sort=yes,mixfmt=no);
run;
Proc Mixed data=ChamberApp; by SiteTime;
Class SiteTime Rep TRT FluxType;
Model Flux=FluxType|TRT /residual OUTP=App3Flux_pred_out;
Random Rep;
LSMEANS FluxType|TRT /pdiff alpha=0.05;
ods output diffs=App3Fluxppp lsmeans=App3Fluxmmm tests3=App3FluxType3;
ods listing exclude diffs lsmeans;
run;
%include 'c:\sas\pdmix800.sas';
*%pdmix800(CumuFluxppp,CumuFluxmmm,alpha=0.10,sort=yes,mixfmt=no);
%pdmix800(App3Fluxppp,App3Fluxmmm,alpha=0.05,sort=yes,mixfmt=no);
*%pdmix800(CumuFluxppp,CumuFluxmmm,alpha=0.01,sort=yes,mixfmt=no);
run;
```

Nitrous Oxide Emissions Analysis

2024 GYD Placement

```
Data Flux;
Input Plot TRT REP DOY166     DOY173      DOY180      DOY193      DOY200
      DOY207      DOY215      DOY227      DOY236      DOY243      DOY250
      DOY257      DOY285;

If Plot=418 then delete;
If TRT=20 then delete;
If TRT=21 then delete;
If TRT=22 then delete;
If TRT=23 then delete;
If TRT=24 then delete;
Cards;
;
run;
Proc Sort data=flux; by Plot;
run;
proc transpose data=flux
      out=TallFlux(where=(Flux ne .) rename=(col1=Flux)) name=DOY;
by Plot TRT REP;
run;
proc datasets lib=work nolist;
modify TallFlux;
attrib _all_ label=' ';
quit;
Proc Sort data=TallFlux;
by DOY;
run;
Proc Mixed data=TallFlux;
Class Rep TRT;
```

```
Model Flux=TRT /residual OUTP=CumuFlux_pred_out;
Random Rep;
LSMEANS TRT /pdiff alpha=0.05;
ods output diffs=CumuFluxppp lsmeans=CumuFluxmmm tests3=CumuFluxType3;
ods listing exclude diffs lsmeans;
run;
%include 'c:\sas\pdmix800.sas';
*%pdmix800(CumuFluxppp,CumuFluxmmm,alpha=0.10,sort=yes,mixfmt=no);
%pdmix800(CumuFluxppp,CumuFluxmmm,alpha=0.05,sort=yes,mixfmt=no);
*%pdmix800(CumuFluxppp,CumuFluxmmm,alpha=0.01,sort=yes,mixfmt=no);
run;
Proc Mixed data=TallFlux; by DOY;
Class Rep TRT;
Model Flux=TRT /residual OUTP=CumuFlux_pred_out;
Random Rep;
LSMEANS TRT /pdiff alpha=0.05;
ods output diffs=CumuFluxppp lsmeans=CumuFluxmmm tests3=CumuFluxType3;
ods listing exclude diffs lsmeans;
run;
%include 'c:\sas\pdmix800.sas';
*%pdmix800(CumuFluxppp,CumuFluxmmm,alpha=0.10,sort=yes,mixfmt=no);
%pdmix800(CumuFluxppp,CumuFluxmmm,alpha=0.05,sort=yes,mixfmt=no);
*%pdmix800(CumuFluxppp,CumuFluxmmm,alpha=0.01,sort=yes,mixfmt=no);
run;
```

2024 GYD Rate

```
Data Flux;
Input Plot TRT REP DOY166     DOY173      DOY180      DOY193      DOY200
      DOY207      DOY215      DOY227      DOY236      DOY243      DOY250
      DOY257      DOY285;
If Plot=418 then delete;
If TRT=15 then delete;
If TRT=18 then delete;
cards;
;
run;
Proc Sort data=flux; by Plot;
run;
proc transpose data=flux
      out=TallFlux(where=(Flux ne .) rename=(col1=Flux)) name=DOY;
by Plot TRT REP;
run;
proc datasets lib=work nolist;
modify TallFlux;
attrib _all_ label=' ';
quit;
Proc Sort data=TallFlux;
by DOY;
run;

Proc Mixed data=TallFlux; by DOY;
Class Rep TRT;
Model Flux=TRT /residual OUTP=CumuFlux_pred_out;
Random Rep;
LSMEANS TRT /pdiff alpha=0.05;
```

```
ods output diffs=CumuFluxppp lsmeans=CumuFluxmmm tests3=CumuFluxType3;
ods listing exclude diffs lsmeans;
run;
%include 'c:\sas\pdmix800.sas';
*%pdmix800(CumuFluxppp,CumuFluxmmm,alpha=0.10,sort=yes,mixfmt=no);
%pdmix800(CumuFluxppp,CumuFluxmmm,alpha=0.05,sort=yes,mixfmt=no);
*%pdmix800(CumuFluxppp,CumuFluxmmm,alpha=0.01,sort=yes,mixfmt=no);
run;
Proc Mixed data=TallFlux;
Class Rep TRT;
Model Flux=TRT /residual OUTP=CumuFlux_pred_out;
Random Rep;
LSMEANS TRT /pdiff alpha=0.05;
ods output diffs=CumuFluxppp lsmeans=CumuFluxmmm tests3=CumuFluxType3;
ods listing exclude diffs lsmeans;
run;
%include 'c:\sas\pdmix800.sas';
*%pdmix800(CumuFluxppp,CumuFluxmmm,alpha=0.10,sort=yes,mixfmt=no);
%pdmix800(CumuFluxppp,CumuFluxmmm,alpha=0.05,sort=yes,mixfmt=no);
*%pdmix800(CumuFluxppp,CumuFluxmmm,alpha=0.01,sort=yes,mixfmt=no);
Run;
```

2024 MRD Placement – Early

```
Data Flux;
Input Plot TRT REP DOY140 DOY145 DOY150 DOY156 DOY158 DOY165 DOY185
      DOY192      DOY199      DOY205      DOY215      DOY219      DOY228
      DOY235      DOY240      DOY247      DOY254      DOY261      DOY269
      DOY276      DOY283      DOY290      DOY297;

If TRT=15 then delete;
If TRT=16 then delete;
If TRT=27 then delete;
If TRT=20 then delete;
If TRT=21 then delete;
If TRT=22 then delete;
If TRT=23 then delete;
If TRT=24 then delete;
cards;
;
run;
Proc Sort data=flux; by Plot;
run;
proc transpose data=flux
      out=TallFlux(where=(Flux ne .) rename=(col1=Flux)) name=DOY;
by Plot TRT REP;
run;
proc datasets lib=work nolist;
modify TallFlux;
attrib _all_ label=' ';
quit;
Proc Sort data=TallFlux;
by DOY;
run;
Proc Mixed data=TallFlux;
Class Rep TRT;
```

```
Model Flux=TRT /residual OUTP=CumuFlux_pred_out;
Random Rep;
LSMEANS TRT /pdiff alpha=0.05;
ods output diffs=CumuFluxppp lsmeans=CumuFluxmmm tests3=CumuFluxType3;
ods listing exclude diffs lsmeans;
run;
%include 'c:\sas\pdmix800.sas';
*%pdmix800(CumuFluxppp,CumuFluxmmm,alpha=0.10,sort=yes,mixfmt=no);
%pdmix800(CumuFluxppp,CumuFluxmmm,alpha=0.05,sort=yes,mixfmt=no);
*%pdmix800(CumuFluxppp,CumuFluxmmm,alpha=0.01,sort=yes,mixfmt=no);
run;
Proc Mixed data=TallFlux; by DOY;
Class Rep TRT;
Model Flux=TRT /residual OUTP=CumuFlux_pred_out;
Random Rep;
LSMEANS TRT /pdiff alpha=0.05;
ods output diffs=CumuFluxppp lsmeans=CumuFluxmmm tests3=CumuFluxType3;
ods listing exclude diffs lsmeans;
run;
%include 'c:\sas\pdmix800.sas';
*%pdmix800(CumuFluxppp,CumuFluxmmm,alpha=0.10,sort=yes,mixfmt=no);
%pdmix800(CumuFluxppp,CumuFluxmmm,alpha=0.05,sort=yes,mixfmt=no);
*%pdmix800(CumuFluxppp,CumuFluxmmm,alpha=0.01,sort=yes,mixfmt=no);
run;
```

2024 MRD Placement – At Planting

```
Data Flux;
Input Plot TRT REP DOY140 DOY145 DOY150 DOY156 DOY158 DOY165 DOY185
      DOY192      DOY199      DOY205      DOY215      DOY219      DOY228
      DOY235      DOY240      DOY247      DOY254      DOY261      DOY269
      DOY276      DOY283      DOY290      DOY297;

If TRT=1 then delete;
If TRT=6 then delete;
If TRT=3 then delete;
If TRT=4 then delete;
If TRT=20 then delete;
If TRT=21 then delete;
If TRT=22 then delete;
If TRT=23 then delete;
If TRT=24 then delete;
cards;
;
run;
Proc Sort data=flux; by Plot;
run;
proc transpose data=flux
      out=TallFlux(where=(Flux ne .) rename=(col1=Flux)) name=DOY;
by Plot TRT REP;
run;
proc datasets lib=work nolist;
modify TallFlux;
attrib _all_ label=' ';
quit;
Proc Sort data=TallFlux;
```

```
by DOY;
run;
Proc Mixed data=TallFlux;
Class Rep TRT;
Model Flux=TRT /residual OUTP=CumuFlux_pred_out;
Random Rep;
LSMEANS TRT /pdiff alpha=0.05;
ods output diffs=CumuFluxppp lsmeans=CumuFluxmmm tests3=CumuFluxType3;
ods listing exclude diffs lsmeans;
run;
%include 'c:\sas\pdmix800.sas';
*%pdmix800(CumuFluxppp,CumuFluxmmm,alpha=0.10,sort=yes,mixfmt=no);
%pdmix800(CumuFluxppp,CumuFluxmmm,alpha=0.05,sort=yes,mixfmt=no);
*%pdmix800(CumuFluxppp,CumuFluxmmm,alpha=0.01,sort=yes,mixfmt=no);
run;
Proc Mixed data=TallFlux; by DOY;
Class Rep TRT;
Model Flux=TRT /residual OUTP=CumuFlux_pred_out;
Random Rep;
LSMEANS TRT /pdiff alpha=0.05;
ods output diffs=CumuFluxppp lsmeans=CumuFluxmmm tests3=CumuFluxType3;
ods listing exclude diffs lsmeans;
run;
%include 'c:\sas\pdmix800.sas';
*%pdmix800(CumuFluxppp,CumuFluxmmm,alpha=0.10,sort=yes,mixfmt=no);
%pdmix800(CumuFluxppp,CumuFluxmmm,alpha=0.05,sort=yes,mixfmt=no);
*%pdmix800(CumuFluxppp,CumuFluxmmm,alpha=0.01,sort=yes,mixfmt=no);
run;
```

2024 MRD Rate

```
Data Flux;
Input Plot TRT REP DOY140 DOY145 DOY150 DOY156 DOY158 DOY165 DOY185
      DOY192      DOY199      DOY205      DOY215      DOY219      DOY228
      DOY235      DOY240      DOY247      DOY254      DOY261      DOY269
      DOY276      DOY283      DOY290      DOY297;

If TRT=1 then delete;
If TRT=3 then delete;
If TRT=4 then delete;
If TRT=6 then delete;
If TRT=15 then delete;
If Plot=304 then delete;
cards;
;
run;
Proc Sort data=flux; by Plot;
run;
proc transpose data=flux
      out=TallFlux(where=(Flux ne .) rename=(col1=Flux)) name=DOY;
by Plot TRT REP;

run;
proc datasets lib=work nolist;
modify TallFlux;
attrib _all_ label=' ';
```

```
quit;
Proc Sort data=TallFlux;
by DOY;
run;
Proc Mixed data=TallFlux;
Class Rep TRT;
Model Flux=TRT /residual OUTP=CumuFlux_pred_out;
Random Rep;
LSMEANS TRT /pdiff alpha=0.05;
ods output diffs=CumuFluxppp lsmeans=CumuFluxmmm tests3=CumuFluxType3;
ods listing exclude diffs lsmeans;
run;
%include 'c:\sas\pdmix800.sas';
*%pdmix800(CumuFluxppp,CumuFluxmmm,alpha=0.10,sort=yes,mixfmt=no);
%pdmix800(CumuFluxppp,CumuFluxmmm,alpha=0.05,sort=yes,mixfmt=no);
*%pdmix800(CumuFluxppp,CumuFluxmmm,alpha=0.01,sort=yes,mixfmt=no);
run;
Proc Mixed data=TallFlux; by DOY;
Class Rep TRT;
Model Flux=TRT /residual OUTP=CumuFlux_pred_out;
Random Rep;
LSMEANS TRT /pdiff alpha=0.05;
ods output diffs=CumuFluxppp lsmeans=CumuFluxmmm tests3=CumuFluxType3;
ods listing exclude diffs lsmeans;
run;
%include 'c:\sas\pdmix800.sas';
*%pdmix800(CumuFluxppp,CumuFluxmmm,alpha=0.10,sort=yes,mixfmt=no);
%pdmix800(CumuFluxppp,CumuFluxmmm,alpha=0.05,sort=yes,mixfmt=no);
*%pdmix800(CumuFluxppp,CumuFluxmmm,alpha=0.01,sort=yes,mixfmt=no);
run;
```

2024 THD Placement

```
Data Flux;
Input Plot TRT REP DOY164     DOY170      DOY177      DOY199      DOY205
      DOY214      DOY221      DOY234      DOY240      DOY247      DOY254
      DOY261      DOY275;

If plot=107 then delete;
If plot=402 then delete;
If TRT=20 then delete;
If TRT=21 then delete;
If TRT=22 then delete;
If TRT=23 then delete;
If TRT=24 then delete;
cards;
;
run;
Proc Sort data=flux; by Plot;
run;
proc transpose data=flux
      out=TallFlux(where=(Flux ne .) rename=(col1=Flux)) name=DOY;
by Plot TRT REP;
run;
proc datasets lib=work nolist;
modify TallFlux;
```

```
attrib _all_ label=' ';
quit;
Proc Sort data=TallFlux;
by DOY;
run;
Proc Mixed data=TallFlux;
Class Rep TRT;
Model Flux=TRT /residual OUTP=CumuFlux_pred_out;
Random Rep;
LSMEANS TRT /pdiff alpha=0.05;
ods output diffs=CumuFluxppp lsmeans=CumuFluxmmm tests3=CumuFluxType3;
ods listing exclude diffs lsmeans;
run;
%include 'c:\sas\pdmix800.sas';
*%pdmix800(CumuFluxppp,CumuFluxmmm,alpha=0.10,sort=yes,mixfmt=no);
%pdmix800(CumuFluxppp,CumuFluxmmm,alpha=0.05,sort=yes,mixfmt=no);
*%pdmix800(CumuFluxppp,CumuFluxmmm,alpha=0.01,sort=yes,mixfmt=no);
run;
Proc Mixed data=TallFlux; by DOY;
Class Rep TRT;
Model Flux=TRT /residual OUTP=CumuFlux_pred_out;
Random Rep;
LSMEANS TRT /pdiff alpha=0.05;
ods output diffs=CumuFluxppp lsmeans=CumuFluxmmm tests3=CumuFluxType3;
ods listing exclude diffs lsmeans;
run;
%include 'c:\sas\pdmix800.sas';
*%pdmix800(CumuFluxppp,CumuFluxmmm,alpha=0.10,sort=yes,mixfmt=no);
%pdmix800(CumuFluxppp,CumuFluxmmm,alpha=0.05,sort=yes,mixfmt=no);
*%pdmix800(CumuFluxppp,CumuFluxmmm,alpha=0.01,sort=yes,mixfmt=no);
run;
```

2024 THD Rate

```
Data Flux;
Input Plot TRT REP DOY164     DOY170      DOY177      DOY199      DOY205
      DOY214      DOY221      DOY234      DOY240      DOY247      DOY254
      DOY261      DOY275;

If plot=107 then delete;
If plot=402 then delete;
If TRT=15 then delete;
If TRT=18 then delete;
cards;
;
run;
Proc Sort data=flux; by Plot;
run;
proc transpose data=flux
      out=TallFlux(where=(Flux ne .) rename=(col1=Flux)) name=DOY;
by Plot TRT REP;

run;
proc datasets lib=work nolist;
modify TallFlux;
attrib _all_ label=' ';
```

```
quit;
Proc Sort data=TallFlux;
by DOY;
run;
Proc Mixed data=TallFlux;
Class Rep TRT;
Model Flux=TRT /residual OUTP=CumuFlux_pred_out;
Random Rep;
LSMEANS TRT /pdiff alpha=0.05;
ods output diffs=CumuFluxppp lsmeans=CumuFluxmmm tests3=CumuFluxType3;
ods listing exclude diffs lsmeans;
run;
%include 'c:\sas\pdmix800.sas';
*%pdmix800(CumuFluxppp,CumuFluxmmm,alpha=0.10,sort=yes,mixfmt=no);
%pdmix800(CumuFluxppp,CumuFluxmmm,alpha=0.05,sort=yes,mixfmt=no);
*%pdmix800(CumuFluxppp,CumuFluxmmm,alpha=0.01,sort=yes,mixfmt=no);
run;
Proc Mixed data=TallFlux; by DOY;
Class Rep TRT;
Model Flux=TRT /residual OUTP=CumuFlux_pred_out;
Random Rep;
LSMEANS TRT /pdiff alpha=0.05;
ods output diffs=CumuFluxppp lsmeans=CumuFluxmmm tests3=CumuFluxType3;
ods listing exclude diffs lsmeans;
run;
%include 'c:\sas\pdmix800.sas';
*%pdmix800(CumuFluxppp,CumuFluxmmm,alpha=0.10,sort=yes,mixfmt=no);
%pdmix800(CumuFluxppp,CumuFluxmmm,alpha=0.05,sort=yes,mixfmt=no);
*%pdmix800(CumuFluxppp,CumuFluxmmm,alpha=0.01,sort=yes,mixfmt=no);
run;
```

2025 GYD Placement – Early

```
Data Flux;
Input Plot TRT REP DOY140     DOY150      DOY160      DOY174      DOY178
      DOY183      DOY189      DOY197      DOY204      DOY211      DOY220
      DOY226      DOY235      DOY255      DOY269;

If TRT=27 then delete;
If TRT=18 then delete;
If TRT=17 then delete;
If TRT=16 then delete;
If TRT=20 then delete;
If TRT=21 then delete;
If TRT=22 then delete;
If TRT=23 then delete;
If TRT=24 then delete;
cards;
;
run;
Proc Sort data=flux; by Plot;
run;
proc transpose data=flux
      out=TallFlux(where=(Flux ne .) rename=(col1=Flux)) name=DOY;
by Plot TRT REP;
run;
```

```
proc datasets lib=work nolist;
modify TallFlux;
attrib _all_ label=' ';
quit;
Proc Sort data=TallFlux;
by DOY;
run;
Proc Mixed data=TallFlux; by DOY;
Class Rep TRT;
Model Flux=TRT /residual OUTP=CumuFlux_pred_out;
Random Rep;
LSMEANS TRT /pdiff alpha=0.05;
ods output diffs=CumuFluxppp lsmeans=CumuFluxmmm tests3=CumuFluxType3;
ods listing exclude diffs lsmeans;
run;
%include 'c:\sas\pdmix800.sas';
*%pdmix800(CumuFluxppp,CumuFluxmmm,alpha=0.10,sort=yes,mixfmt=no);
%pdmix800(CumuFluxppp,CumuFluxmmm,alpha=0.05,sort=yes,mixfmt=no);
*%pdmix800(CumuFluxppp,CumuFluxmmm,alpha=0.01,sort=yes,mixfmt=no);
run;
```

2025 GYD Placement – At Planting

```
Data Flux;
Input Plot TRT REP DOY140     DOY150      DOY160      DOY174      DOY178
      DOY183      DOY189      DOY197      DOY204      DOY211      DOY220
      DOY226      DOY235      DOY255      DOY269;

If TRT=1 then delete;
If TRT=9 then delete;
If TRT=10 then delete;
If TRT=11 then delete;
If TRT=12 then delete;
If TRT=20 then delete;
If TRT=21 then delete;
If TRT=22 then delete;
If TRT=23 then delete;
If TRT=24 then delete;
cards;
;
run;
Proc Sort data=flux; by Plot;
run;
proc transpose data=flux
      out=TallFlux(where=(Flux ne .) rename=(col1=Flux)) name=DOY;
by Plot TRT REP;
run;
proc datasets lib=work nolist;
modify TallFlux;
attrib _all_ label=' ';
quit;
Proc Sort data=TallFlux;
by DOY;
run;
Proc Mixed data=TallFlux;
Class Rep TRT;
```

```
Model Flux=TRT /residual OUTP=CumuFlux_pred_out;
Random Rep;
LSMEANS TRT /pdiff alpha=0.05;
ods output diffs=CumuFluxppp lsmeans=CumuFluxmmm tests3=CumuFluxType3;
ods listing exclude diffs lsmeans;
run;
%include 'c:\sas\pdmix800.sas';
*%pdmix800(CumuFluxppp,CumuFluxmmm,alpha=0.10,sort=yes,mixfmt=no);
%pdmix800(CumuFluxppp,CumuFluxmmm,alpha=0.05,sort=yes,mixfmt=no);
*%pdmix800(CumuFluxppp,CumuFluxmmm,alpha=0.01,sort=yes,mixfmt=no);
run;
Proc Mixed data=TallFlux; by DOY;
Class Rep TRT;
Model Flux=TRT /residual OUTP=CumuFlux_pred_out;
Random Rep;
LSMEANS TRT /pdiff alpha=0.05;
ods output diffs=CumuFluxppp lsmeans=CumuFluxmmm tests3=CumuFluxType3;
ods listing exclude diffs lsmeans;
run;
%include 'c:\sas\pdmix800.sas';
*%pdmix800(CumuFluxppp,CumuFluxmmm,alpha=0.10,sort=yes,mixfmt=no);
%pdmix800(CumuFluxppp,CumuFluxmmm,alpha=0.05,sort=yes,mixfmt=no);
*%pdmix800(CumuFluxppp,CumuFluxmmm,alpha=0.01,sort=yes,mixfmt=no);
run;
```

2025 GYD Rate

```
Data Flux;
Input Plot TRT REP DOY140     DOY150      DOY160      DOY174      DOY178
      DOY183      DOY189      DOY197      DOY204      DOY211      DOY220
      DOY226      DOY235      DOY255      DOY269;

If TRT=1 then delete;
If TRT=9 then delete;
If TRT=10 then delete;
If TRT=11 then delete;
If TRT=12 then delete;
If TRT=17 then delete;
If TRT=18 then delete;
cards;
;
run;
Proc Sort data=flux; by Plot;
run;
proc transpose data=flux
      out=TallFlux(where=(Flux ne .) rename=(col1=Flux)) name=DOY;
by Plot TRT REP;
run;
proc datasets lib=work nolist;
modify TallFlux;
attrib _all_ label=' ';
quit;
Proc Sort data=TallFlux;
by DOY;
run;
Proc Mixed data=TallFlux;
```

```
Class Rep TRT;
Model Flux=TRT /residual OUTP=CumuFlux_pred_out;
Random Rep;
LSMEANS TRT /pdiff alpha=0.05;
ods output diffs=CumuFluxppp lsmeans=CumuFluxmmm tests3=CumuFluxType3;
ods listing exclude diffs lsmeans;
run;
%include 'c:\sas\pdmix800.sas';
*%pdmix800(CumuFluxppp,CumuFluxmmm,alpha=0.10,sort=yes,mixfmt=no);
%pdmix800(CumuFluxppp,CumuFluxmmm,alpha=0.05,sort=yes,mixfmt=no);
*%pdmix800(CumuFluxppp,CumuFluxmmm,alpha=0.01,sort=yes,mixfmt=no);
run;
Proc Mixed data=TallFlux; by DOY;
Class Rep TRT;
Model Flux=TRT /residual OUTP=CumuFlux_pred_out;
Random Rep;
LSMEANS TRT /pdiff alpha=0.05;
ods output diffs=CumuFluxppp lsmeans=CumuFluxmmm tests3=CumuFluxType3;
ods listing exclude diffs lsmeans;
run;
%include 'c:\sas\pdmix800.sas';
*%pdmix800(CumuFluxppp,CumuFluxmmm,alpha=0.10,sort=yes,mixfmt=no);
%pdmix800(CumuFluxppp,CumuFluxmmm,alpha=0.05,sort=yes,mixfmt=no);
*%pdmix800(CumuFluxppp,CumuFluxmmm,alpha=0.01,sort=yes,mixfmt=no);
run;
```

2025 RND Placement

```
Data Flux;
Input Plot TRT REP DOY177     DOY182      DOY190      DOY197      DOY205
      DOY211      DOY217      DOY226      DOY231      DOY246      DOY253
      DOY262      DOY269      DOY274      DOY281      DOY288      DOY295;

If TRT=20 then delete;
If TRT=21 then delete;
If TRT=22 then delete;
If TRT=23 then delete;
If TRT=24 then delete;
cards;
;
run;
Proc Sort data=flux; by Plot;
run;
proc transpose data=flux
      out=TallFlux(where=(Flux ne .) rename=(col1=Flux)) name=DOY;
by Plot TRT REP;
run;
proc datasets lib=work nolist;
modify TallFlux;
attrib _all_ label=' ';
quit;
Proc Sort data=TallFlux;
by DOY;
run;
Proc Mixed data=TallFlux;
Class Rep TRT;
```

```
Model Flux=TRT /residual OUTP=CumuFlux_pred_out;
Random Rep;
LSMEANS TRT /pdiff alpha=0.05;
ods output diffs=CumuFluxppp lsmeans=CumuFluxmmm tests3=CumuFluxType3;
ods listing exclude diffs lsmeans;
run;
%include 'c:\sas\pdmix800.sas';
*%pdmix800(CumuFluxppp,CumuFluxmmm,alpha=0.10,sort=yes,mixfmt=no);
%pdmix800(CumuFluxppp,CumuFluxmmm,alpha=0.05,sort=yes,mixfmt=no);
*%pdmix800(CumuFluxppp,CumuFluxmmm,alpha=0.01,sort=yes,mixfmt=no);
run;
Proc Mixed data=TallFlux; by DOY;
Class Rep TRT;
Model Flux=TRT /residual OUTP=CumuFlux_pred_out;
Random Rep;
LSMEANS TRT /pdiff alpha=0.05;
ods output diffs=CumuFluxppp lsmeans=CumuFluxmmm tests3=CumuFluxType3;
ods listing exclude diffs lsmeans;
run;
%include 'c:\sas\pdmix800.sas';
*%pdmix800(CumuFluxppp,CumuFluxmmm,alpha=0.10,sort=yes,mixfmt=no);
%pdmix800(CumuFluxppp,CumuFluxmmm,alpha=0.05,sort=yes,mixfmt=no);
*%pdmix800(CumuFluxppp,CumuFluxmmm,alpha=0.01,sort=yes,mixfmt=no);
run;
```

2025 RND Rate

```
Data Flux;
Input Plot TRT REP DOY177      DOY182      DOY190      DOY197      DOY205
      DOY211      DOY217      DOY226      DOY231      DOY246      DOY253
      DOY262      DOY269      DOY274      DOY281      DOY288      DOY295;

If TRT=9 then delete;
If TRT=10 then delete;
If TRT=11 then delete;
If TRT=12 then delete;
If TRT=15 then delete;
If TRT=18 then delete;
cards;
;
run;
Proc Sort data=flux; by Plot;
run;
proc transpose data=flux
      out=TallFlux(where=(Flux ne .) rename=(col1=Flux)) name=DOY;
by Plot TRT REP;
run;
proc datasets lib=work nolist;
modify TallFlux;
attrib _all_ label=' ';
quit;
Proc Sort data=TallFlux;
by DOY;
run;
Proc Mixed data=TallFlux; by DOY;
Class Rep TRT;
```

```
Model Flux=TRT /residual OUTP=CumuFlux_pred_out;
Random Rep;
LSMEANS TRT /pdiff alpha=0.05;
ods output diffs=CumuFluxppp lsmeans=CumuFluxmmm tests3=CumuFluxType3;
ods listing exclude diffs lsmeans;
run;
%include 'c:\sas\pdmix800.sas';
*%pdmix800(CumuFluxppp,CumuFluxmmm,alpha=0.10,sort=yes,mixfmt=no);
%pdmix800(CumuFluxppp,CumuFluxmmm,alpha=0.05,sort=yes,mixfmt=no);
*%pdmix800(CumuFluxppp,CumuFluxmmm,alpha=0.01,sort=yes,mixfmt=no);
run;
Proc Mixed data=TallFlux;
Class Rep TRT;
Model Flux=TRT /residual OUTP=CumuFlux_pred_out;
Random Rep;
LSMEANS TRT /pdiff alpha=0.05;
ods output diffs=CumuFluxppp lsmeans=CumuFluxmmm tests3=CumuFluxType3;
ods listing exclude diffs lsmeans;
run;
%include 'c:\sas\pdmix800.sas';
*%pdmix800(CumuFluxppp,CumuFluxmmm,alpha=0.10,sort=yes,mixfmt=no);
%pdmix800(CumuFluxppp,CumuFluxmmm,alpha=0.05,sort=yes,mixfmt=no);
*%pdmix800(CumuFluxppp,CumuFluxmmm,alpha=0.01,sort=yes,mixfmt=no);
run;
```

2025 THD Placement – Early

```
Data Flux;
Input Plot TRT REP DOY150     DOY161      DOY165      DOY171      DOY177
      DOY183      DOY190      DOY203      DOY210      DOY217      DOY225
      DOY233      DOY239      DOY247;

If TRT=16 then delete;
If TRT=17 then delete;
If TRT=18 then delete;
If TRT=27 then delete;
If TRT=20 then delete;
If TRT=21 then delete;
If TRT=22 then delete;
If TRT=23 then delete;
If TRT=24 then delete;
cards;
;
run;
Proc Sort data=flux; by Plot;
run;
proc transpose data=flux
      out=TallFlux(where=(Flux ne .) rename=(col1=Flux)) name=DOY;
by Plot TRT REP;
run;
proc datasets lib=work nolist;
modify TallFlux;
attrib _all_ label=' ';
quit;
Proc Sort data=TallFlux;
by DOY;
```

```
run;
Proc Mixed data=TallFlux;
Class Rep TRT;
Model Flux=TRT /residual OUTP=CumuFlux_pred_out;
Random Rep;
LSMEANS TRT /pdiff alpha=0.05;
ods output diffs=CumuFluxppp lsmeans=CumuFluxmmm tests3=CumuFluxType3;
ods listing exclude diffs lsmeans;
run;
%include 'c:\sas\pdmix800.sas';
*%pdmix800(CumuFluxppp,CumuFluxmmm,alpha=0.10,sort=yes,mixfmt=no);
%pdmix800(CumuFluxppp,CumuFluxmmm,alpha=0.05,sort=yes,mixfmt=no);
*%pdmix800(CumuFluxppp,CumuFluxmmm,alpha=0.01,sort=yes,mixfmt=no);
run;
Proc Mixed data=TallFlux; by DOY;
Class Rep TRT;
Model Flux=TRT /residual OUTP=CumuFlux_pred_out;
Random Rep;
LSMEANS TRT /pdiff alpha=0.05;
ods output diffs=CumuFluxppp lsmeans=CumuFluxmmm tests3=CumuFluxType3;
ods listing exclude diffs lsmeans;
run;
%include 'c:\sas\pdmix800.sas';
*%pdmix800(CumuFluxppp,CumuFluxmmm,alpha=0.10,sort=yes,mixfmt=no);
%pdmix800(CumuFluxppp,CumuFluxmmm,alpha=0.05,sort=yes,mixfmt=no);
*%pdmix800(CumuFluxppp,CumuFluxmmm,alpha=0.01,sort=yes,mixfmt=no);
run;
```

2025 THD Placement – At Planting

```
Data Flux;
Input Plot TRT REP DOY150     DOY161      DOY165      DOY171      DOY177
      DOY183      DOY190      DOY203      DOY210      DOY217      DOY225
      DOY233      DOY239      DOY247;

If TRT=9 then delete;
If TRT=1 then delete;
If TRT=10 then delete;
If TRT=11 then delete;
If TRT=12 then delete;
If TRT=20 then delete;
If TRT=21 then delete;
If TRT=22 then delete;
If TRT=23 then delete;
If TRT=24 then delete;
Cards;
;
run;
Proc Sort data=flux; by Plot;
run;
proc transpose data=flux
      out=TallFlux(where=(Flux ne .) rename=(col1=Flux)) name=DOY;
by Plot TRT REP;
run;
proc datasets lib=work nolist;
modify TallFlux;
```

```
attrib _all_ label=' ';
quit;
Proc Sort data=TallFlux;
by DOY;
run;
Proc Mixed data=TallFlux;
Class Rep TRT;
Model Flux=TRT /residual OUTP=CumuFlux_pred_out;
Random Rep;
LSMEANS TRT /pdiff alpha=0.05;
ods output diffs=CumuFluxppp lsmeans=CumuFluxmmm tests3=CumuFluxType3;
ods listing exclude diffs lsmeans;
run;
%include 'c:\sas\pdmix800.sas';
*%pdmix800(CumuFluxppp,CumuFluxmmm,alpha=0.10,sort=yes,mixfmt=no);
%pdmix800(CumuFluxppp,CumuFluxmmm,alpha=0.05,sort=yes,mixfmt=no);
*%pdmix800(CumuFluxppp,CumuFluxmmm,alpha=0.01,sort=yes,mixfmt=no);
run;
Proc Mixed data=TallFlux; by DOY;
Class Rep TRT;
Model Flux=TRT /residual OUTP=CumuFlux_pred_out;
Random Rep;
LSMEANS TRT /pdiff alpha=0.05;
ods output diffs=CumuFluxppp lsmeans=CumuFluxmmm tests3=CumuFluxType3;
ods listing exclude diffs lsmeans;
run;
%include 'c:\sas\pdmix800.sas';
*%pdmix800(CumuFluxppp,CumuFluxmmm,alpha=0.10,sort=yes,mixfmt=no);
%pdmix800(CumuFluxppp,CumuFluxmmm,alpha=0.05,sort=yes,mixfmt=no);
*%pdmix800(CumuFluxppp,CumuFluxmmm,alpha=0.01,sort=yes,mixfmt=no);
run;
```

2025 THD Rate

```
Data Flux;
Input Plot TRT REP DOY150     DOY161      DOY165      DOY171      DOY177
      DOY183      DOY190      DOY203      DOY210      DOY217      DOY225
      DOY233      DOY247;

If TRT=1 then delete;
If TRT=9 then delete;
If TRT=10 then delete;
If TRT=11 then delete;
If TRT=12 then delete;
If TRT=17 then delete;
If TRT=18 then delete;
cards;
;
run;
Proc Sort data=flux; by Plot;
run;
proc transpose data=flux
      out=TallFlux(where=(Flux ne .) rename=(col1=Flux)) name=DOY;
by Plot TRT REP;
run;
proc datasets lib=work nolist;
```

```
modify TallFlux;
attrib _all_ label=' ';
quit;
Proc Sort data=TallFlux;
by DOY;
run;
Proc Mixed data=TallFlux;
Class Rep TRT;
Model Flux=TRT /residual OUTP=CumuFlux_pred_out;
Random Rep;
LSMEANS TRT /pdiff alpha=0.05;
ods output diffs=CumuFluxppp lsmeans=CumuFluxmmm tests3=CumuFluxType3;
ods listing exclude diffs lsmeans;
run;
%include 'c:\sas\pdmix800.sas';
*%pdmix800(CumuFluxppp,CumuFluxmmm,alpha=0.10,sort=yes,mixfmt=no);
%pdmix800(CumuFluxppp,CumuFluxmmm,alpha=0.05,sort=yes,mixfmt=no);
*%pdmix800(CumuFluxppp,CumuFluxmmm,alpha=0.01,sort=yes,mixfmt=no);
run;
Proc Mixed data=TallFlux; by DOY;
Class Rep TRT;
Model Flux=TRT /residual OUTP=CumuFlux_pred_out;
Random Rep;
LSMEANS TRT /pdiff alpha=0.05;
ods output diffs=CumuFluxppp lsmeans=CumuFluxmmm tests3=CumuFluxType3;
ods listing exclude diffs lsmeans;
run;
%include 'c:\sas\pdmix800.sas';
*%pdmix800(CumuFluxppp,CumuFluxmmm,alpha=0.10,sort=yes,mixfmt=no);
%pdmix800(CumuFluxppp,CumuFluxmmm,alpha=0.05,sort=yes,mixfmt=no);
*%pdmix800(CumuFluxppp,CumuFluxmmm,alpha=0.01,sort=yes,mixfmt=no);
run;
```